DESIGN AND PERFORMANCE STUDY OF CO_2 BASED VORTEX TUBE COOLING SYSTEM IN TURNING OF Ti-6Al-4V

Submitted in partial fulfillment of the requirements

for the award of degree of

DOCTOR OF PHILOSOPHY

in

Mechanical Engineering

by

KHIROD KUMAR MAHAPATRO

(Roll. No. 718027)

under the supervision of

Dr. P. Vamsi Krishna
Professor
Department of Mechanical Engineering

DEPARTMENT OF MECHANICAL ENGINEERING
NATIONAL INSTITUTE OF TECHNOLOGY WARANGAL
WARANGAL-506004, TELANGANA, INDIA.
NOVEMBER -2022

DESIGN AND PERFORMANCE STUDY OF CO_2 BASED VORTEX TUBE COOLING SYSTEM IN TURNING OF Ti-6Al-4V

Submitted in partial fulfillment of the requirements

for the award of degree of

DOCTOR OF PHILOSOPHY

in

Mechanical Engineering

by

KHIROD KUMAR MAHAPATRO

(Roll. No. 718027)

under the supervision of

Dr. P. Vamsi krishna
Professor
Department of Mechanical Engineering

DEPARTMENT OF MECHANICAL ENGINEERING
NATIONAL INSTITUTE OF TECHNOLOGY WARANGAL
WARANGAL-506004, TELANGANA, INDIA.
NOVEMBER -2022

DEPARTMENT OF MECHANICAL ENGINEERING
NATIONAL INSTITUTE TECHNOLOGY WARANGAL,
WARANGAL – 506004, TELANGANA (INDIA)

CERTIFICATE

This is to certify that the work presented in the thesis entitled "**Design and performance study of CO_2 based vortex tube cooling system in turning of Ti-6Al-4V**" which is being submitted by **Mr. Khirod Kumar Mahapatro (Roll No. 718027),** is a bonafide work submitted to the Department of Mechanical Engineering, National Institute of Technology Warangal in partial fulfillment of the requirement for the award of the degree of Doctor of Philosophy in Mechanical Engineering.

Dr. P. Vamsi Krishna
Supervisor
Professor
Department of Mechanical Engineering,
National Institute of Technology Warangal.

Prof. V. Suresh Babu
Chairman-DSC
Head of the Department
Department of Mechanical Engineering
National Institute of Technology Warangal

DEPARTMENT OF MECHANICAL ENGINEERING
NATIONAL INSTITUTE TECHNOLOGY WARANGAL,
WARANGAL – 506004, TELANGANA (INDIA)

DECLARATION

This is to certify that the work presented in the thesis entitled "**Design and performance study of CO_2 based vortex tube cooling system in turning of Ti-6Al-4V**" is a bonafide work done by me under the supervision of Dr. P. Vamsi Krishna, Associate Professor, Department of Mechanical Engineering, NIT Warangal, India was not submitted elsewhere for the award of any degree.

I declare that this written submission represents my ideas in my own words and where others' ideas or words have been included, I have adequately cited and referenced the original sources. I also declare that I have not misrepresented or fabricated or falsified any idea / data/ fact / source in my submission. I understand that any violation of the above will be a cause for disciplinary action by the Institute and can also evoke penal action from the sources which have thus not been properly cited or from whom proper permission has not been taken when needed.

.....
(Signature)

.....
(Name of the student)

.....
(Roll No.)

Date: .....

Dedicated

To

My Family

ABSTRACT

The use of titanium alloys in aerospace and manufacturing sectors has significantly increased due to their high strength-to-weight ratio, high corrosion resistance, and ability to maintain high strength at elevated temperatures. Titanium alloys are difficult to machine as they possess low thermal conductivity, high chemical affinity, low Young's modulus, etc. The energy utilized during the machining process is converted into heat and causes high heat generation in the machining zone. The generated heat is distributed among the chip, tool, and workpiece respectively. The distribution of heat depends upon various factors such as tool material, tool geometry, thermal conductivity of the workpiece, and cutting conditions. In titanium alloys, the maximum portion of the heat generated is directed to the tool (i.e. around 80%) due to low thermal conductivity of the titanium alloy. This in turn is responsible for the rise in temperature near the cutting edge of the tool. Further elevated temperatures will lead to rapid tool wear in titanium machining. The distribution of cutting temperature in titanium alloys results in an abrupt rise in temperature due to a smaller heat-affected zone near the cutting edge. Therefore, the area of contact decreases between the chip and the tool which causes further rise in the cutting temperature.

In this study, a new cooling method known as Vortex Tube Cooling System (VTCS) was used with CO_2 gas as a working fluid to provide the cooling effect in the machining zone. CO_2 gas was used due to its low response time to reach the desired temperature, low friction coefficient, and positive Joule Thomson coefficient. In VTCS high pressure CO_2 gas was cooled while passing through the vortex tube and turned to cold compressed gas. The vortex tube is a device that produces high and cold streams of gases from compressed gas. The cold compressed CO_2 gas at high pressure with low temperatures can easily provide a adequate penetration into the machining zone to reduce the cutting temperature.

In the first phase, a the single nozzle VTCS was developed and used as a source of coolant in the machining of Ti-6Al-4V. The flow parameters (coolant pressure, cold fraction, and coolant temperature) were varied in the machining process at constant machining conditions. The effect of flow parameters on responses such as cutting force, cutting temperature, and surface roughness was evaluated. It is observed that the cutting temperature and surface roughness are reduced with an increase in CO_2 gas pressure and cold fraction, whereas with a decrease in CO_2 temperature. Cutting force is increased with a rise in pressure, cold fraction, and with decrease in temperature

of CO_2 gas. Response surface methodology (RSM) was used to predict and optimize the cutting temperature, cutting force, and surface roughness respectively. The validation of the results was carried out by experimenting with optimized input parameters. The responses at optimized conditions in VTCS were compared with the dry cutting. The cutting temperature and surface roughness are reduced by 31% and 69 % by the use of VTCS whereas cutting forces are increased by 35% compared to dry cutting due to strain hardening effect and impulse force applied by the coolant.

In the second phase, the experimental setup of VTCS was modified and a single nozzle was replaced by two similar nozzles. The experiments were performed under the same condition with single nozzle VTCS and dual nozzle VTCS. It was observed that there was a drop of 15 % in cutting force in dual nozzle VTCS and changes in cutting temperature and surface roughness were lower than 5%. It indicates that the dual nozzle VTCS is effective in minimizing the cutting force. The experiments were carried out at constant cutting and flow parameters during turning at different levels of nozzle angle, nozzle position to tool-tip distance, and diameter of the nozzle. From the results, it was observed that an increase in nozzle angle reduced cutting force and surface roughness and increased cutting temperature. Decreasing the nozzle diameter reduced both cutting temperature as well as surface roughness but increased the cutting force. An increase in the distance between the tool and the tip of the nozzle, led to reduction in the cutting force is reduced and the other two are first reduced and then increased. The model was developed to identify the most impacting parameter which turned out to be the nozzle diameter.

In the third phase, the experiments were performed at different levels of flow parameters such as coolant pressure, cold fraction, and diameter of the nozzle. The responses included cutting force, cutting temperature, and surface roughness when the nozzle angle, nozzle position and machining parameters were maintained constant throughout the experimentation. From the results, low cutting force was observed at lower coolant pressure coupled with low cold fraction and higher nozzle diameter. The cutting temperature was minimized by increasing the coolant pressure and cold fraction and by decreasing the nozzle diameter. A better surface finish was observed at high coolant pressure and cold fraction and lower nozzle diameter.

The variation of cutting force, cutting temperature, and surface roughness with cutting speed, feed, and depth of cut were recorded. The nozzle and flow parameters were maintained

constant throughout the experiment. From the experimental results, the cutting force and surface roughness followed a similar trend that increased with decreasing speed and increasing feed and depth of cut. The cutting temperature increased with three variables. RSM model was developed for both experimental results to determine the most impacting parameters. It was found that coolant pressure and cold fraction are significantly affected flow parameters and cutting speed was found to be the most influential machining parameter.

In the final phase, the performance of CO_2 -VTCS was evaluated by comparing it with other alternate cooling methods unde optimum conditions. The optimum conditions of the most influential parameters were evaluated using RSM optimization. Responses such as cutting force, cutting temperature, and surface roughness CO_2 -VTCS were compared with other alternate sustainable cooling methods viz. dry condition, compressed air, compressed CO_2 gas, and air VTCS. The responses such as chip morphology, surface morphology, tool wear, and surface residual stresses were analyzed for both dual nozzle CO_2 -VTCS and dry environment. Uge of VTCS system reduced cutting temperature and surface roughness in Ti-6Al-4V machining compared to those of dry cutting. However, marginally higher cutting forces were observed in VTCS due to strain hardening phenomenon. The uges of VTCS reduced the width of segmented chips and decreased flank wear by up to 48% relative to dry cutting. The width of the crater wear zone was reduced slightly and notch wear was almost eliminated. Appearance of chip segments and accumulated edge fragments on the machined surface were greatly reduced. Compressive residual stresses developed on the machined surface in Ti-6Al-4V machining with dual nozzle CO_2 -VTCS.

Table of contents

List of tables

List of figures

Nomenclature

VTCS : Vortex Tube Cooling System

CO_2 : Carbon-di-Oxide

RSM : Response Surface Methodology

F_x : Axial component of cutting force

F_y : Radial component of cutting force

F_z : Tangential or main cutting force

BUE : Build up Edge

MQL : Minimum Quality Lubrication

CVD : Chemical Vapour eposition

CBN : Cubic Boron Nitride

FEM : Finite Element Method

LAM : Laser-Assisted Machining

NDM : Near Dry Machining

HPC : High Pressure Cooling

ADL : Aerosol Dry Lubrication

SEM : Scanning Electron Microscope

RHVT : Ranque-Hilsch Vortex Tube

CAMQL : Cooling Air Minimum Quality Lubrication

MQCL : Minimum Quantity Cooling Lubrication

EP : Extreme Pressure

AW : Anti-Wear

LN2 : Liquid Nitrogen

$SCCO_2$: Supercritical Carbon Dioxide

LCO_2 : Liquid Carbon-di-Oxide

NGMQL : Nitrogen Gas Minimum Quantity Lubrication

CFD : Computational Fluid Dynamics

COP : Coefficient Of Performance

L/D ratio : Length to Diameter Ratio

VTS : Vortex tubes arranged in series

VTP : Vortex tubes arranged in parallel

ANOVA : Analysis of Variance

TLBO : Teaching-Learning Based Optimization

GA : Genetic Algorithm

k : Thermal Conductivity

E : Young's Modulus

BHN : Brinell Hardness Number

IFOV : Instantaneous Field of View

IR : Infrared

XRD : X-ray diffraction

d : Inter-planar spacing for stressed samples

d_0 : Inter-planar spacing for unstressed samples

P_c : Pressure of cold fluid

P_h : Pressure of hot fluid

P_{atm} : Atmospheric Pressure

T_h : Temperature of hot fluid

T_c : Temperature of cold fluid

γ : Specific heat ratio of the gas

η_{is} : Isentropic efficiency

Q_r : Rate of cooling

W : Work Input

C_p : Specific heat of the gas

$\dot{m}_i$: Mass flow rate of the gas at inlet

$\dot{m}_c$: Mass flow rate through the cold end of the vortex tube

$\dot{m}_h$: Mass flow rate through the hot end of the vortex tube

A : Surface area exposed to the fluid in m^2

h : Convective heat-transfer coefficient in w/m^2-^oC.

ṁ : Mass flow rate of CO_2 gas

µ : Coefficient of Friction

T_c : Coolant Temperature

P_c : Coolant pressure

C_f : Cold Fraction

Ra : Average surface roughness

T_m : Cutting temperature

ρ : Density of the coolant

v : Velocity of the coolant

θ : Nozzle Angle

Tg : Temperature of coolant supplied to the machining zone

Nu	: Nusselt number
Re	: Reynolds number
Pr	: Prandtl number
L	: Characteristic length
MRR	: Material Removal Rate
f	: Feed rate
r	: Nose radiu

1 INTRODUCTION

1.1 Introduction

Nowadays, the use of titanium alloys in the aerospace and manufacturing sectors has significantly increased due to their high strength-to-weight ratio, high corrosion resistance, and ability to maintain high strength at elevated temperatures. Among all the manufacturing processes, machining holds around 30% stake out of the total fabrication activities. It is worthy of note that the surface finish and dimensional accuracy of the specimen are affected by the machining process, workpiece material, tool material, lubricating conditions, and cutting parameters. Characterized by its commendable dimensional accuracy and superior surface finish, machining is extensively employed in aerospace and engineering applications. With the ever growing demand for titanium alloys, it is the need of the hour to develop an effective and capable machining technology. Additionally low thermal conductivity of titanium alloys further complicates the machining operation. Though conventional machining has proven its capability all these years, it is losing its effectiveness in the modern engineering world. One such situation is the lack of an efficient and sustainable mechanism that can remove heat generated in the machining. Cutting fluids have been a promising solution so far but are currently losing their edge due to straight rules posed by the environmental protecting agencies. It becomes imperative to develop a novel and an efficient cooling system for effectively machining materials such as titanium alloys.

1.2 Machining

Traditionally different machining processes such as turning, milling, boring, grinding, shaping, etc. have been used to remove the material from the workpiece to obtain the final product. In the machining process, the cutting tool plays an important role as it removes material in the form of chips by shearing and tearing action of cutting edge. In this process, a large amount of power is consumed which also gets converted into heat. The heat distribution occurs among chips, cutting tool, and workpiece in machinining process. Accordingly, three heat zones are identified where the heat generation occurs. Figure 1.1 showcases the existence of these three zones viz. primary deformation zone, secondary deformation zone and tool work interface. Out of these, plastic deformation takes place only in two specific zones namely the primary and secondary

deformation zone. The rubbing action takes place along the cutting tool rake and flank faces with the chip and workpiece in secondary deformation and tool work interface [1].

The main reasons for heat generation during machining would be work done during plastic deformation, friction between chip and tool rake face (as the chip flows over it), and rubbing of the machined surface (workpiece)on the flank face. The heat generation causes increase in cutting temperature that leads to decrease in the tool life [2]. It also causes the tool wear and leads to a poor surface finish of the machined component. Because of the high temperature, the chips stick to the cutting tool edges, and the workpiece leads to form the built-up edge (BUE) and increases the surface roughness of the machined component. To avoid these, it is necessary to remove the heat generation in the machining zone which is done by supplying cutting fluids into the machining zone. Cutting fluids minimize the heat generation at the primary and secondary zone and also carry away the generated heat, hence cooling the machining zone. The lubricating action of cutting fluid reduces the friction between the mating parts and thereby minimize the heat generation due to rubbing action. The quality of the machined surface is affected by the type of cutting fluid and its method of application. Cutting force is one of the influential factor concerning the quality of the surface. Higher cutting forces in machining leads to the surface finish deterioration. To estimate the quality of the machining it is necessary to study the cutting temperature, cutting force, tool wear in machining, surface roughness, residual stresses of the machined component [3].

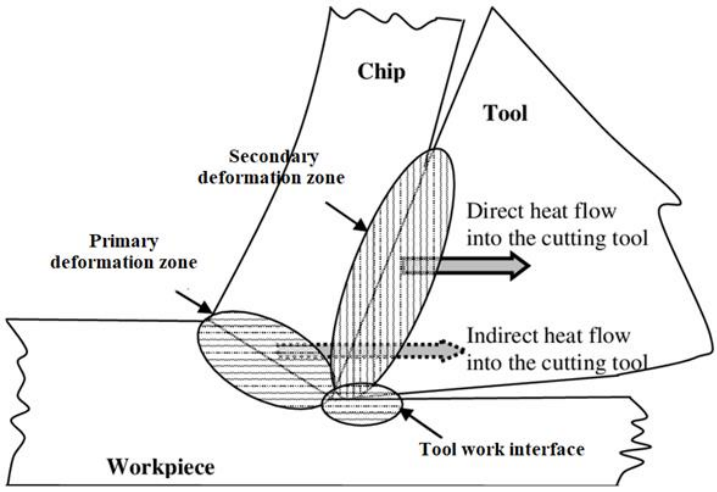

Figure 1.1: Sources of heat generation in machining [1]

1.3 Cutting temperatures

Cutting temperature is the most influential parameter during the machining that directly influences the rate of tool wear and surface finish. A large amount of energy is used during the machining process, which causes higher heat generation in the machining zone. At the contact area of the chip and tool, the workpiece material which is in contact with the cutting tool is sheared and the face of the tool is strained after the conversion of work into heat. The heat generated at the rake face is transferred to the cutting tool through conduction. The amount of heat transferred depends on the thermal conductivity of the material. It is influenced by cutting conditions and cutting fluid used in the machining process [4]. The generated heat is distributed among the chip, tool, and workpiece respectively. In general, a large portion of (around 70-80%) the generated heat is transferred to the chips which are flowing away from the machining zone. The total heat carried by the workpieces is 10% to 20% of the total heat generated and 5% to 10% of heat is flowing into the tool [5]. In titanium alloys, heat distribution is different and the maximum portion of the heat generated is directed to the tool (i.e., around 80%) due to the low thermal conductivity of the titanium alloy this causes further rise in temperature near the cutting edge of the tool. Heat distribution in machining zone depends upon various factors such as tool material, tool geometry, thermal conductivity of the workpiece, cutting conditions, etc. By providing sufficient clearance angle, maximum portion of the heat is directed towards the workpiece and also avoids rubbing the tool against the workpiece. The contact between tool and workpiece increases the tool flank wear causing heat generation and thus leading to catastrophic failure of the tool. This effect will lead to rapid tool wear, which is commonly observed during the machining of Titanium alloys [6]. Studies show that the distribution of cutting temperature in titanium alloys results in an abrupt rise of temperature due to smaller heat-affected zone near the cutting edge. Therefore, the area of contact decreases between the chip and the tool which causes further rise in the temperature. The cutting parameters in machining operation are also influence the cutting temperature since higher cutting speed, feed rate, and depth of cut lead to higher cutting temperature. This can be minimized by proper selection of cutting fluid, cutting tool, cutting condition. Reduction in cutting tempaerature enhances the tool life and improves the quality of machined surface with a reduction in tool wear [7].

1.4 Cutting forces

Comprehensive analysis of cutting forces is necessary to select proper parameters in machining. Power consumption, machinability, online condition monitoring of cutting tool and machine tools can be estimated by using cutting force analysis. The cutting force is resultant of forces acting in three directions, which are F_x, F_y, and F_z, as shown in figure 1.2. The force in the direction of primary motion is known as tangential or main cutting force (F_z) is around 70-80% in the total cutting force and it is used to measure the power consumption in machining. The forces perpendicular to F_z are axial component F_x (acts in the direction of tool transverse) and radial component F_y (acts along tool shank). F_x and F_y are less significant in power consumption but a higher F_y value leads to dimensional inaccuracy and vibration during machining [8]. In machining, mechanical and thermal stresses are developed and these effect the performance of machined component. To minimize the failure or breakage of the tool, it is crucial to identify the tool behavior with respect to the load acting on it. Therefore, the analysis of tool wear, i.e. measuring and analyzing the mechanical load on the tool, is useful for improving the cutting process, selection of geometry of the cutting tool, coating requirement of the tool, coolant requirement etc. [9]. Analyzing the cutting forces during machining is beneficial because it provides the information for machinability of material and selection of tool, identifying overload, chatter vibration, and tool conditions.

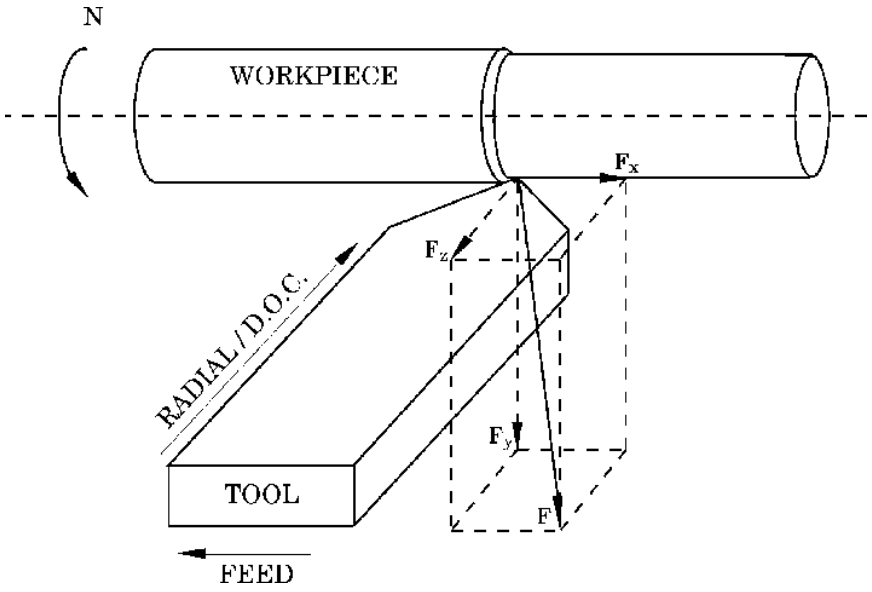

Figure 1.2: Cutting forces components in turning operation [8]

1.5 Surface roughness

Surface roughness is one of the critical factors in machining because it influences the fatigue strength, corrosion resistance, service life, and reliability of the component. Good surface finish improves the performance and durability of the component. Wear will be higher at the rough surface because of the higher coefficient of friction. The surface roughness values during machining help in identifying the tool condition such as tool wear, tool breakage etc. The surface finish of the machined surface mainly depends upon the cutting conditions, cutting tool and workpiece variables, lubrication [10].

Cutting conditions: The surface quality of the machined surface is affected significantly by machining speed, feed, and depth of cut. Cutting forces are high at lower cutting speed and the formation of BUE by workpiece material on the cutting tool is speeded up. On the other hand, due to increase in temperature at high cutting speed, the formation of BUE and the frictional stress reduces at the rake face of the tool. BUE formation does occur at a very small speed and low temperature. That's why surface quality is positively influenced by both of the above mentioned conditions [11]. Feed directly influences the surface quality as compared to the depth of cut. An indication of surface roughness which is peak to valley height is proportional to the square of feed per revolution. Cutting forces and deflections are altered by the depth of cut and higher depth of cuts produces higher waviness on the machined surface.

Cutting tool variables: Quality of machined surface is significantly influenced by material of cutting tool, tool geometry, hardness, frictional behavior, and toughness of the cutting tool material. A lower coefficient of friction between the mating parts improves the quality of the surface. High rake and relief angles provide a better surface finish without affecting the cutting edge of the tool. A high rake angle cutting tool reduces the cutting force thereby minimizing the peak to valley height of the machined surface. By providing adequate relief angles, the rubbing action between the tool and workpiece can be minimized. It also reduces the formation of BUE. The surface roughness can be reduced by providing sufficient nose radius to the tool which further decreases the feed marks on the finished surface. A better surface is produced by increasing the side cutting edge angle by improving the chip flow and by decreasing the true feed. Lower end cutting edge angle decreases the height of feed marks which leads to better surface finish [12].

Variables of workpiece material: Surface quality is influenced by chemical composition, metallurgical uniformity, microstructure, and hardness of the workpiece material. A good surface finish can be attained with the help of high hardness, fine grain size, and low ductility. Metallurgical consistency of the workpiece material is beneficial for maintaining uniformity in the finished machined surface. The irregular wavy pattern on the machined surface is caused by longer and slender workpieces due to static and dynamic forces. Thus, better surface quality can be obtained by using short length workpiece clamped rigidly to the machine tool's chuck [13].

Cooling and lubrication: Cooling the machining zone would hamper the tool wear thereby improving the tool life. Surface finish is indirectly affected by lubrication which reduces the friction between tool-chip and tool-workpiece interfaces. Lubricant plays a vital role in attaining the required dimensional accuracy and surface quality in the machining process. If the coolant possesses higher penetrating ability, then employing larger amounts of such coolant can result in a better surface finish [14].

1.6 Tool wear

The loss of material from the interacting surfaces of the tool during machining is termed as tool wear. Some of the features related to the phenomena of tool wear are, unable to cut the material effectively, spoiled surface finish, deformation of cutting tool edge, vibrations, increase in cutting force, etc. Resharpening of the tool is required after a certain degree of wear and sharpness of cutting tool affects the surface quality, dimensional accuracy and extent of machine tool vibrations [9]. The different tool wears are described in th fiure 1.3 .Different mechanisms of tool wear are [3]:

- **Adhesive wear:** It occurs due to very strong bonding between two mating surfaces owing to welding of surface asperities when they are in close contact. Adhesive wear takes place at low cutting speeds and is associated with shear plane deformation.
- **Abrasive wear:** It occurs due to loss of material when hard surface or particles rubbed on soft surface.
- **Diffusion wear:** It occurs due to the chemical affinity between the mating surfaces. The atoms from one surface diffuse into another and cause material loss which is predominant at high cutting speeds.

- **Plastic deformation:** It occurs because of overstressing of the tool material. The cutting tool can be deformed due to high compressive stress acting on the tool rake face during the machining process.
- **Fatigue wear :** It occurs due to strain induced on the surface by number of repeated cycles of load .

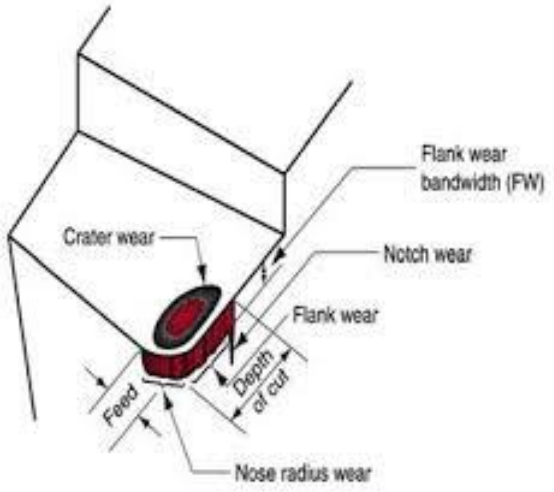

Figure 1.3 :Different types of tool wear in machining [9]

Flank wear, crater wear, and nose wear are most generally observed wears in machining. The flank wear is mainly due to abrasive and adhesive wear, while crater wear is due to diffusion. Flank wear can be measured in terms of length of wear land which increases with time. Crater wear is measured in terms of the depth of the crater. The crater is normally formed at some distance from the cutting edge and the chances of its formation are high at a higher temperature. Nose wear is considered as separate part of the tool wear. It wears out the tool corner which is the mating part of the flank and face and it occurs due to the combined effect of crater wear and flank wear [15].

1.7 Residual stress

In machining, the residual stresses are one of the most important responses because of their influence on the durability and performance of the component. Residual stresses are most significant in the conditions where surface finish and dimensional accuracy take high priority as in like aircraft engines. They are also affected by cutting parameters and cooling conditions in the

machining. Compressive residual stresses are developed at higher speed, feed, and depth of cut. Magnitude of compressive residual stress increases with increase in these parameters. X-ray diffraction technique is used for measuring the residual stresses. Strain in the metal's atomic crystal lattice is measured in this technique and later residual stresses are calculated from the strain values [16].

Residual stresses are produced maybe because of localized yielding, surface hardening and shot peening, deformation gradients, etc. Among these factors deformation gradients play a crucial role in developing residual stresses in machining which are generated by a thermal gradient. In preventing the failure of the component residual stresses play an important role. Residual stresses may be tensile on the surface and compressive below the surface or vice versa. The tensile stresses prevent crack nucleation, on the other hand it increases the service stress which can lead to component failure. Whereas compressive stress reduces the service stresses and enhances both life and performance of the component. When tensile stress is applied to a component that is already experiencing residual stresses, it increases the magnitude of the stress thus making a component unreliable. Sometimes the residual tensile stresses are sufficient to cause corrosion cracking. The effect of applied tensile stress can be reduced due to compressive residual stress on the surface which improves fatigue strength and resistance to corrosion cracking in most cases. The state, distribution, and amplitude of residual stresses near the surface layer are mainly influenced by edge preparation, tool geometry, lubrication method, tool wear, cutting parameters as well as the physical properties of the tool [17].

1.8 Chip morphology

In machining, the mechanical behavior such as cutting temperature, surface roughness and tool wear are directly affected by the chip formation. The chip geometry and the way in which the chip stays in contact with the cutting tool affect the response parameters. Vibrations are generated when either continuous or discontinuous chips are in contact between the flank and rake interface. It may lead to poor surface quality accentuated wear, and chatter marks on the surface. Chip formation mechanisms also influence the chip tool contact length on rake face and crater wear evaluation. Chip morphology is closely related to machining efficiency and the surface integrity of the machined product. The variables that mainly affect chip morphology are cutting speed, feed,

depth of cut, workpiece material properties, lubrication and cooling conditions. Therefore, it is important to recognize the nature of the chip based on the variation of the cutting parameters [18].

To understand the tool wear and machinability while machining titanium alloys, chip morphology and segmentation are essential. Different chip morphologies can be observed under different cutting speeds, due to changes in flow localization in the cutting zone and crack initiation and propagation. The thermomechanical behavior at the interface of the tool and the part is strongly influenced by the morphology of the chip which also influences the tool life. It is important to study the mechanics of chip segmentation and its effects on machinability to increase tool life and productivity [19].

Serrated chips are observed in machining of Ti–6Al–4V at wide range of cutting speeds. The chip is divided into segments by bands that are very thin with localized shear strain. The chip segmentation can be related to the vibration encountered in the machining process. Even though the mechanisms of chip formation are not yet fully clear, two predominant theories attempts to describe the occurrence of chip segmentation. The first relates to crack initiation and propagation with the second relating to adiabatic shear favored by the lower thermal conductivity of the workpiece. The chips obtained are regularly serrated in shape and frequency at lower speeds. However, increasing the speed can lead to severe deformation. At a lower depth of cut, random cracks may appear and these cracks can get wider as the depth of cut increases [20].

1.9 Cutting fluids

Cutting fluids can regulate cutting force, cutting temperature and surface finish to a considerable extent. To obtain a better surface quality and better dimensional accuracy in the machining of alloys, cutting fluids are one of the major choice of manufacturers [21]. The main purpose of using cutting fluids is to cool the machining area, reduce friction and surface roughness, reduce thermal distortion, prevent corrosion and improve tool life. Important properties of cutting fluids are stability, non-toxicity, and compatibility with other lubricants and machine elements. Additives in the cutting fluid react with the workpiece material surface, resulting in the formation of low shear film to withstand high temperatures. Chips shear easily during sliding because welding between the chip and the tool is limited. Another function of cutting fluid is to reduce the amount of heat generated during rubbing and this is called the lubricating action. Certain additives such as fatty acids, chlorine, sulfur, and phosphorus are added to cutting fluids to reinforce the

lubricating action. The use of cutting fluids increasing day by day because of the increasing demand for machined components in manufacturing industries. The use of cutting fluids increases the cost of machining and environmental pollution and adversly affects the health of the workers. Disposal of these conventional cutting fluids after usage was difficult because it is contaminated with metallic chips and chemicals which affect aqua life [22].

1.9.1 Cooling methods alternative to conventional cooling

The limitations of cutting fluids make it necessary to develop a new cooling system as an alternative to the conventional methods. the main alternatives to conventional methods are dry cutting, compressed air cooling, Minimum quality lubrication (MQL), Cryogenic cooling, Solid lubricants, nanofluids, gaseous refrigeration [21] .

In dry machining process, the machining is performed without supplying any cutting fluid into the machining zone. The absence of cutting fluids in machining has led to high heat generation adhesion mechanisms, an increase in friction between tool and workpiece, and poor chip evacuation [23]. All these factors decrease the machinability, especially in titanium alloy machining where a large amount of heat generates due to its inherent properties. Compressed air cooling in which the high pressure air is supplied into the machining zone removes some portion of the heat and reduces the cutting temperature. However, the lack of lubrication effect in compressed air cooling produces high coefficient friction in the machining zone. In MQL, mixture of compressed air lubricant is used as a coolant and supplied into the machining zone which provides better results compared to dry and compressed air cooling. Consumption of cutting fluid reduced drastically by around 10000 times than the conventional methods [24]. Cryogenic cooling is a method in which cutting fluid is supplied at a sub-zero level to reduce the machining temperature. The gases like. Nitrogen, carbon dioxide, oxygen, helium, etc., are used as cryogenics coolants. Gases that exist in the environment are converted into liquid form and are evaporated and converted into gases at room temperature [25]. Solid lubricants are in the form of fine powders or composite materials and applied between the mating zone. This reduces the friction, minimizes the wear, and minimizes the surface damage. The environmental friendly, non-toxic, and biodegradable nature of solid lubricant makes it more attractive to use as an alternative to conventional methods. Graphite, molybdenum disulfide, calcium fluoride, and boric acid are generally used as solid lubricants [7]. Nanofluids are a mixture of conventional cutting fluids and

nanoparticles. The addition of nanoparticles enhances the thermal conductivity of the cutting fluid thereby improving the heat transfer rate. Nanofluids require relatively less quantity than conventional cutting fluids for the same performance [26]. In the gaseous refrigeration system, the compressed gas is cooled by using any refrigerating system and supplied in the machining zone. The refrigeration effect can be produced in different ways like liquid nitrogen cooling, vapor-compression refrigeration, cooling by adiabatic expansion, or by using a vortex tube [27]. In this context, a gaseous refrigeration system is used for minimizing the heat generation in the machining zone and the cooling effect is produced by the vortex tube cooling system.

1.10 Vortex tube cooling system (VTCS)

In VTCS, the refrigerated or chilled gas is produced and it is used to carry away the heat generated during machining. It includes a high-pressure gas source, vortex tube, and an effective nozzle system. The gas with the required pressure is supplied into the vortex tube which develops a stream of cold gas. The cold stream of gas is forced into the machining zone by a suitable nozzle that carries away the heat generated.

1.10.1 Vortex tube

The vortex tube is a device that separates high pressure gas stream into two steams of high temperature and low temperature. It consists of a generator surrounded by annular space and when the high-pressure gas contacts the nozzle of the generator, a portion of pressure is lost which in turn creates a spin at a higher velocity. The maximum portion of the air moves towards the hot end in the form of a vortex and is maintained at the walls of the vortex tube because of centrifugal force. The amount of air leaving through the hot end valve depends upon its position and some portion of the air is restricted to pass through it and forced to the cold end side (inner vortex). Figure 1.4 shows the working principle of the vortex tube. The ratio of the volume flow rate at cold and to the total gas supplied is known as the cold fraction. By varying the cold fraction the amount of cold gas out from the vortex tube can be controlled. The vortex tube is generally used to cool electrical components and spot cooling applications [28].

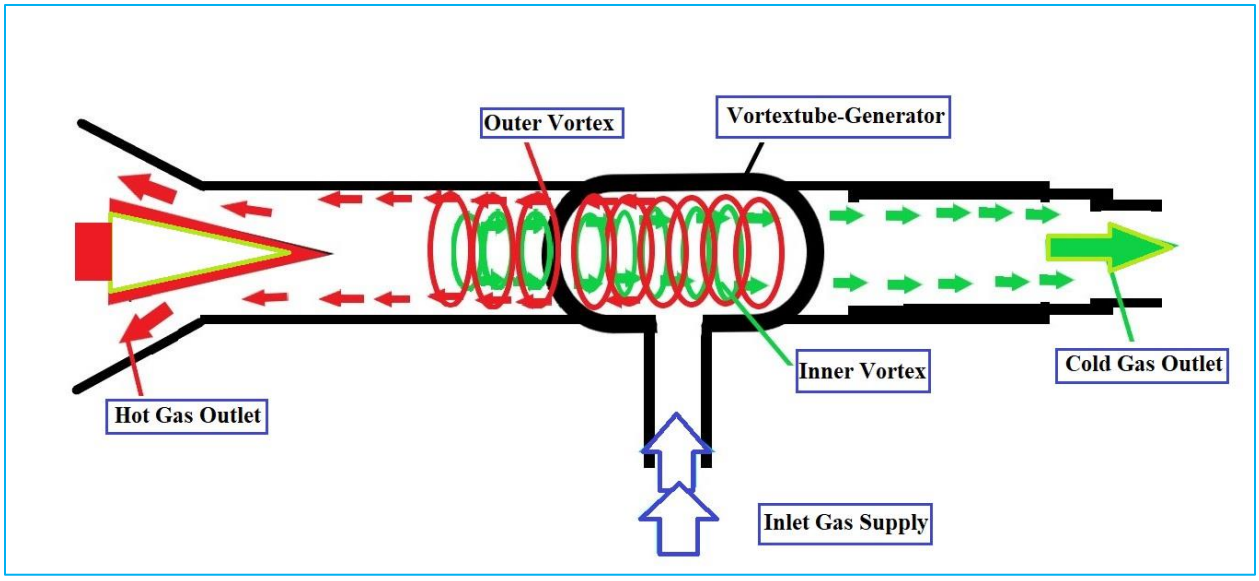

Figure 1.4 :Vortex tube – Working principle

1.10.2 Working fluid in the vortex tube

Air is the common working fluid used in vortex tube due to abundant availability in the atmosphere. In manufacturing industries, compressed air is used for different applications because there is no need of maintaining an additional setup for supplying compressed air into the vortex tube. The temperature drop in the vortex tube depends on the coolant pressure and cold fraction. For air, the values of temperature drop are well established for different cold fractions and pressures (Figure 1.5). Gases like nitrogen, and CO_2 also can be used as a working fluid but usage of these gases is limited. The research articles related to other gases except air are limited. But these gases required an additional setup to store high-pressure gas. Alongside usage of nitrogen CO_2 gas in vortex tube providing better machinability.

This study CONSIDERS the effect of incorporation of vortex tube cooling system on machinability of the Ti-6Al-4V. The variableS includes coolant pressure, cold fraction, coolant velocity coolant temperature, etc. Machinability is studied by analyzing the response parameter such as cutting temperature, cutting force, surface roughness, tool wear, residual stress, chip morphology, etc. The effectiveness of VTCS is analyzed by comparing the results with other cooling methods. The best combination of input parameters is obtained in the Ti-6Al-4V machining under VTCS environment.

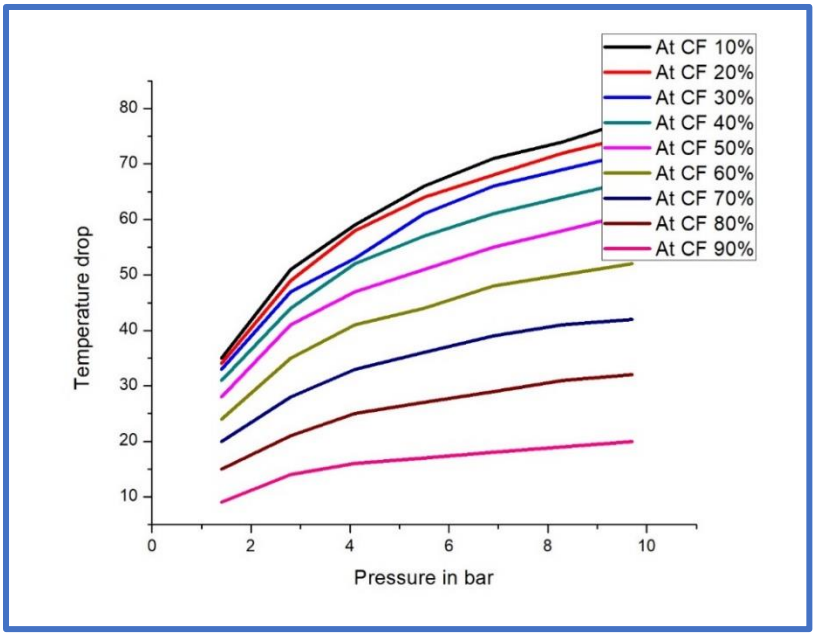

Figure 1.5 ***:****Variation of temperature for pressure and % cold fraction in the vortex tube for [28]*

1.11 Thesis outline

Chapter 1 Outlines the problems associated with the machining of difficult to cut materials like Ti-6Al-4V alloy with conventional machining. The importance of parameters like of cutting force, cutting temperature, surface roughness, tool wear, residual stresses, and chip morphology of machined components in machining is presented. Then, a brief introduction of the VTCS process is discussed along with its components.

Chapter 2: this chapterReviews the previous research work done in machining under dry cutting, MQL, pressurized gas, CO_2 gas, and VTCS process. The effect of cooling medium on the machining of Ti-6Al-4V is reviewed at different machining conditions.

Chapter 3: Deals with the experimental procedures in dry cutting and VTCS. Various types of equipment, tools, measuring devices used and their specifications are presented in this chapter.

Chapter 4: Discusses the results of preliminary experiments and also the introduction of a single nozzle vortex tube cooling system. The effects of flow parameters on machinability ARE examined and the same parameters are optimized.

Chapter 5: This chapter explores the dual nozzle vortex tube cooling system and studied the influence of nozzle parameters, flow parameters and machining parameters on the machinability

of Ti-6Al-4V. The effectiveness of dual nozzle VTCS is described in terms of response parameters by comparing the results with other alternative cooling methods.

Chapter 6: This chapter presents the overall observations, conclusions, and also the scope of future works.

2 LITERATURE REVIEW

2.1 Introduction

In this section, the literature related to the machining of Ti6-Al4-V such as issues arising during machining, properties of the alloys, the effect of coatings etc. are discussed. The use of cutting fluids in machining and the subsequent developments related to machining are also covered. Alternative methodologies concerning the cutting fluids such as dry cutting, MQL, high pressure coolants, cryogenic coolants, CO_2 cooling and vortex tube cooling have been listed and explored.

2.2 Machining of titanium alloy

Titanium is one of the most sought-after materials for engineering applications. However, it is often associated with machining related issues. Ezugwu et al. [5] discussed the major problems encountered and reviewed the various cutting tools used in titanium alloy machining. It was found that the straight tungsten carbide is more efficient compared to other tool materials. It is also found that ceramics and CVD coated carbides should not be used as cutting tools because of their properties like high reactivity with titanium alloy, poor thermal conductivity, and lower fracture toughness. Ezugwu et al. [29] conducted experiments to assess the performance of different Cubic Boron Nitride (CBN) tool grades in turning Ti-6Al-4V (IMI 318) alloy at higher cutting speed using different cutting fluids. The studies showed that the uncoated carbide tools are better than CBN tools in terms of bond strength and tool life. The use of uncoated carbide tools provided a better surface finish and longer tool life compared to the usage of the CBN tool.

Parida et al.[30] studied the machinability of titanium alloys at different temperatures (250°C, 350°C, and 600°C) along with room temperature. Finite element method (FEM) analysis was done on Ti-5553 and Ti-6Al-4V alloys at various cutting speeds. In both cases, a change in chip morphology and reduction in cutting forces was observed at higher temperatures compared to room temperature. The thrust and cutting forces were higher in Ti-5553 compared to Ti-6Al-4V at all temperatures. It was also observed that higher temperatures reduced the chip thickness and increased the contact between tool and chip. Leak et al.[31] studied the micro-textured tool effects during machining of titanium alloy under dry cutting using a 3D FE model. These textures include grooves that are parallel, perpendicular, and diagonal to the main cutting edge. The distribution of

forces, stress, temperature, and wear rate were predicted under these micro-textured conditions. Better stress distribution and a reduction in the cutting force were observed using perpendicular and diagonal micro-textured tools compared to parallel textured tools. Rashid et al. [32] investigated the behavior of Ti–6Cr–5Mo–5V–4Al workpiece in terms of cutting force and cutting temperature using Laser-Assisted Machining (LAM) which reduces the cutting forces required for machining by softening the workpiece and increasing metal removal rates. It was found that LAM reduces the cutting force significantly compared to conventional methods within a certain range of speed and feed. Dandekar et al. [33] studied the tool life and material removal rate in LAM and hybrid machining using TiAlN coated carbide tool for titanium alloy. It was found that LAM showed better results in the range of low to medium cutting speeds (60-107 m/min), in terms of machinability while hybrid machining was better from medium to high cutting speed (150–200 m/min). In hybrid machining, Tool life was improved by two to three times over conventional machining at cutting speeds of 200 m/min with TiAlN coated carbide cutting tool. The above discussed works commonly conclude that cutting temperature holds a significant impact over the machinability of titanium either directly or indirectly.

2.3 Cutting fluids

The advent of cutting fluids has certainly changed the machining science altogether for good. Sharma et al.[7] reviewed the usage of air and water vapor as cutting fluids by comparing it with other cooling techniques like NDM (Near Dry Machining), HPC (High Pressure Cooling), cryogenic cooling, etc. The flank wear, chip formation, lubrication, friction, MRR, etc were considered as responses. It was found that water vapour shows better results in terms of lubrication and water as a coolant removes 2.5 times more heat compared to oils. Sujan et.al [21] classified the cutting fluids based on their state and type as shown in Figure 2.1. moreover, the drawbacks of using conventional cutting fluids were elaborated including environmental damage and negative effect on workers' health. Busch et al. [34] observed the behavior of different cooling strategies such as CO_2 and ADL (Aerosol Dry Lubrication) to reduce the thermal load and friction during machining of Ti-6Al-4V and Inconel 718. The cooling strategies highly influence the quality of the surface. It was concluded that aerosol as a coolant was better in terms of performance but the only drawback was high instability and it can be stabilized by supplying CO_2. Shokrani et al. [22] discussed the difficulties arising due to the usage of cutting fluids in the machining of hard-to-cut materials like nickel and titanium alloys and reviewed different cooling approaches alternative to

cutting fluids like Dry cutting, MQL, Cryogenic machining, and Air cooling. And also, discussed their applications, advantages, and limitations.

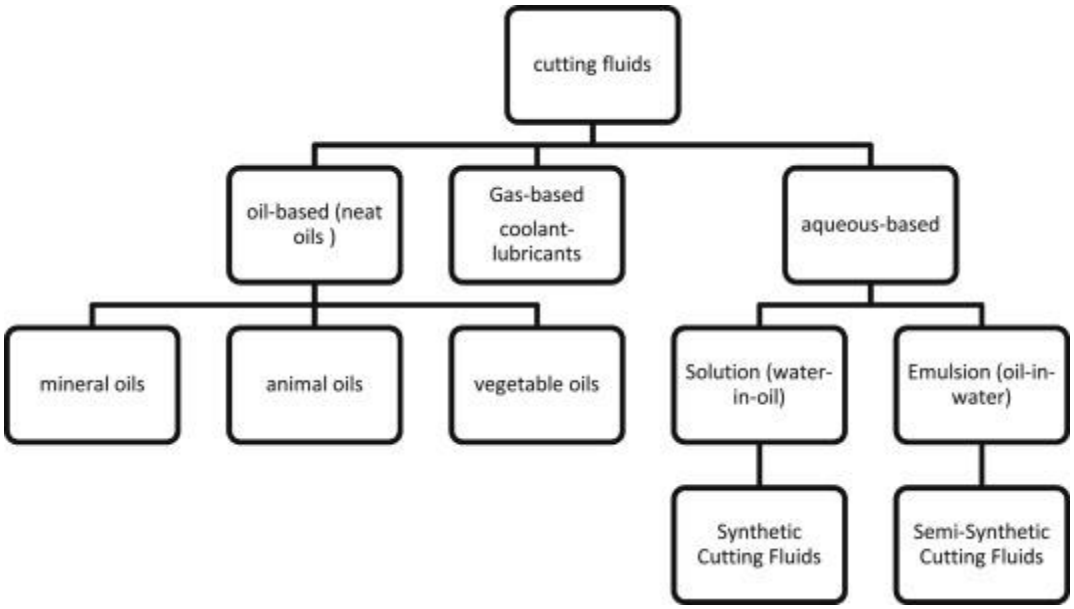

Figure 2.1:Classification of cutting fluids

2.4 Dry machining

There are several instances where machining can give better results even in the absence of any cutting fluid. Such a group of operations can be termed dry machining. Liew et al. [35] discussed the performance of dry, MQL, HPC, nanofluid, and cryogenic environments for different materials in terms of tool wear, environmental effects, and product quality and cost. It was found that dry turning is more effective in turning the alloys of steel and cast iron in terms of cost and environmental aspects compared to other environments. But it is ineffective in terms of stress profile, compressive residual stress, and surface finish. Debnath et al. [36] investigated the effects of different cutting fluids while machining and compared them with a newly developed vegetable oil-based coolant. It was found that the dry cutting technique is more environmentally friendly compared to other techniques except for drilling operations. The limitations of dry cutting include abrasion of the tool, diffusion, high friction, higher heat generation in the machining zone, etc. Shokrani et al. [37] performed an experimental study to analyze the power consumption in Ti-6Al-4V machining. It was found that dry cutting consumes 40% and 1.5% less power compared to flood cooling and cryogenic LN2 respectively. But in terms of specific machining energy, dry cutting gives poor results because of lower cutting speeds as the higher cutting speeds generate

more amount of heat. Jawaid et al. [38] studied the surface integrity in the machining of Ti-6Al-4V under a dry environment and cemented carbide tool was used as the cutting tool. It was found that severe plastic deformation and tearing of machining surfaces were identified through SEM images. Despite all the merits and flaws, dry cutting was ineffective when used for titanium alloys due to their low thermal conductivity.

2.5 Minimum quantity lubrication

Many a time the quantity of the lubricant seems to be the issue rather than the lubricant itself. MQL is a lubrication technique that involves employing only the minimum needed lubricant quantity with no excess at all. Sharma et al. [7] reviewed the effects of different cooling environments like dry machining, NDM, HPC and solid lubricants during machining. It was found that usage of MQL results in reduced cost, improved surface quality, and reduced coolant usage. It was also stated that using vegetable oils as lubricants provided better results compared to mineral oils in terms of cost, health, safety, and environment. Singh et al. [39] performed a turning operation on pure Titanium alloy using MQL and RHVT MQL as a cooling medium by varying cutting conditions and taking Surface roughness, cutting force, tool wear, and consumption of power as responses. A reduction of 15% to 18% in the surface roughness was obtained and also the tool wear was reduced significantly while using RHVT MQL compared to MQL. Gupta et al.[40] performed a turning operation on grade-2 titanium alloy under MQL environment considering cutting forces, tool wear, and surface quality as responses at different levels of inputs. The effect of individual parameters on response was discussed and optimized conditions were obtained using RSM and found that lower cutting speeds, lower feed rates, and higher angles of approach give better outcomes.

Su et al. [27] performed turning of Inconel 718 Nickle alloy and milling of AISI D2 tool steel under different cooling environments like MQL, dry, cool air, and cooling air and MQL (CAMQL) to investigate the tool wear, the shape of the chip, and surface quality. A new cooling method was used to produce a cooling effect which was presented in Figure 2.2. It was found that in the case of turning of Inconel 718, cooling air and CAMQL provided better results whereas, in the case of milling of AISI D2, cool air has shown better results. Pereira et al. [41] performed milling operation on Inconel 718 alloy under different environments such as emulsion, MQL, and cryoMQL (where CO_2 gas is used as a working fluid).it was found that cryo MQL improved the

tool life by 57% and 12% when compared with emulsion and MQL environments respectively. However, there was 11% increase in cutting force was observed due to strain hardening.

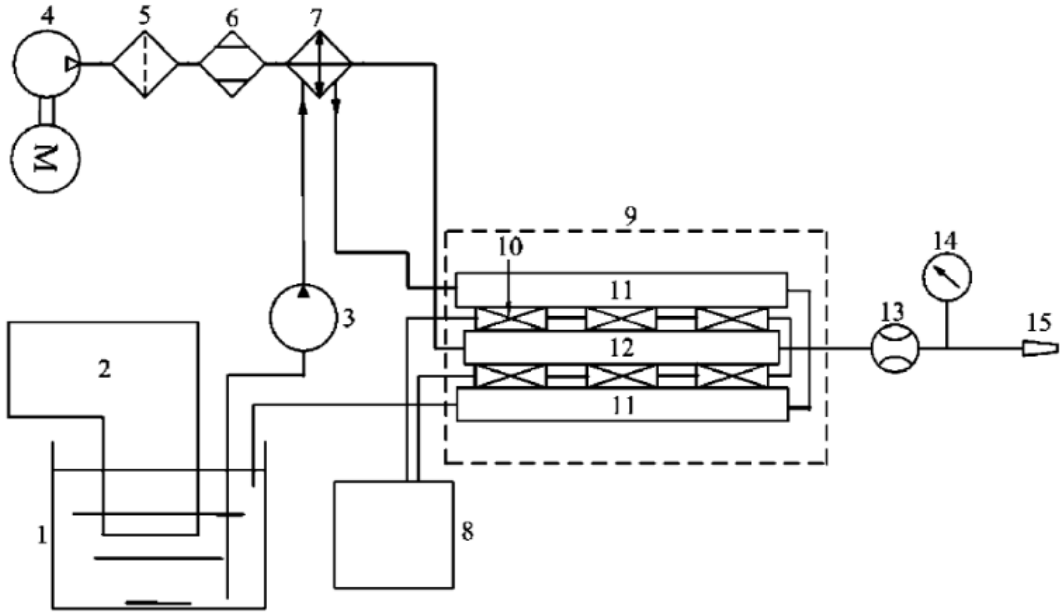

Figure 2.2 : Schematic diagram of the new cooling gas equipment

1, water container; 2, vapor-compression refrigeration system; 3, water pump; 4, compressor 5, filter; 6, drier; 7, heat exchanger; 8, control box; 9, semiconductor refrigeration system; 10, thermopile; 11, heat absorber; 12, cooler; 13, flow meter; 14, pressure gauge; 15, nozzle.[17]

Maruda et al. [42] examined the tribological properties of AISI 1045 steel after machining under dry, MQL, minimum quantity cooling lubrication (MQCL), extreme pressure- MQCL (EP+MQCL), and MQCL+EP/AW (anti-wear) conditions. it was found that MQCL+EP/AW reduced the tool wear by 16% and 27% compared to MQCL and dry machining. It was also found that both temperature and friction coefficient were reduced in the case of MQCL+EP/AW compared to other methods. Shokrani et al. [6] performed an end milling operation on Ti-6Al-4V under hybrid cryogenic MQL at different cutting speeds. The tool life and productivity were considered as responses and compared with different cooling techniques like flood cooling, MQL and cryogenic cooling. It was found that the hybrid cryogenic MQL technique improved the tool life 30 times and the productivity by 50%. The alternative methods used in literature is presented in Table 2.1.

Table 2.1: Alternative cooling system used in literature

Authors	Field of study	Contribution
Liew et al. [35]	• Dry cutting • Near dry / MQL • Cryogenic cooling • High pressure coolants • Nanofluids	It was found that the MQL technique was more environmentally friendly compared to other techniques as it can be used to supply both coolant and lubricant. The amount of coolant was less compared to the conventional machining which reduces the health hazards and environmental pollution that occurred due to the usage of cutting fluids.
Adam Race et al. [43]	• Dry cutting • Near dry / MQL • flood cooling	Studied tool wear, surface quality, energy consumed during milling of carbon steel under dry, and MQL environments. It was found that these techniques provide better outcomes compared to flood cooling along with this, the cost of operation and environmental pollution can be minimized. The cost of usage of MQL was reduced by 50% compared to flood cooling.
Vishal Sharma et al. [7]	• Dry cutting • Near dry machining • High pressure coolants • Solid lubricants	It was found that usage of MQL results in reduced cost, improved surface quality, and reduced coolant usage. It was also stated that using vegetable oils as lubricants provided better results compared to mineral oils in terms of cost, health, safety, and environment.
Debnath et al. [36]	• Dry cutting • Near dry / MQL • flood cooling	Studied machinability in terms of surface roughness, tool wear, coefficient of friction, etc. It was that MQL is the best alternative when dry cutting fails and flood cooling cannot be applied i.e. operations like drilling operations.
Muhammad Jamil et al. [44]	• CO_2 snow as coolant • MQL • Nanofluid-based MQL	It was found that better surface finish and tool life were observed while using nanofluid-based MQL compared to CO_2 snow.

2.6 High-pressure coolant

The pressure at which the coolant is supplied is also pivotal as it influences the heat transfer coefficient. Liew et al. [35] presented an analysis for turning of different materials under different cooling strategies like dry turning, MQL, nanofluids, high pressure cooling, and cryogenic

environment. The product quality, tool life, and environmental effects were observed and it was found that cryogenic cooling was more efficient in terms of product quality but in terms of tool life, pressurized coolant was efficient. Sharma et al. [7] studied different responses like machining cost, tool life, surface finish, etc under an environment of high pressure coolant jet. it was found that the usage of HPC in turning operation results in better tool life, better surface finish, and reduced cutting force. Also, the direction of the nozzle plays a vital role while machining. Nandy et al. [45] used the high-pressure coolant jets (oil and water-soluble oil) as a cooling medium to study the machining performance for Ti-6Al-4V alloy in turning. It is revealed that the use of a high-pressure coolant jet significantly increased the tool life and reduced tool wear compared to wet cooling. Busch et al. [34] discussed the usage of the different cooling systems like HPC, wet machining, Cryogenic-CO_2, etc., and studied machinability in terms of chip control, tool life, energy consumption, etc. it was found that high pressure coolant can provide better tool life, and better chip control compared to other cooling techniques. There is a 50% reduction in machining time observed and adhesion between the toll and workpiece was minimized compared to dry cutting. Palanisamy et.al. [46] discussed the effect of high pressure coolant on the life of the cutting tool and chip removal of titanium alloy in machining. It was found that by the usage of this cooling process increased the tool life by three times, the evacuation of the chip became efficient and the surface quality also improved compared to conventional methods.

Sahoo et al. [47] studied the wear behavior and machinability of AISI D2 steel with a compressed air-water spray cooling system as an alternative to conventional cutting fluid. It was found that the usage of water droplets, absorbs more amount of latent heat and minimizes the cutting temperature. Also, the tool wear and formation of built-up edge were reduced, and cutting performance was improved using spray impingement cooling compared to dry cutting. Rubio et al. [4] reviewed the effect of cold compressed air during the machining of different materials like stainless steel, cast iron, and alloys of Nickle, aluminum, and titanium. It was found that the usage of cold compressed air as a cooling medium increased the tool life, surface finish, chip evacuation, and minimized the cutting temperature effectively. Also, it increases productivity by reducing production costs as the air is naturally available.

2.7 Cryogenic coolants

Cryogenic coolants are characterized by their sub-zero temperatures and many researchers have reported some valuable information concerning the performance of these coolants in machining. Rotella et al. [48] compared the responses of Ti-6Al-4V under different cooling strategies which are dry, MQL, and cryogenic cooling at various speeds and feeds. It studied the product quality in terms of microstructure, grain refinement, and surface quality. It was found that the cryogenic cooling condition improves the given responses significantly. Along with this, in the perspective of sustainability, cryogenic cooling is environmentally friendly compared to other techniques. Sun et al. [49] developed a cooling method in which cold compressed gas was used as a cooling medium during the machining of Ti-6Al-4V and the cooling effect was produced by supplying the high pressure gas through copper tubes that are positioned inside the Liquid Nitrogen (LN2) cylinder which is described in Figure 2.3. The usage of cryogenic compressed gas reduced the cutting temperature and produced segmented type chips which are easy to evacuate compared to compressed air and dry environments. However, cutting forces were increased marginally by using this cooling method because of the strain hardening effect compared to other environments. Sharma et al. [7] reviewed different cooling techniques for difficult to cut materials and stated that cryogenic coolants improve the tool life effectively compared to other cooling environments and these can be used as both coolant and lubricant and increase productivity even at higher feed rates. Also, It was found that usage of cryogenic cooling with carbide tools reduces the diffusion, adhesion, and abrasion wear. Arauzo et al. [25] studied surface finish and tool wear in SAE 1045 steel machining in the environments of refrigerated and non-refrigerated pressurized air. The vapor compression refrigeration system used for providing a refrigeration effect to the compressed air. the experiments are performed under constant machining conditions and found that the usage of refrigerated gas provided better outcomes.

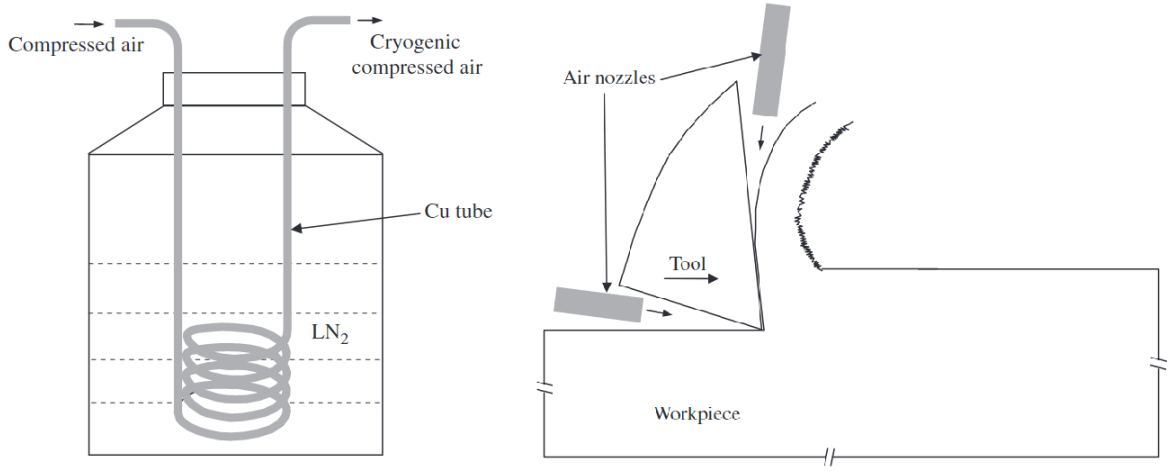

Figure 2.3: Schematic illustrations of (a) generation and (b) delivery of cryogenic compressed air to the cutting edge [49]

Sartori et al. [50] developed a novel approach involving cooling with LN2 with a cooling temperature between 0ºC to -150ºC. This approach was used to study the performance in terms of tool wear and surface integrity in the semifinished turning of TI-6Al-4V. The cooling temperature of -100 ºC performed better in terms of reduced flank wear and tool wear and better surface integrity was found compared to cutting fluids and the surface defects were eliminated which were observed under dry and LN2 environments. Mozammel et al. [36] reviewed various cooling environments that can be applied while machining and discussed their properties. It was found that cryogenic coolants require less force compared to other techniques and also concluded that cryogenic coolants provide better properties in terms of friction, surface quality, heat generation, etc. the different types of wear like adhesion, diffusion, abrasion are minimized by the usage of cryogenic coolant.

Mia et al. [51] studied cutting force, cutting temperature, surface roughness, specific energy, and material removal rate under the LN2 environment supplied by single and dual jets during machining of TI-6Al-4V. Supply of LN2 using a dual jet was more effective in terms of specific energy, cutting temperature, and quality of surface due to effective heat removal at higher speed and lower feeds. It was also pointed out that the cryogenic environment was a clean and eco-friendly cooling medium compared to conventional methods. Jamil et al. [24] compared the performance of cooling techniques like LN2, MQL, CO_2 -snow, and dry cutting while machining Ti-6Al-4V in terms of temperature, surface quality, and tool wear. It was found that a lower cutting

temperature was observed in the LN2 environment compared to other cooling environments. It was also found that the maximum efficiency of 30.72% is obtained under the LN2 environment at a cutting speed of 110 m/min, and a helix angle of 30^0 in up milling direction. Shokrani et al. [37] performed the end milling operation on Ti-6Al-4V and studied the tool wear under cryogenic LN2, flood, and dry environments at constant cutting conditions. It was found that cryogenic LN2 resulted in reduced tool wear with a minimum value of 10microns at a speed of 200m/min, energy consumption reduced by 88%, and increased productivity compared to conventional cooling. Shane Hong et al. [52] conducted experiments on Ti-6Al-4V to study the effect of cryogenic LN2 on cutting force and friction coefficient between tool chip interfaces during machining. Cutting force was increased in cryogenic cooling due to strain hardening of the workpiece and the coefficient of friction was reduced due to the lubricating effect of cutting fluid when compared to dry cutting.

Khanna et al. [53] discussed the performance of various cooling environments while drilling Titanium alloy in terms of hole quality, power consumption, chip morphology, etc. It was found that the LN2 environment provides better results in terms of power consumption, and accuracy of hole geometries. Also, discontinuous chips, higher penetrating ability, and increased thrust forces were observed by the usage of cryogenic LN2. Jerold et al. [54] conducted a turning operation on AISI 1045 steel under CO_2, LN2, and wet environments in terms of tool wear, cutting temperature, and chip control. It was concluded that in terms of lower cutting temperature LN2 is the best alternative compared to other environments. Kim et al. [25] developed a cooling strategy for machining Titanium alloy and analyzed the cutting force and life of the tool. Cryogenic LN2 was used as the coolant and supplied it indirectly to the machining zone and compared the results with conventional methods. It was found that there is a reduction in cutting force by 54% and an improvement in tool life by 90% while the usage of cryogenic LN2. Shokrani et al. [55] investigated tool life, surface roughness, power consumption, and specific machining energy in CNC end milling of Ti-6Al-4V under cryogenic LN2 and compared the results with flood cooling. Their investigation concluded that cryogenic LN2 improved the tool life three times and reduced the surface roughness by 40%. Furthermore, the following works (Table 2.2) can provide an even better insight into the performance of cryogenic coolants.

Table 2.2: Literature related to cryogenic cooling in the machining of titanium alloy

Author	Field of study and contribution
Paul et al. [56]	Studied the tool life in Ti-6Al-4V machining where uncoated carbide inserts are used under dry, wet, and LN2 environments. LN2 media provided better tool life by minimizing adhesion and diffusion tool wear and controlled the cutting temperature effectively compared to other cooling media.
Mia et al. [57]	Used liquid nitrogen as a coolant media while turning Ti-6Al-4V and studied the surface roughness, tool life, and chip-tool interface temperature. In this study, a single jet (aimed at rake face) and duplex jet (aimed at rake and flank surface) were used and found that The duplex jet cooling increases the tool life by 30% and 60% compared to single jet and dry cutting environments respectively. Also, the tool cost, temperature, and energy consumption were reduced and surface quality was improved in the case of the duplex jet.
Jamil et al. [58]	Studied cutting temperature, surface roughness, tool life and cost of machining under dry, MQL, and cryogenic LN2 modes in hard turning of a-b titanium alloy. The machining cost, tool wear, cutting temperature, and surface roughness were minimized under cryogenic cooling compared to other techniques. Besides this, the environmental pollution and negative effect on workers' health were minimized in the case of cryogenic coolants.
Shane et al. [59]	Developed a setup with two micro nozzles in which LN2 is used as a cooling medium during machining of Ti-6Al-4V. This technique improved the tool life by five times and reduced the cutting temperature by providing effective cooling even with a small amount of LN2 compared to emulsion cooling. The usage of two nozzles reduces the flow rate, coefficient of friction and also, found that adequate positioning of the nozzles improved the machining performance
Sivaiah et al. [60]	Developed a sustainable cooling method in which cryogenic coolant with LN2 was sprayed in the chip-tool interface during machining of precipitated hardenable stainless steel. Machining performance studied at different depths of cut and compared with dry cutting and MQL. It was observed that this method provided better results in terms of cutting temperature, surface integrity, chip thickness, and tool wear.

2.8 CO_2 cooling

Despite being a greenhouse gas, CO_2 can also be utilized as a coolant in machining operations. Busch et.al. [34] compared the effectiveness of different cooling strategies while machining Ti-6Al-4V and Inconel 718. It was concluded that cryogenic CO_2 was more effective and completely residue-free. But it cannot provide lubrication i.e. an additional lubricant has to be supplied during machining. Machai et al. [61] studied tool life and notch wear by performing a turning operation on Ti–10V–2Fe–3Al using CO_2 snow as coolant. It was concluded that the tool life was doubled by using this coolant compared to flood emulsions and also the burr formation and notch wear are reduced significantly. but a poor penetration ability of CO_2 gas into the chip-tool interface was observed. Sadik et al. [62]performed experiments on the face milling of Ti-6Al-4V with PVD coated inserts and liquid CO_2 coolant. It was found that tool life was improved with the flow rate of coolant and also the propagation of thermal cracks and cutting edge chipping were delayed by the usage of CO_2 gas coolant.

Jamil et al. [24] discussed the surface quality, tool wear, and cutting temperature while milling Ti-6Al-4V under different cooling environments such that MQL, CO_2 -snow, LN2, and dry cutting. From their analysis, better surface finish and tool life were observed under the CO_2 environment compared to other environments. Stephenson et.al. [63] used a $SCCO_2$ (supercritical Carbon dioxide) based MQL as a cooling medium while machining Inconel 750 and compared the results with flood cooling. The $SCCO_2$ -MQL gives better tool life, and an increase in metal removal rate compared to flood cooling because of effective coolant supply through specially designed jet tool holders. But the crater wear and chip hammering were increased in case of $SCCO_2$ -MQL compared to other environments. Rahim et al. [64] performed machining operation on AISI 1045 medium carbon steel under two different cooling environments such that MQL, and $SCCO_2$ gas, and studied cutting force, cutting temperature, and chips. $SCCO_2$ provided effective machinability in terms of all the above response parameters. Machai et al.[61] used CO_2 snow as a coolant supplied from pressurized gas bottles to the tool chip interface during machining of Ti-10V-2Fe-3Al. He found that there was an increase in tool life under the CO_2 environment compared to emulsion cooling even at higher speeds. Jamil et al. [65] studied the heat transfer effect during machining of Ti-6Al-4V using different cooling media like LN2, CO_2 snow, and the dry environment under constant cutting conditions and flow rate. Machinability was analyzed in

terms of cutting forces, tool wear, surface quality, maximum chip curl diameter and observed that the CO_2 snow environment provides better outcomes followed by LN2 and dry environments.

Khanna et al. [53] performed drilling operations of Titanium alloy under different cooling environments such that dry, flood LN2, and LCO_2 and studied its properties. A lower thrust force, lower surface roughness, and better lubrication were observed under LCO_2 conditions compared to dry and flood cooling techniques. Jamil et al. [44] compared the performance of nanofluid-based MQL and CO_2 snow at different cutting parameters. It was found that using CO_2 snow as coolant reduced the cutting temperature by 22.36% compared to nanofluid based MQL at a speed of 80m/min and a feed of 0.12 mm/revolution. Jerold et al. [54] analyzed cutting temperature, tool wear, cutting force, and surface finish by comparing LN2, CO_2, and flood cooling in the turning of AISI 1045 steel. The usage of cryogenic CO_2 reduces the cutting force, tool wear, and surface roughness compared to LN2 and wet environments. Iqbal et al.[66] studied the machinability of Ti-6Al-4V in terms of tool displacement area, cutting energy, and tool wear by using CO_2 snow with MQL and emulsion-based coolant. It was found that CO_2 snow with MQL provided better results in every aspect compared to the emulsion-based coolant. Sartori et al.[67] investigated about two cooling strategies i.e. one for cooling and the other for lubrication while performing the turning operation on wrought Ti-6Al-4V. The MQL system along with CO_2 and LN2 were used as coolants and studied the tool wear which was analyzed using SEM. It was observed that both the lubricants reduce the tool wear but there is a significant drop in the tool wear while using CO_2 as a coolant.

2.9 Vortex tube cooling

Employing refrigeration systems for coolant can yield better results. However, such systems are associated with additional energy requirements which in turn can affect the sustainability of the whole process. Vortex tube cooling system is capable of providing refrigeration with no internal or external energy input. Yuksel et al. [68] performed CNC turning operation assisted by RHVT on chromium-molybdenum steel alloy (42CrMo4) by considering cooling temperature, feed, and cutting speed as inputs, and surface roughness, cutting temperature, and cutting force as responses. The lowest cutting temperature was found as 74.17^0C at 250 m/min cutting speed and 0.25 mm/rev feed and -4^0C coolant temperature under vortex tube cooling conditions. The lowest surface roughness was found as 0.77 µm at 400 m/min cutting speed and 0.15 mm/rev feed under vortex tube cooling conditions. Whereas the cutting forces were not

affected significantly (the change is less than 1%). It was found the lower temperature of the coolant. minimizes the cutting temperature and surface roughness in the machining. Taha et al. [69] studied cutting temperature, surface roughness, and power consumption during machining of mild steel under ambient and vortex tube cooling conditions. Lower cutting temperature was recorded in machining under vortex tube conditions. However, better surface finish and lower power consumption are observed under ambient conditions.

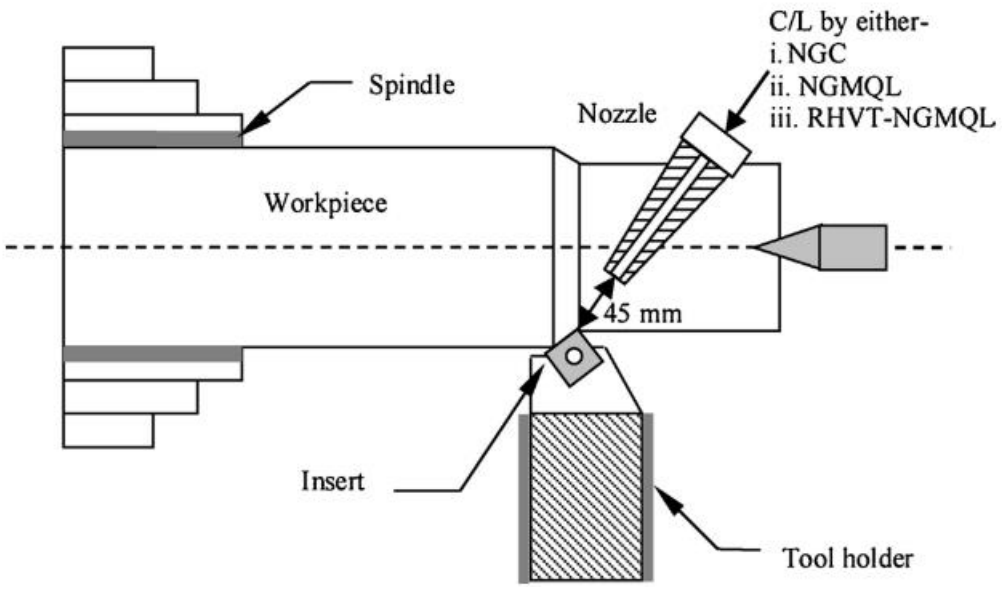

Figure 2.4: Schematic diagram of the experimental setup[70]

Mia et al. [70] used the nitrogen gas in the vortex tube as a cooling medium in turning Al 6061-T6 along with Nitrogen Gas Minimum Quantity Lubrication (NGMQL) to reduce the flank wear (V_b) and surface roughness. Uncoated tungsten carbide was used as the cutting tool at two levels of speed and feed with canola oil as the lubricant. the experimental setup used by the author is presented in Figure 2.4. It was observed that the NGMQL method reduced the surface roughness and flank wear compared to dry cutting. Khazaei et al.[71] developed a CFD model to study the effect of properties of gas on the performance of vortex tube and observed that cold temperature difference (difference between temperatures of inlet and cold side of vortex tube) increased with an increase in specific heat capacity ratio and decrease in molecular weight. And it was also found that hot end dimensions and shape don't influence the temperature distribution significantly because of lower swirl velocity at the hot end of the vortex tube. Kirmaci [72] conducted an

experimental investigation to study the performance of vortex tube concerning the number of nozzles and inlet pressure. Oxygen and air were used as working fluids at a constant cold fraction and length to diameter ratio of 0.5 and 15 respectively. It was observed that the cold stream temperature was increased with an increase in inlet pressure for both the fluids and an increase in the number of nozzles decreased the temperature gradient between hot and cold ends.

Golhar et al. [73] studied the effect of nozzle diameter on the efficiency and energy separation of cooling in counter-flow vortex tube keeping all other parameters constant. It was found that maximum temperature drop occurs in the nozzle diameter range of 3.4 mm to 4 mm. Chou et al. [74] performed turning of hyper eutectic Si-Al alloys under vortex tube cooling to study the tool wear and cutting temperature and the results were compared with dry machining. Usage of vortex tube reduced the tool wear and cutting temperature at lower feeds and speeds whereas higher values of these parameters diminish the cooling effect. Zhang et al. [75] discussed the energy separation, mass separation, cooling, and heating performance of the vortex tube with different working fluids like air, N2, Ar, CO_2, etc. The effect of different properties like thermal conductivity, molecular weight, thermal diffusivity, and specific heat capacity of pure gas fluid on the performance of the Vortex tube was discussed. Agrawal et al. [76] investigated the performance of vortex tube under cooling media like air, nitrogen, and CO_2 by considering length to diameter ratio (L/D ratio), cold fraction, and inlet pressure as influencing parameters. It was found that an L/D ratio of 17.5 and a cold fraction of 60% are optimum conditions and CO_2 is the better coolant compared to the other two because of its high molecular weight and low specific heat ratio.

Attalla et al.[77] compared the coefficient of performance (COP) of two similar vortex tubes arranged in series (VTS) and parallel (VTP) at various inlet pressures and cold fractions. Their investigation revealed that a pressure of 6 bar and the cold fraction of 0.4 provides a higher cold temperature difference for both systems. The refrigeration COP was higher for VTS and the heat pump COP qas higher for VTP. Ahmed et al.[78] investigated the energy separation and cooling performance of counter flow vortex tube by varying the number of nozzles and inlet pressure. It was concluded that better performance i.e. the highest cold temperature difference of 25^0C and a COP of 0.21 is obtained with three nozzles. Aydın et al. [79] studied the performance, flow visualization, and most influencing parameter among coolant pressure, length, cold fraction, diameter at the inlet, and angle of control valve while using a counterflow vortex tube. Both the flow pattern and energy transfer in this system can be visualized as depicted in Figure 2.5. It was

observed that coolant pressure and cold fractions are the most influencing parameters in different coolants such as air, oxygen, and nitrogen.

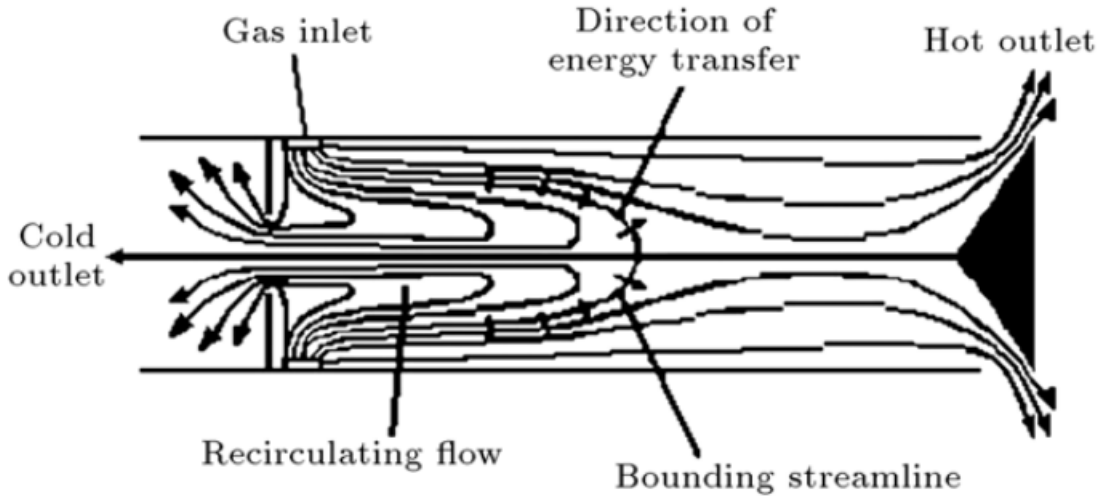

Figure 2.5: Schematic diagram of vortex tube (counter-flow)[71]

Dincer [80] investigated to study the optimum conditions for pressure, cold fraction, and temperature difference under three situations such as conventional, threefold cascade type (combination of three RHVTs), and six cascade types (combination of six RHVTs). Results revealed that better performance was obtained in the third situation at a pressure of 400kPa, the maximum temperature difference of 67.60, and the cold fraction of 0.9. Salaam et al. [69] investigated the effect of RHVT on surface quality, and power consumption while turning mild steel at a fixed cutting speed and by varying depth of cut. It was found that a better reduction in cutting temperature was obtained while using RHVT and better surface quality and lower power consumption are found at ambient conditions except at a feed rate of 0.28mm/rev. Munish Kumar Gupta et al. [81] discussed the effect of cooling techniques like dry, N2 cooling, N2MQL, and RHVT-N2MQL on surface quality, chip formation, and tool wear while Al 7075-T6 turning by varying cutting speed and feed. It was concluded that RHVT-N2MQL improves the surface quality by up to 77%, reduces chip disposal, and reduces the tool wear up to 118%.

2.10 Optimization

Singh et al. [39] compared the performance of MQL and RHVT-MQL in terms of Surface roughness, cutting force, tool wear, and consumption of power and performed an ANOVA analysis using Teaching-Learning Based Optimization (TLBO) technique. It was found that RHVT-MQL

provides better results in all aspects and feed rate was the most influencing parameter. M. Boujelbene [82] performed an experimental study about the tangential force at different cutting speeds and feeds at a constant depth of cut in orthogonal turning. A model was obtained for cutting force in terms of input parameters using RSM. Using this model it was found that cutting force was mainly influenced by cutting speed and feed it can be decreased by increasing the cutting speed and decreasing the feed and depth of cut. Rubio et al. [83] experimentally investigated the surface quality of Ti-6Al-4V by taking spindle speed, feed, depth of cut, measurement location, type of cooling system, and tool type and performed an ANOVA analysis. The analysis has shown that spindle speed, feed, and measurement location are the most influencing parameters individually and while in terms of interactions tool type, and type of cooling system with spindle speed were mostly influencing.

Bhagyashree et al. [84] performed a dry cutting operation of Ti-6Al-4V at different levels of cutting parameters. The RSM and GA (Genetic Algorithm) techniques were used to analyze the data and find the optimum conditions by taking feed force and cutting force as responses. The analysis has given that the optimum values for speed, feed, and depth of cut are 120 m/min, 0.10 mm/rev, and 0.5 mm respectively. Asit et al.[85] investigated the influence of cutting parameters while turning Monel-400 by taking flank wear and surface roughness as responses. It was found that workpiece temperature and cutting speed are the most influencing parameters for flank wear and surface roughness. The maximum error between predicted and experimental values were found to be 13%, and 7% for flank wear and surface roughness respectively.

2.11 Motivation for the work

Nowadays industries like manufacturing and aerospace are widely using Titanium alloys because of their excellent properties like large specific strength, high resistance to fracture, and corrosion. Titanium alloy machining is hard because of its material properties like low thermal conductivity (k), low Young's modulus (E), and high chemical reactivity. The lower thermal conductivity of the Titanium alloys does not allow the heat to be transferred from the machining zone which causes for further increase in the cutting temperature. It needs to be minimized because it affects the surface roughness of the machined component and the life of the tool. Traditionally cutting temperature is minimized by using cutting fluids, but the utilization of cutting fluids leads to several difficulties like higher cost, which also shows a negative effect on the environment and

workers' health. So it is necessary to develop an alternative solution to the usage of cutting fluid which usually removes the heat from the machining zone. Hence, the present study aims at developing a cooling system that controls the cutting temperature in machining Ti-6Al-4V.

In this study, the gaseous refrigeration technique used is known as vortex tube-based cooling system in which the refrigeration effect is produced by using a vortex tube and CO_2 gas as a working fluid. Previous researchers have mostly focused on the use of cryogenic LN2 and some worked on using cryogenic CO_2 to minimize the cutting temperature as an alternative to cutting fluid, but the use of refrigerated CO_2 as a coolant in the machining of titanium alloy is seldom found. Even though many articles are available on vortex tube cooling, the air was used as working fluid in those studies, and use of CO_2 was limited. In VTCS, CO_2 gas is used due to its low response time to reach the desired temperature, its lower coefficient of friction between tool and workpiece interface and positive Joule Thomson coefficient also help to produce more cooling effect. Many researchers focused on the use of high pressure coolants and obtained better results in terms of minimizing cutting temperature, surface roughness, and tool wear. Focus on the position, nozzle size, and angle of impingement was seldom found while supplying coolant in the high pressure coolant system. Also, the effect of nozzle diameter and cold fraction on the machinability of Ti-6Al-4V in vortex tube cooling has not been extensively reported use in the literature. The use of dual nozzle along with vortex tube in cooling applications during machining is also needs to be explored.

The main objectives of this research work are listed as follows:

1. To design and develop a vortex tube cooling system that can beused to minimize the cutting temperature in the machining of Ti-6Al-4V.
2. To study the effect of nozzle parameters (Nozzle angle, Nozzle position, and Nozzle diameter) on machinability during turning of Ti-6Al-4V and optimization of these parameters for better responses.
3. To study the influence of flow parameters (coolant pressure, cold fraction, and nozzle diameter) on response parameters (Cutting temperature, Cutting force, and Surface roughness) in VTCS assisted turning.
4. To study the influence of machining parameters (cutting speed, feed, and depth of cut) on response parameters in VTCS assisted turning.

5. To analyze the performance of vortex tube by comparing the responses with other alternative cooling methods.

2.12 Research methodology

The machining of Ti-6Al-4V alloy produces a large amount of heat leading to a rise in cutting temperature. It significantly affects surface finish, dimensional accuracy and tool life. For better machinability, it is required to minimize the cutting temperature. Traditionally cutting fluids were using for this purpose but these had drawbacks that were described in earlier sections of this chapter. In this study, a novel cooling system is developed known as vortex tube cooling system was employed with CO_2 gas is used as the coolant. The effect of VTCS on the responses was analyzed and the results were compared to the other alternative cooling methods. The effects of nozzle, flow and machining parameters on the responses in VTCS have been discussed briefly. The flow chart of work carried out is represented in Figure 2.6.

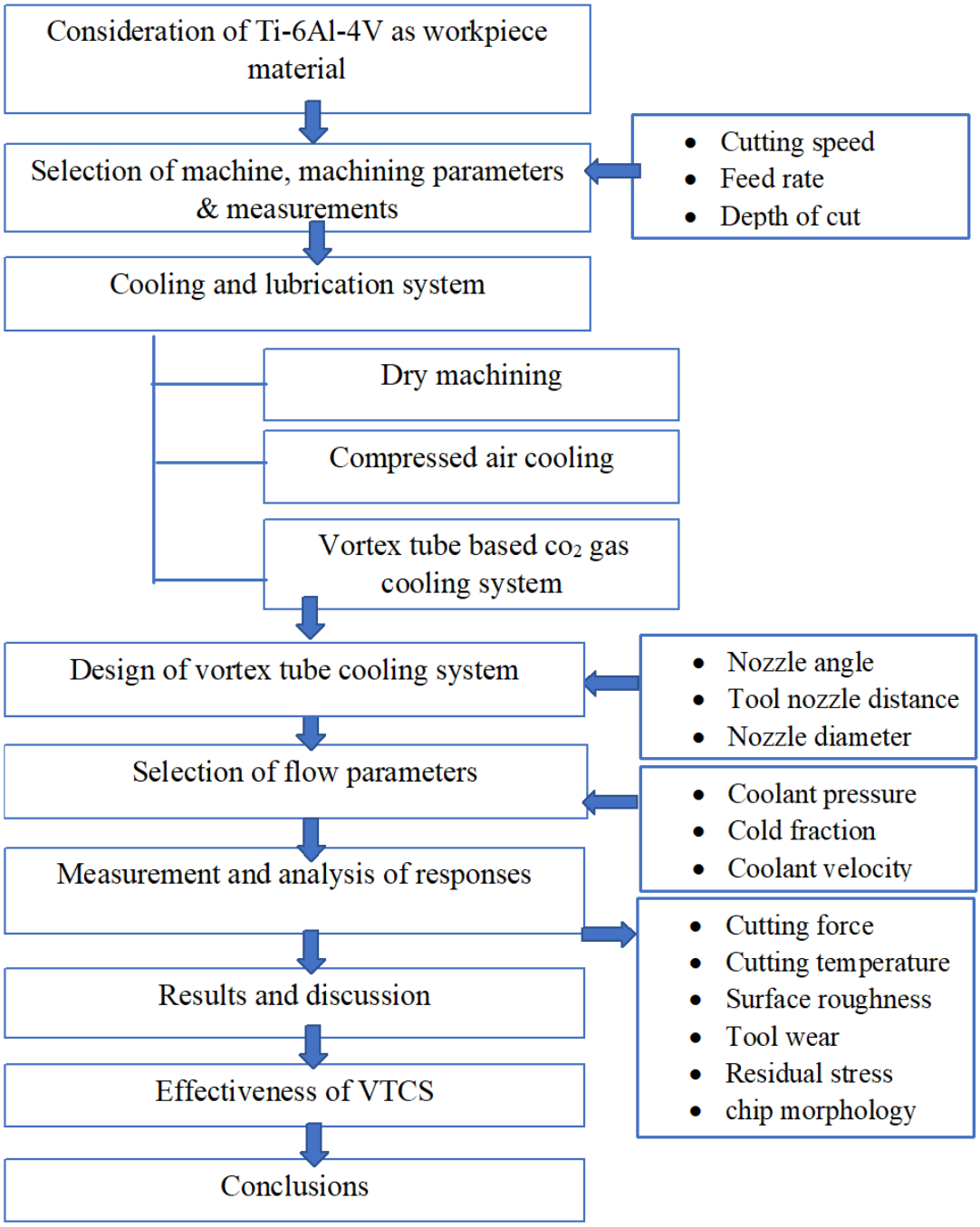

Figure 2.6: Flow chart of research methodology

3 EXPERIMENTATION

3.1 Introduction

This chapter mainly includes details of the experimental setup used in the current work. The working principle and the underlying aspects of the system are also explored. The major constituent of the VTCS is the vortex tube and it is necessary to calibrate for different cold fractions before conducting experiment. Different types of equipment, instruments, and tools were used to systematically record and evaluate the performance of VTCS and the properties of the machined component are discussed. CO_2 gas is selected as a coolant for VTCS owing to its traits. The experimental procedure was implemented for both online and offline data acquisition. Schematic illustrations of the general setup and individual instruments are discussed in the following sections.

3.2 Vortex tube cooling system

VTCS is an external aid connected to the machine tool which provides coolant with the required pressure, speed, and temperature to suppress heat generation in the machining area. The VTCS consists of three subsystems, namely, gas supply system, vortex tube, and coolant spray system (nozzle). The line diagram of VTCS is shown in Figure 3.1. The gas supply system consists of a CO_2 gas cylinder and a pressure gauge. It delivers gas at high pressure and can be regulated using a pressure gauge. The vortex tube is a device that separates high-pressure gas stream into two vapors of high temperature and low temperature.

It consists of a generator surrounded by an annular space and when high pressure gas comes in contact with the nozzle of the generator, some of the pressure is lost which in turn creates a higher speed rotation. The maximum part of the air moves towards the hot end as a vortex and is maintained at the walls of the vortex tube due to centrifugal force. The amount of air exiting through the hot end valve depends on its position and some of the air is restricted from passing through it and forced to the cold end side (inner vortex). Figure 3.2 shows the working principle of the vortex tube. The ratio of the gas flow leaving the cold end to the total gas flow is called “cold fraction”. It can be controlled in the vortex tube by the controller to produce a different amount of cooling rate. By changing the position of the regulator, the portion of cold gas and hot gas can be changed but the total flow rate remains the same and is equal to the inlet flow rate. The gas supply system and the vortex tube are connected by a tube insulated with glass wool. This can

help to minimize heat loss from the gas expanding from cylinder pressure to vortex tube inlet pressure.

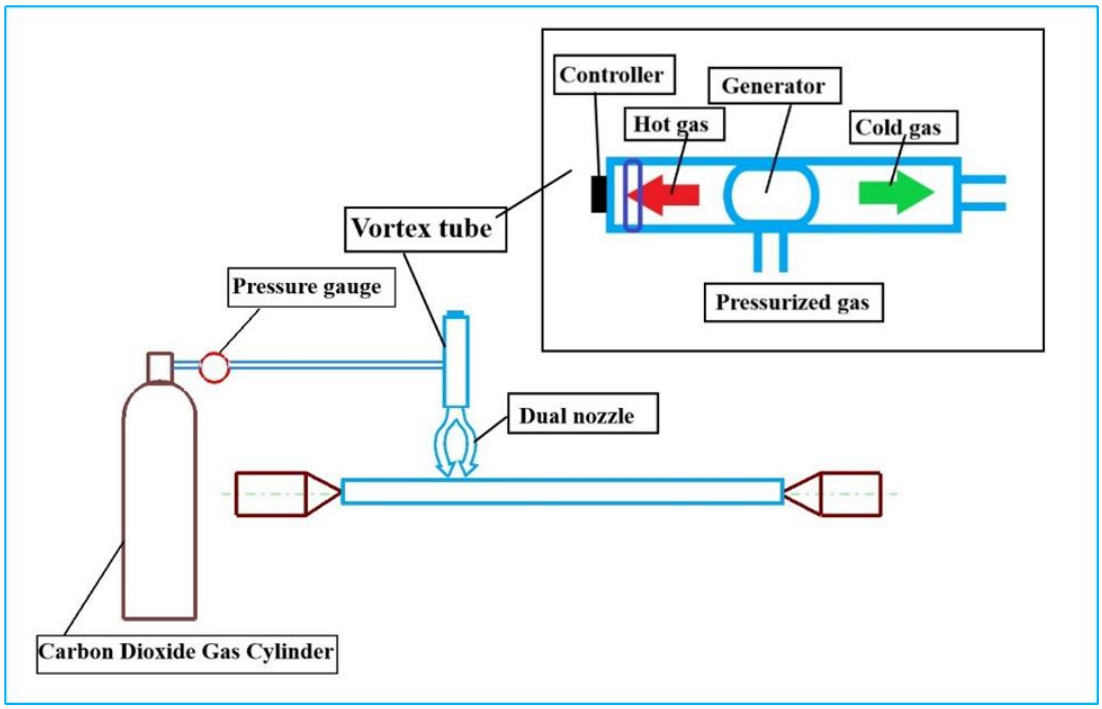

Figure 3.1:The line diagram of the experimental setup

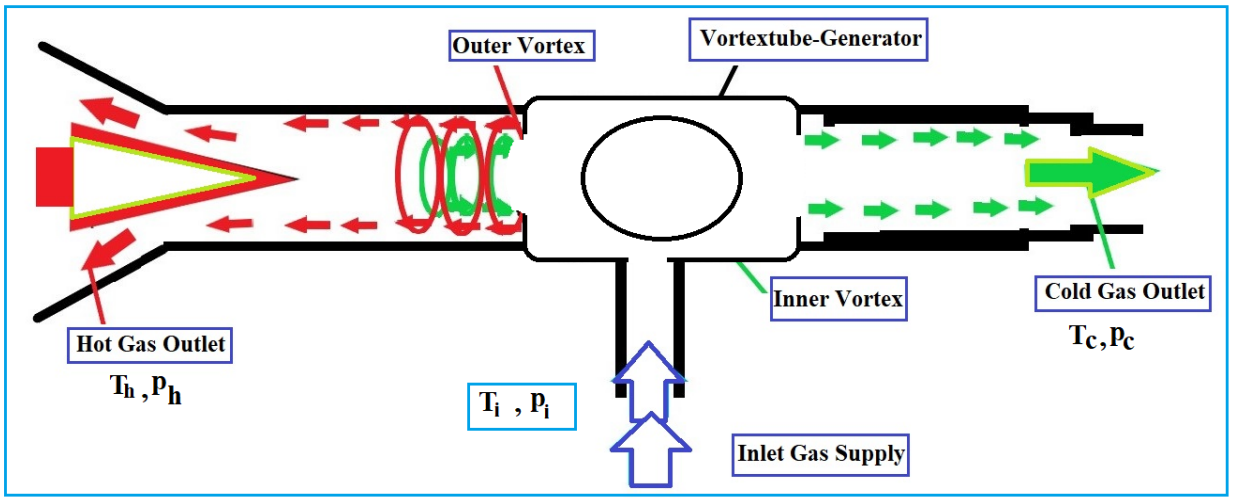

Figure 3.2 :Working procedure of vortex tube

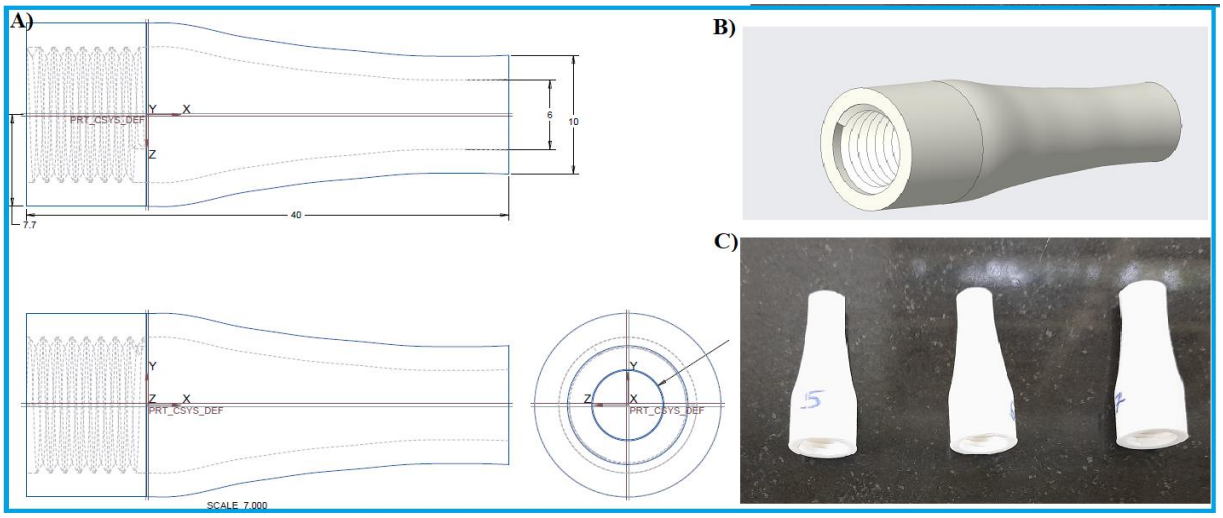

Figure 3.3:Nozzle A) CAD model (All dimensions are in mm) B) 3D image C) Prototype

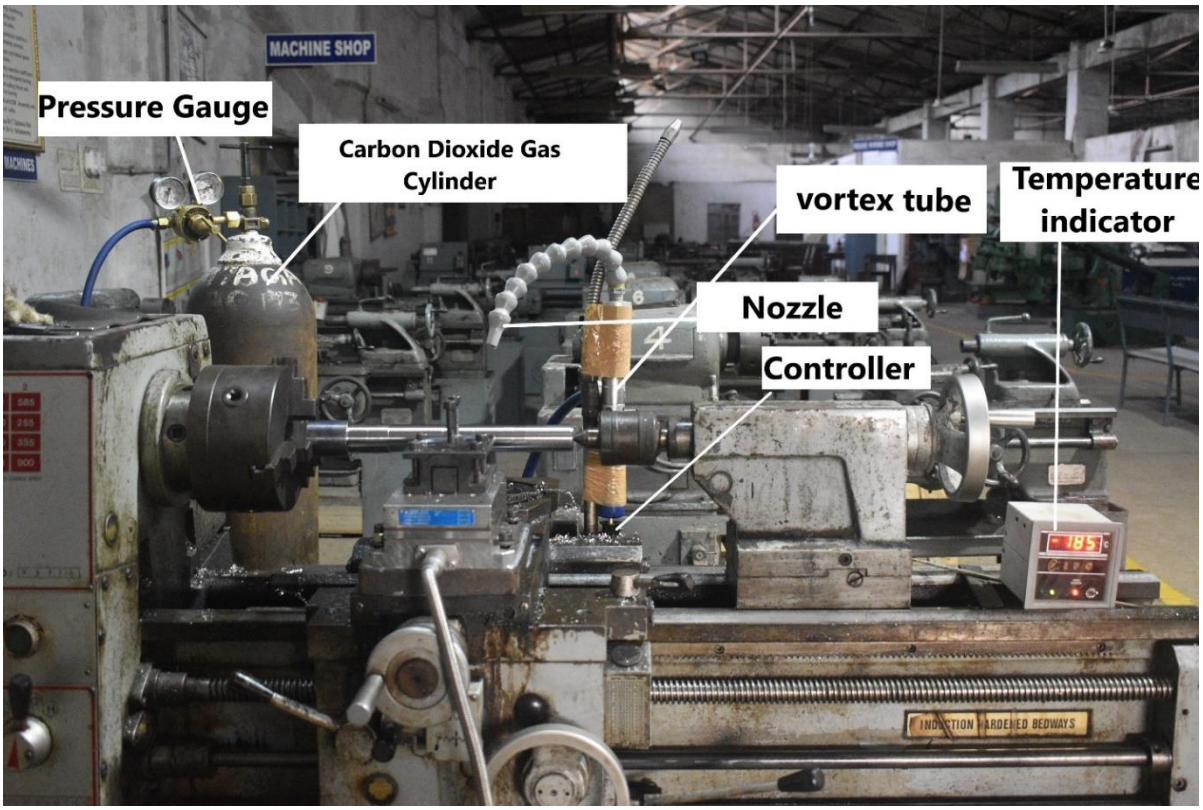

Figure 3.4 :Experimental setup of CO2 based VTCS

The coolant spray system consists of a single/dual nozzle through which coolant is forced into the machining zone and removes heat based on forced convection principles. The coolant velocity is the parameter that is controlled in the coolant spray system using different nozzle sizes. Different nozzle diameters are designed and prepared using a 3D printer which is shown in Figure 3.3 and the material used is polylactic acid. CO_2 gas from the cylinder was regulated to the vortex tube and its output pressure was regulated using a pressure gauge connected to the cylinder. The temperature of the gas stream at the cold end mainly depends on the inlet pressure and the cold fraction and it was supplied into the machining zone at different speeds which were produced using different nozzle sizes. The cold stream of gas obtained from VTCS was used to minimize cutting temperature, improve tool life and surface finish, and provide proper lubrication between mating parts. Two experimental setups were developed by altering the number of nozzles in the coolant spray system known as single nozzle VTCS and dual nozzle VTCS, as shown in figures 3.4 and 3.5 respectively.

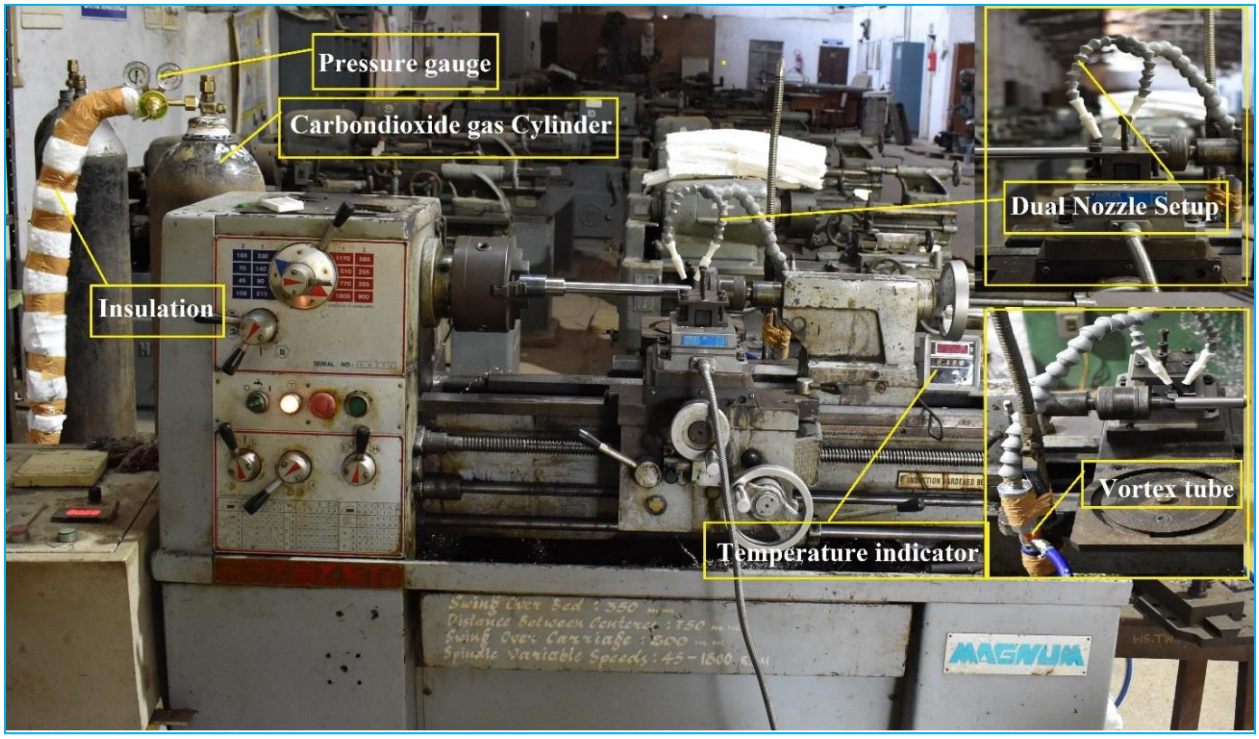

Figure 3.5 : Experimental setup of dual nozzle CO_2 based VTCS

3.3 Calibration of vertex tube

The calibration of the vortex tube was carried out for setting a desired cold fraction (10%, 20%, and 30%) for performing the experiments. For this purpose, the gas flow meter was connected to the inlet and outlet of the vortex tube. The pressure for supplying the gas through the vortex tube was controlled by using a pressure gauge connected immediately after the CO_2 gas cylinder. The pressure was maintained at 3 bar, after which CO_2 gas passed through the vortex tube and flow rates were noted. The outlet flow through the cold end of the vortex tube was varied with the help of the controller. The ratio of cold outlet and inlet flow of 10%, 20%, and 30% was calibrated by varying the cold side flow rate. The ratio was in the range of 0.1 to 0.3 which indicates a 10% to 30% cold fraction. For each cold fraction, a marking was done on the controller to ensure the setting. In VTCS selection cold fraction is an important aspect because it influences temperature drop, COP, and isentropic efficiency of the vortex tube. Initially, the vortex tube is calibrated for different cold fractions. The calibration procedure of the vortex tube is shown in figure 3.6.

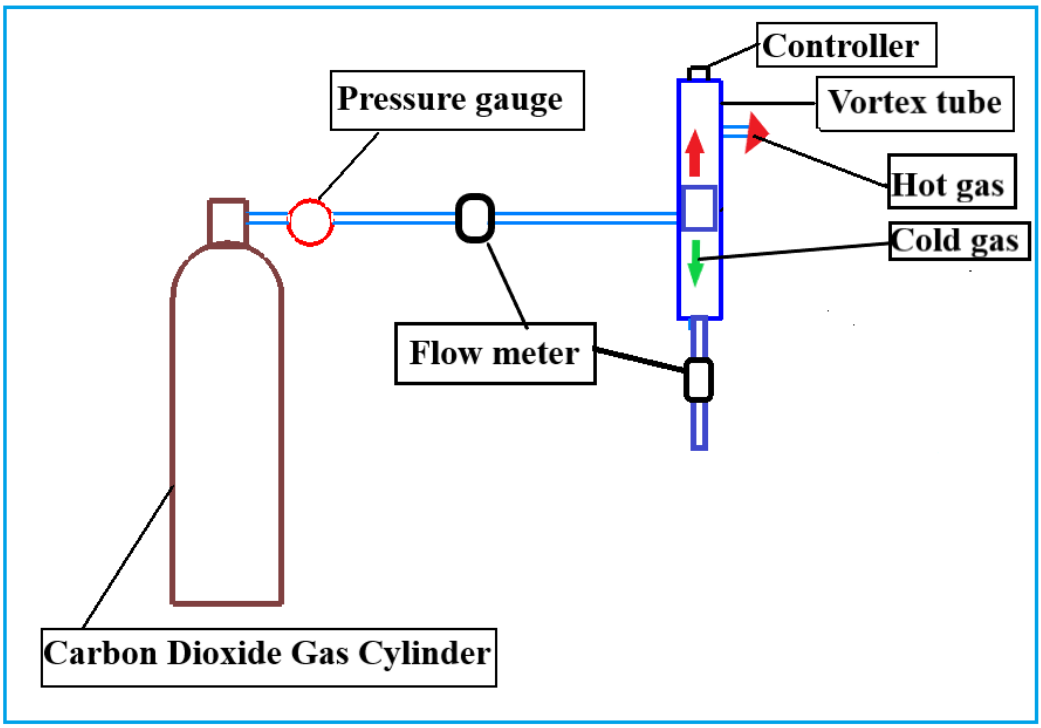

Figure 3.6: Calibration of vortex tube for different cold fractions

3.4 Selection of cutting fluid

In the current work, CO_2 gas was selected as a working fluid because

- It is has a positive Joules Thomson coefficient which produces better cooling effect compared to other gases while expanding [86].
- Storage and supply of CO_2 gas is easy compared to other gases and no insulation is required for supplying tubes [41].
- It is stable under atmospheric conditions [34].
- It needs little time to reach minimum temperature after expansion in the vortex tube when compared to other gases [34].
- It is a triatomic gas having a low specific heat ratio value compared to other monoatomic and diatomic gases which provide higher isentropic efficiency [87].

3.5 Experimentation

The Turning operations were performed in different environments involving dry, compressed air, cold compressed air, compressed CO_2 gas as well as and VTCS single and dual nozzle configurations. The responses (cutting forces, cutting temperature, surface roughness, etc.) were measured at different levels of input parameters. The cutting conditions were selected based on the material of the cutting tool and workpiece in addition to machining tool available in the machine shop to carry out the experiment.

3.5.1 Machine tool

Turning experiments were performed on high precision grade 1 accuracy Precision lathe-SSM 1430, featuring flame hardened bed ways with over 300 BHN hardness, hardened and ground alloy steel Spindle running in anti-friction taper roller bearings. It was attached to a specially designed and fabricated tool post to accommodate the dynamometer and experimental setup. For increasing the rigidity of the machining system, work-piece material was held between three-jaw chuck for all types of experiments. The specification of the precision lathe machine is given in Table 3.1.

Table 3.1: Machine tool specifications

Type	Feature	Specification
Make and Model	Company	MAGNUM
	Model	MA-1430
Mechanical system	Swing over bed	356 mm
	Width of bed ways	206 mm
	The total length of bed ways	1430 mm
	Swing over cross slide	220 mm
	Height of centers	178 mm
	Distance between centers	750 mm
	Variable spindle speed	45-1800 rpm
	Feed rate	0.04-7 mm/rev
	Pitch of the lead screw	6 mm
Electrical system	Spindle motor speed (dynamically variable)	8 KW infinitely variable Speed
	Stabilizer & Transformer	3 KVA
Attachments	Dynamometer for force measurement	Yes
	VTCS Setup	Yes

3.5.2 Work specimen

Ti-6Al-4V was used as a workpiece material. Ti-6Al-4V is widely used in industries due to its properties like high strength to weight ratio, corrosion resistance, etc. The mechanical and chemical properties are described in Tables 3.2 and 3.3 which are taken from supplier data. These values were compared with the data in Ziterature and they were found to be similar. To ensure stress-free condition, the Ti-6Al-4V alloy workpiece was annealed at 590^{o}C for 2 hours and followed by furnace cooling before the start of the experimentation.

Table 3.2: Chemical composition of the workpiece material [88]

Titanium	Aluminum	Vanadium	Carbon	Oxygen	Nitrogen	Hydrogen	Iron
90%	6%	4%	<0.10%	<0.20%	<0.05%	<0.0125%	<0.3%

Table 3.3: Mechanical properties of the workpiece material

Ti alloy	Ti-6Al-4V
Rockwell	36
Elastic modulus (MPa)	114
Tensile strength (MPa)	1000
Melting point	1649 ± 15^0C
Specific heat ($J/^0C/kg$)	560
Thermal conductivity (W/mK)	7.2

3.5.3 Tool holder and Cutting insert

In the turning operation, an uncoated carbide-tipped tool insert (CNMG120408) was used as a cutting tool and PCLNR2525M12 was used as a tool holder. The cutting tool has a rake angle of -6°, an insert inclination angle of 80^0, and a nose radius of 0.8 mm as shown in figure 3.7. The specifications of the cutting insert are presented in Table 3.5.

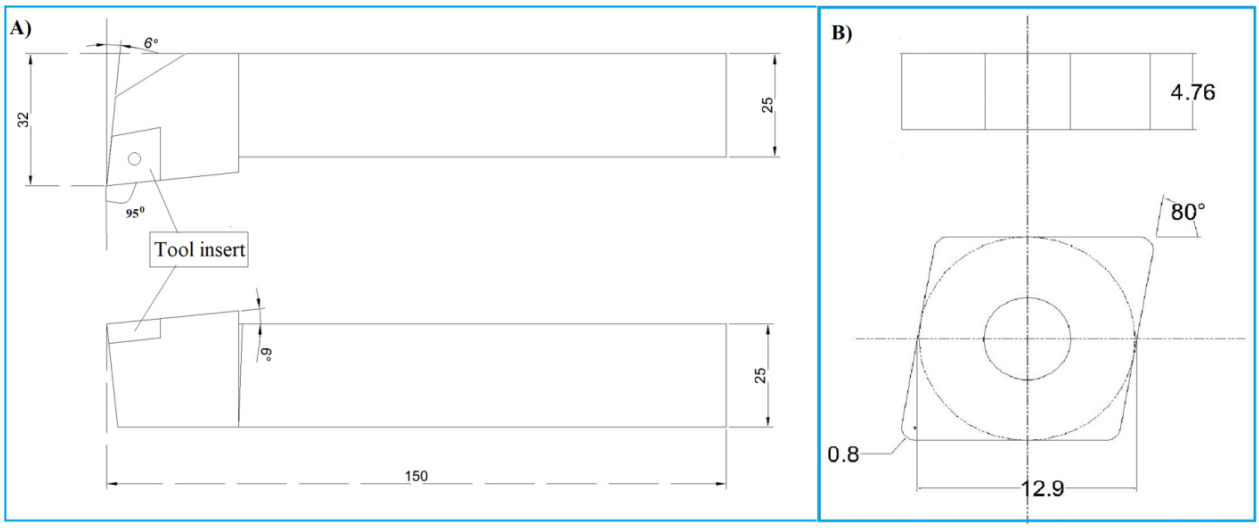

Figure 3.7 :Specifications of a) Tool holder b) Cutting insert (All dimensions are in mm)

Table 3.4: Machine specifications and machining parameters

Machine	Lathe (10 Hp) (Magnum Tools, Romulus, MI)
Work material	Ti-6Al-4V
Tool geometry	rake angle of -6°, insert Inclination angle of 80^0, a nose radius of 0.8 mm
Tool holder	PCLNR2525M12
Cutting insert	CNMG120408 THM

Table 3.5: Specifications of cutting insert

Description	**Value**
Tool material	Cemented carbide
Insert included angle	80^o
Rake angle	-6^o
Clearance angle major	0 Degree
Cutting edge length	12.896 mm
Inscribed circle diameter	12.7 mm
Insert thickness	4.76 mm
Corner radius	0.8 mm

3.5.4 Input parameters

In the experiment, the coolant pressure, cold fraction, nozzle diameter, tool-tip distance, nozzle angle, cutting speed, feed, and depth of cut were varied individually or combinedly to identify the effect on response parameters. The input parameters and their magnitudes are presented in Table 3.6. The coolant pressure, cold fraction, and nozzle diameter were considered flow parameters and varied in the gas supply system, vortex tube, and spray system respectively. Cutting speed, feed, and depth of cut were considered cutting/machining parameters and were varied in the machine tool.

Table 3.6: Input parameters and their magnetudes

S.No	Parameter	Values
1	Coolant pressure (bar)	5 bar, 6 bar, 7 bar, 8 bar and 9 bar
2	Cold fraction (%)	10%, 20% and 30%
3	Nozzled dia (mm)	5mm, 6mm and 7mm.
4	Tip nozzle distance	2.5 mm, 3.5 mm and 4.5mm
5	Nozzle angle	30^0,45^0 and 60^0
4	Cutting speed.	60 m/min , 70 m/min , 80 m/min , 90 m/min , 100 m/min
5	Feed rate	0.21 mm/rev , 0.25 mm/rev, and 0.29 mm/rev
6	Depth of cut	0.8 mm, 1 mm and 1.2 mm

3.6 Measurement of response parameters

3.6.1 Cutting temperature

The measurement of the temperature at the machining zone was carried out by Fluke thermal imager TI400 (shown in figure 3.8) which measures temperatures from -20 °C to +1200 °C (-4 °F to +2192 °F). The thermal imager was positioned about 350 mm above the tool chip interface. The cutting temperature is considered as an average of three values measured after 45 sec from the initiation of the machining process. Specification of the thermal imager is given in Table 3.7.

Figure 3.8 :Thermal imager

Table 3.7: Specifications of thermal imager

Description	**Value**
Temperature Measurement Range	-20^{o} +1200 ^{oC}
Best Temperature Measurement Accuracy	2 ^{o}C
Spatial Resolution IFOV	1.31mrad
Maximum Temperature Measurement	+1200 C
Refresh Rate	9Hz
Image Enhancement	IR-Fusion
Minimum Focus Distance	15cm
Focus Type	Automatic, Manual
Detector Resolution	320 x 240pixel
Visual Camera	Yes
Minimum Focus	15 cm
Display Resolution	640 x 480pixel
Auto Capture on Camera	Yes
Weight	1.04kg
Model Number	TI400
Emissivity	0.1 1

3.6.2 Cutting force

The cutting forces were measured using plug dynamometer shown in figure 3.9 by fixing it to the lathe tool post and the forces were measured by Dyno ware software. Cutting forces were obtained along X, Y, and Z directions. A charge amplifier (5070A) displays the values of the force and indicates the status of force measurement every second.

Dynamometer: Kistler (9257 B) type dynamometer was used for force measurement and it is shown in figure 3.9. The dynamometer consists of a four three-component force sensors fitted under high preload between a base plate and a top plate. Each sensor consists of three pairs of quartz plates, one sensitive to pressure in the z-direction and the other two responding to the shear in x and y directions respectively. The six components (three orthogonal components of a force Fx, Fy, and Fz and three torque components Mx, My, and Mz) were measured practically without displacement. These precision sensors are featured with high stiffness, high sensitivity, excellent repeatability, and long-term stability. They exhibit the inherent ruggedness of bonded strain gauge transducers and this is incorporated with rustproof material and protected against penetration of splash water and cooling agents. The top mounting surface of the sensor is equipped with a mounting tool post to hold lathe cutting tools. The forces and torque acting on the tool were transmitted to the top plate of a six-component dynamometer sensor. The charges yielded by the quartz plates were collected with electrodes connected to the connector of the sensor.

Figure 3.9 : Kistler six-component 9257 B type dynamometer

Figure 3.10 :Cutting force -charge amplifier &Data acquisition system

Charge Amplifier: The 5070A, 4-channel strain gauge amplifier was used for amplifying the output of the dynamometer from micro-volts to milli-volts as shown in Figure 3.10. It is a cost-effective, compact instrument suitable for high-resolution measurements. The front panelof the charge amplifier consists of a rotating knob, and an adjust and measure push-button for setting the ranges of the measuring characteristics. It has both analog and digital capabilities. In the analog mode, the output signal is rated up to +/- 10 volts and is suitable for input into an A/D convertor or some other device. In the digital mode, the output consists of an RS-232 serial connection. Amplifier Inputs and outputs are conveniently provided through single connectors located on the backside of the case.

Data Acquisition: Dyno Ware data acquisition and display software were used for further analysis of the signals obtained from the output through the charge amplifier.

3.6.3 Surface roughness

The surface roughness was measured by using surtonic S128 surface roughness tester (Figure 3.11) at different locations. The specifications of the surface roughness tester are presented in Table 3.8. Surface roughness was considered as an average of three values measured on the surface by using a roughness tester after machining.

Figure 3.11 :Surface roughness tester

Table 3.8: Specifications of surface roughness tester

Feature	Specification
Manufacturer	Taylor Hobson
Model	S128
Standard measuring range	400µm
Resolution	50nm
Sampling length	0.25-25.0mm

3.6.4 Coolant temperature

The coolant temperature of the coolant which was supplied through the nozzle of VTCS was measured using a K- type thermocouple which can be used to measure the temperature in the range of -20^0 to 1260°C (-326°F to 2300°F). The readings of the thermocouple were obtained by the temperature indicator as shown in Figure 3.12.

Figure 3.12:Temperature indicator

3.6.5 Tool wear

The generation of localized adiabatic zones adjacent to the cutting edge of the tool increases the tool wear during the machining of Ti-alloy due to its low thermal conductivity. A Scanning Electron Microscope is used to measure the flank wear of the tool in the machining process. SEM was used to examine the topography, morphology, composition, and crystallographic information. SEM uses electrons rather than light to form an image. The basic principle of SEM is an electron beam produced from the tungsten filament is focused with magnetic lenses and hits the specimen. The electron beam collides with the top surface of the specimen and signals are generated by the interaction of the electron beam with the specimen. Each of these signals is sensitive to a different aspect of the specimen and gives a variety of information about the specimen by detecting the signals which are emitted. The SEM setup [TESCAN make, Model: Vega LMU 3] used in this study is shown in Figure 3.13. and its specifications are shown in Table 3.9.

Table 3.9: Specifications of Scanning Electron Microscope

Component	Details
Make and Model	TESCAN, Vega LMU 3
Electron gun	Tungsten heated cathode
Resolution	High Vacuum Mode (SE): 3 nm at 30 kV / 2 nm at 30 kV Low Vacuum Mode: 3.5 nm at 30 kV / 2.5 nm at 30 kV
Magnification	2 1,000,000
Scanning Speed	From 20 ns to 10 ms per pixel adjustable in steps or continuously
Chamber Vacuum	High Vacuum Mode: < 10-3 9 Pa Medium Vacuum Mode: 3 150 Pa Low Vacuum Mode: 3 500 Pa*
Chamber and Column Suspension	Pneumatic
Specimen Stage	Movements: X = 80 mm (40 mm to +40 mm) Y = 60 mm (30 mm to +30 mm) Z = 47 mm Rotation : 360° continuous Tilt : 80° to +80° Maximum Specimen Height: 54 mm (with rotation stage) 81 mm (without rotation stage)

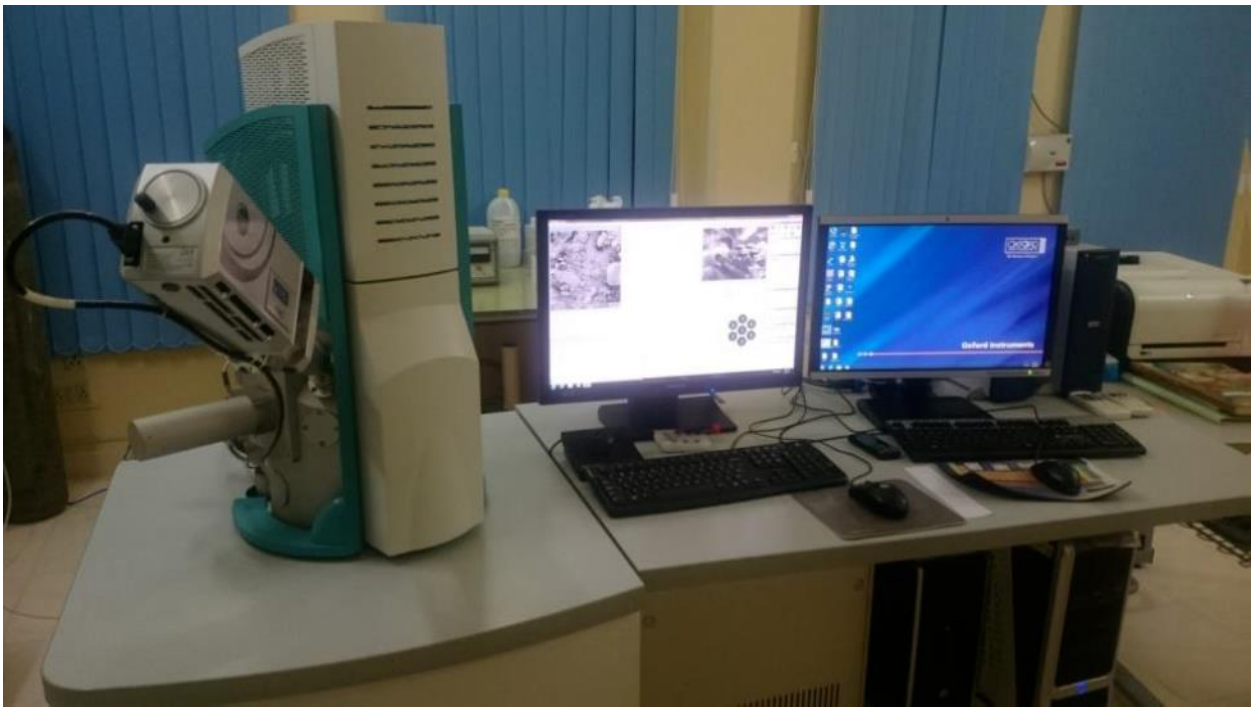

Figure 3.13 :Scanning electron microscopy

3.6.6 Chip morphology

The physical phenomena (phase changes, heat transfer, heat treatment, hardening) generated in the machining process will help in the analysis of the chips. The cutting parameters like cutting speed, feed, and depth of cut influence the physical phenomena and the chips produced can be directly observed using SEM. The chip analysis exposes physical phenomena that are generated in the machining process (heat transfer, hardening, phase changes, heat treatments, etc.). These physical phenomena are directly influenced by the cutting parameters applied to the process (feed, cutting speed, and depth**).** The chip produced by machining is observed by using SEM.

3.6.7 Residual stresses

To measure the residual stress on the surface, XRD (X-ray diffraction), a popular non-destructive testing technique, can be used. This technique measures the inter-atomic spacing of the material and can measure the residual stresses of the surface down to 30μm using portable or laboratory equipment. The wavelength of the X-Rays will be in terms of angstroms (Å), which is similar to the magnitudes of inter-planar or inter-atomic distances of polycrystalline solids. The development of the diffracted beams involves the constructive interference of scattered X-Rays from a polycrystalline solid. Inter-planar spacing (d) is obtained from the angles of maximum diffraction intensities of the planes of diffraction using Bragg's law. The value of 'd' is different for stressed and unstressed samples (d_0). The difference ($d-d_0$) is directly proportional to the residual stress magnitudes present in the workpiece. The grains are used as the internal strain gauges for residual stresses in practice. To measure the profiles of stresses, Panalytical X'pert pro MRD with X'pert stress software was used. Specifications of the X-Ray diffractometer are presented in Table 3.14.

Figure 3.14 :XRD equipment

Table 3.10: Specifications of the X-Ray diffractometer

Component	Details
Make & model	Panalytical X'Pert Pro
Source of X-rays	Cu-Kα, 1.54 Å wavelength
Detector	Pixel and Scintillation detector
Stage for sample	Fixed, with X-Ray source & Detector rotation
Filters	Nickel and copper
Range of masks	2 mm to 20 mm
Measurement range	5^o to 140^o

3.7 Summary

Experiments were conducted on turning of Ti-6Al-4V alloy under dry cutting, compressed air, single nozzle VTCS, and dual nozzle VTCS environments to evaluate its performance based on cutting force, cutting temperature, surface roughness, tool wear, residual stresses, and chip morphology. Standard equipment were used for every measurement.

4 SINGLE NOZZLE VORTEX TUBE COOLING SYSTEM

4.1 Introduction

This chapter includes the results of preliminary experiments performed on Ti-6Al-4V by supplying cold CO_2 gas in the machining zone. The cooling effect is produced by Joule Thomson expansion principle by expanding high pressure CO_2 gas. Based on the literature study it was found that supplying cold CO_2 gas provided better machinability. This leads to the development of a system that produces cooling effect with the vortex tube. fallowing this, the selection of a range of cold fractions is done based on COP, isentropic efficiency, and temperature drop. In VTCS the experiments were performed by varying the flow parameters i.e cold fraction, coolant pressure, and coolant temperature. The responses such as cutting force, cutting temperature, and surface roughness were measured by respective devices discussed in the experimentation chapter. RSM model was developed by using the experimental results and regression equations are generated. The most influencing parameters on the responses and the optimum combinations of flow parameters are derived by using the model. The experimental results obtained at the optimum combination are compared with the results of dry cutting under similar cutting conditions.

4.2 Single nozzle Vortex tube cooling system

In VTCS, cold compressive gas produced was directed towards the machining zone. From the preliminary experiments it was observed that cold compressed CO_2 as a coolant improves machinability in terms of cutting temperature, surface roughness and tool wear. In the current study, cooling effect was produced by the rotodynamic effect of vortex tube which is discussed in section 3.2. The selection of cold fraction plays an vital role in the use of vortex tube in coolng appliactions.

4.2.1 Selection of cold fraction range

Let p_i and Ti be inlet pressure and temperature of gas supplied to the vortex tube respectively. P_c and P_h are the pressures of cold and hot fluids. Tc and T_h are the temperatures of hot and cold fluids at the outlet of the vortex tube and γ is the specific heat ratio of the gas.

The isentropic efficiency of the vortex tube is given by [89],

$$\eta_{is} = \frac{T_i - T_c}{(T_i - T_c)_{rev}} \qquad (4.1)$$

$(\boldsymbol{T_i - T_c})_{\mathbf{rev}}$ of reversible expansion is given by

$$(\boldsymbol{T_i - T_c})_{\mathbf{rev}} = \boldsymbol{T_i}((\frac{\boldsymbol{P_i}}{\boldsymbol{P_{atm}}})^{(\gamma-1)/\gamma} - \mathbf{1})$$

$$\boldsymbol{\eta_{is}} = \frac{\boldsymbol{T_i - T_c}}{\boldsymbol{T_i}[(\frac{\boldsymbol{P_i}}{\boldsymbol{P_{atm}}})^{(1-1/\gamma)} - \mathbf{1}]} \qquad (4.2)$$

From Equation 4.2, it is observed that the isentropic efficiency of the vortex tube depends upon the coolant supply pressure and specific heat ratio of the gas. The gases having low specific heat ratio provide higher efficiency.

COP (Coefficient of performance) of the vortex tube is given by [89]

$$\boldsymbol{COP} = \frac{\boldsymbol{Q_r}}{\boldsymbol{W}} \qquad (4.3)$$

Where Q_r is the rate of cooling and W is the work input in watts.

$$\boldsymbol{Q_c} = \dot{\boldsymbol{m}}_{\mathbf{c}}\boldsymbol{C_p}(\boldsymbol{T_f - T_c})$$

$$\boldsymbol{W} = \dot{\boldsymbol{m}}_{\boldsymbol{i}}\boldsymbol{C_p}\boldsymbol{T_i}((\frac{\boldsymbol{P_i}}{\boldsymbol{P_a}})^{(\gamma-1)/\gamma} - \mathbf{1})$$

$$\boldsymbol{COP} = \frac{\dot{\boldsymbol{m}}_{\boldsymbol{c}}}{\dot{\boldsymbol{m}}_{\boldsymbol{i}}}\left[\frac{\boldsymbol{T_i - T_c}}{\boldsymbol{T_i}\left[\left(\frac{\boldsymbol{P_i}}{\boldsymbol{P_{atm}}}\right)^{(1-1/\gamma)} - \mathbf{1}\right]}\right] \qquad (4.4)$$

Where $\boldsymbol{C_p}$ is the specific heat of the gas, $\dot{\boldsymbol{m}}_{\boldsymbol{i}}$ is the mass flow rate of the gas supplied to the vortex tube, $\dot{\boldsymbol{m}}_{\boldsymbol{c}}$ and $\dot{\boldsymbol{m}}_{\boldsymbol{h}}$ are the mass flow rate through the hot and cold end of the vortex tube. The ratio of the mass flow rate at the cold end to the total mass flow supplied into the vortex tube ($\frac{\dot{\boldsymbol{m}}_{\boldsymbol{c}}}{\dot{\boldsymbol{m}}_{\boldsymbol{i}}}$) is known as cold fraction, and is denoted by $\boldsymbol{\epsilon}$. From equations 2 and 4 COP of the vortex tube is given by:

$$\boldsymbol{COP} = \boldsymbol{\epsilon} \times \boldsymbol{\eta_{is}} \qquad (4.5)$$

The COP of the vortex tube depends on the cold fraction, inlet pressure, and type of gas used (specific heat ratio).

In VTCS, selecting the cold fraction is an important aspect because it influences temperature drop, COP, and isentropic efficiency of the vortex tube. Initially, the vortex tube was calibrated for different cold fractions. This was done by measuring the cold outlet and inlet flow rate of CO_2 gas

and considering their ratio. The ratio is in the range of 0.1 to 0.9 which indicates 10% to 90% cold fraction. The temperature drop was evaluated experimentally by supplying gas through a vortex tube at different cold fractions at a constant pressure of 7 bar. COP and Isentropic efficiency of the vortex tube were evaluated by empirical relations given in Equations 4 and 5 presented in Table 4.1.

Table 4.1 :Analysis of vortex tube under different cold fractions at a pressure of 7 bar

Cold fraction (%)	**Temperature Drop (^{0}C)**	**Isentropic efficiency (%)**	**COP**
10	68	30.78557	0.030786
20	62	28.06919	0.056138
30	56	25.35282	0.076058
40	49	22.18372	0.088735
50	43	19.46734	0.097337
60	38	17.2037	0.103222
70	30	13.58187	0.095073
80	26	11.77095	0.094168
90	15	6.790934	0.061118

Figure 4.1 shows the variation of output parameters with cold fraction at a constant pressure of 7 bar. The secondary vertical axis in the figure indicates COP. It is observed that the drop in temperature and, isentropic efficiency decreased with an increase in cold fraction while COP of the vortex tube increased. For selecting the optimum cold fraction, RSM was used, and it was observed that a cold fraction of 25.3% provided the optimum values of temperature drop, isentropic efficiency, and COP. The vortex tube provided better cooling results in the cold fraction zone of 20 to 30 %. So, the values of cold fraction were selected as 10% ,20% and 30% for further experiments.

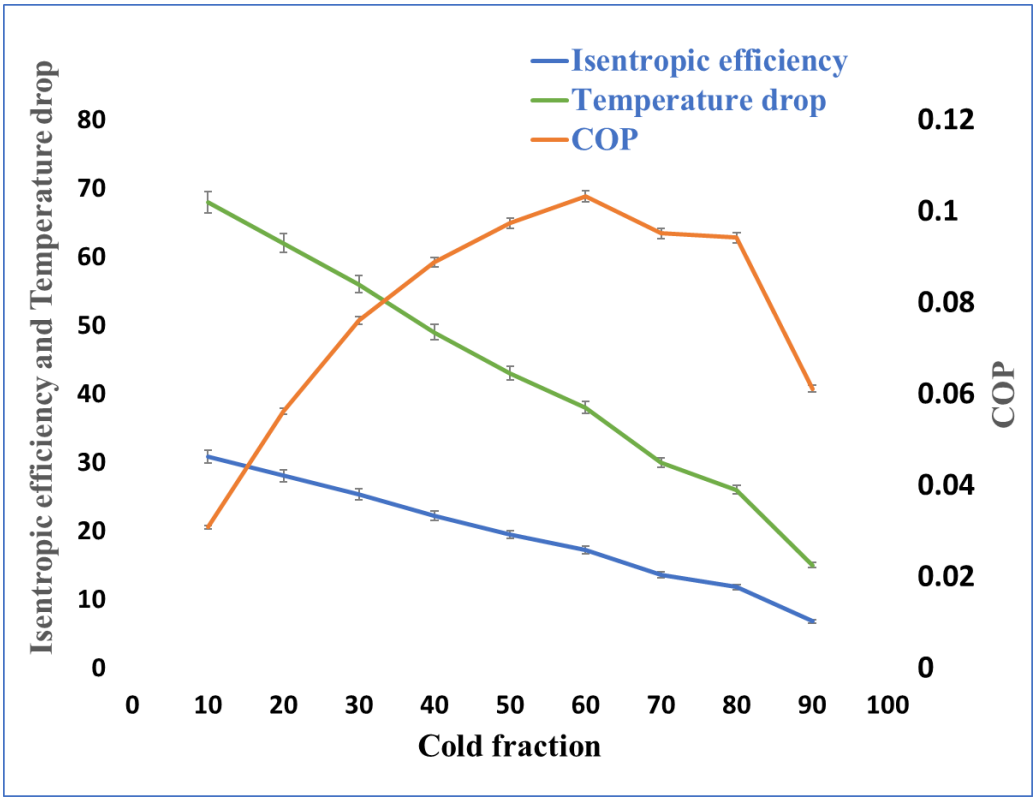

Figure 4.1:Analysis of vortex tube under different cold fraction at a pressure of 7 bar

4.2.2 Experimental results

The turning operation was performed by varying the flow parameters using VTCS after deciding the cold fraction range. The machining parameters i.e cutting speed, feed and were maintained at a constant value of 80 m/min, 0.25 mm/rev, and 1 mm respectively throughout the experiment. The responses were measured and analyzed at different levels of flow parameters discussed in the following sections. The VTCS flow parameters and outputs are shown in Table 4. 2.

Table 4.2: Experimental results in turning of titanium alloy

NO	Cooling Method	Coolant Temperature (^{0}C)	Pressure (bar)	Cold Fraction (%)	Cutting force (Newtons)	Cutting temperature (^{0}C)	Ra (microns)
1	VTC	-5	9	10	767	556.3	0.979
2	VTC	-15	9	10	787	550.7	0.773
3	VTC	-25	9	10	791	543.4	0.684

4	VTC	-5	9	20	895	547.8	0.743
5	VTC	-15	9	20	904	533.7	0.702
6	VTC	-25	9	20	917	518.4	0.596
7	VTC	-5	9	30	924	538.9	0.692
8	VTC	-15	9	30	939	522.5	0.631
9	VTC	-25	9	30	947	505.3	0.562
10	VTC	-5	7	10	667	602.5	1.08
11	VTC	-15	7	10	695	594.8	0.99
12	VTC	-25	7	10	724	585.2	0.74
13	VTC	-5	7	20	755	599.1	0.981
14	VTC	-15	7	20	787	579.5	0.975
15	VTC	-25	7	20	857	564.6	0.71
16	VTC	-5	7	30	892	582.9	0.773
17	VTC	-15	7	30	902	564.9	0.732
18	VTC	-25	7	30	913	558.2	0.656
19	VTC	-5	5	10	627	646.5	1.28
20	VTC	-15	5	10	635	639.4	1.14
21	VTC	-25	5	10	647	630.8	0.994
22	VTC	-5	5	20	675	635.3	1.04
23	VTC	-15	5	20	688	620.8	0.99
24	VTC	-25	5	20	704	605.5	0.726
25	VTC	-5	5	30	711	625.4	0.975
26	VTC	-15	5	30	735	609.8	0.773
27	VTC	-25	5	30	755	597.7	0.725

4.2.3 Effect of flow parameters on cutting temperature

The effect of coolant pressure and coolant temperature on cutting temperature during turning operation is shown in Figure 4.2 for 10%, 20%, and 30% of cold fraction. It is observed that cutting temperature reduced with a decrease in coolant temperature for all cold fractions. On the other hand, the increase in pressure reduced the cutting temperature. The maximum temperature of 646^0C was reported at a pressure of 5 bar for a coolant temperature of -5^{o}C for 10% of cold

fraction. The increase in coolant pressure reduced the cutting temperature significantly because of the higher convective heat transfer coefficient between the machining area and the cooling environment at a particular cold fraction.

$$\boldsymbol{Q = hA\Delta T} \qquad (4.6)$$

Where $\boldsymbol{Q}$ is the heat transfer rate in w, A is the surface area exposed to the fluid in m^2, $\boldsymbol{\Delta T}$ is the difference between cutting temperature and coolant temperature in ºC and 'h' is the convective heat-transfer coefficient in w/m^2-ºC. It can be observed from equation 4.6 that heat transfer can be enhanced either by increasing 'h' or by achieving alarge temperature difference or a combination of both as the machining area will remain constant. A higher temperature difference is achieved by lowering the coolant temperature and an increase in 'h' is obtained by increasing the pressure. The increase in 'h' is due to the increase in pressure of coolant (2000 W/m^2 K at 4-7 bar) compared to dry machining (20 W/m^2-K)[49]. Furthermore, there is a significant temperature drop due to the lower temperature of CO_2. CO_2 gas is cooled by the rotodynamic effect when passing through the vortex tube. This increases the rate of heat removal and helps to lower the cutting temperature. This is due to the combined effect of h and $\mathbf{\Delta T}$. The increase in cold fraction reduced the cutting temperature as CO_2 absorbs heat produced during machining operation which is expressed by Equation 4.7. It is also observed that the cutting temperature decreased slightly from decreasing the coolant temperature. From equation 4.6, the heat transfer rate is proportional to $\mathbf{\Delta T}$ which is the difference between the cutting tool temperature and coolant temperature. The change is $\mathbf{\Delta T}$ value is lower when the cutting temperature is varied between -5^0C and -25^0C which leads to low change in heat transfer. Due to this, the change in cutting temperature is also marginal as can be observed in figure 4.2.

$$\boldsymbol{Q = \dot{m}c\Delta T} \qquad (4.7)$$

Where Q is the heat absorbed in w, $\dot{\mathbf{m}}$ is the mass flow rate of CO_2 gas in kg/s, and $\mathbf{\Delta T}$ is the difference in temperature between the exposed surface and CO_2 gas in ºC. Figure 4.2 indicates that cutting temperature decreased at higher cold fraction. This is due to a large amount of CO_2 gas available to absorb heat on the machining surface at higher cold fraction, as illustrated in equation 4.7

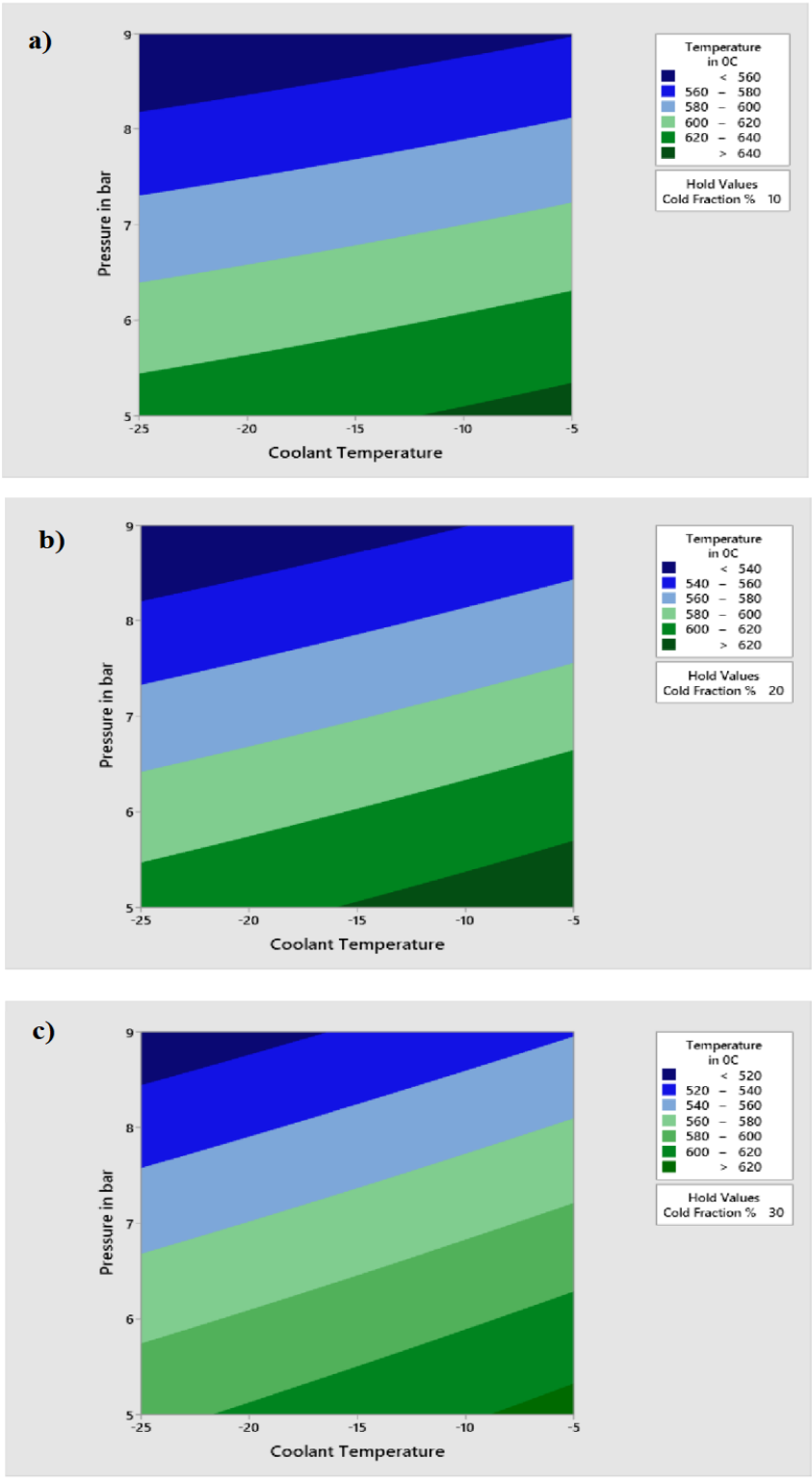

Figure 4.2: Variation of cutting temperature with coolant temperature and pressure at (a) 10% of cold fraction, (b) 20% of cold fraction (c) 30% of cold fraction

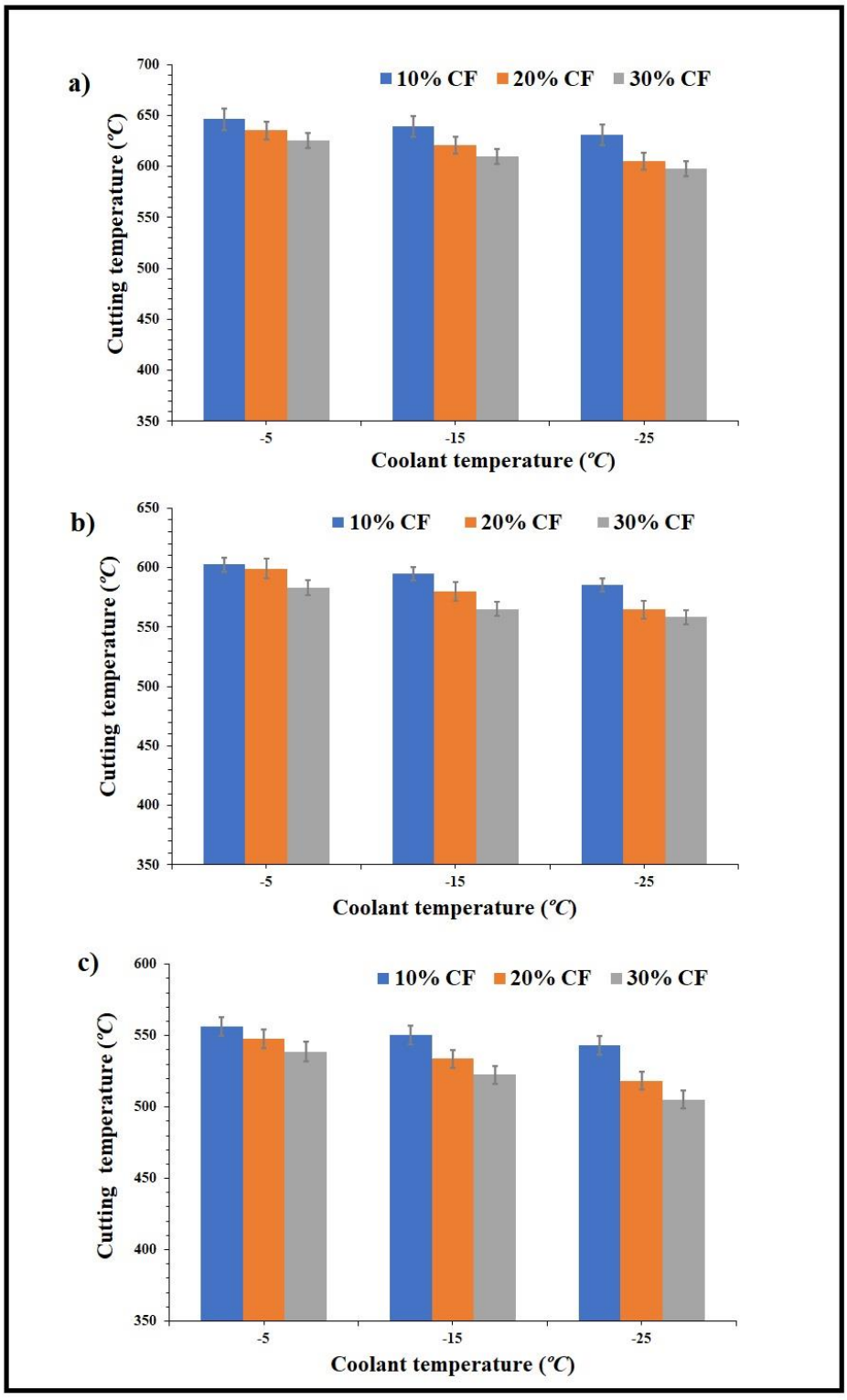

Figure 4.3: Variation of cutting temperature with coolant temperature and cold fractions at a pressure of (a) at 5 bar (b) at 7 bar (c) at 9 bar

4.2.4 Effect of flow parameters on cutting force

Figure 4.4 shows the effect of pressure and coolant temperature on cutting temperature during the turning operation for a cold fraction of 10%, 20%, and 30% respectively. It was observed that coolant temperature impacted cutting force significantly. Subsequently, the increase of cold fraction and pressure increased the cutting force even more. For example, at a pressure of 5 bar and a cold fraction of 10% the force obtained was 647 N; on the other hand at 9 bar pressure, and 10% of cold fraction the cutting force value obtained was 791 N at the same coolant temperature of -25^{o}C. Hence, cutting force increased by 22.25% with an increase of pressure from 5 bar to 9 bar. The minimum cutting force was observed at 5 bar,10% cold fraction, and at -5^{o}C of coolant temperature.

Figure 4.5(a), (b), and (c) show the effect of cold fraction on cutting force for different coolant temperatures at 5,7, and 9 bar pressures respectively. It was observed that cutting force at all coolant temperatures increased with an increase in cold fraction of CO_2. The increase in cutting forces was due to the following reasons: Primarily, the flow of gas at higher speed from the nozzle into the machining zone increases the pressure on the tool due to the application of impulse force. Impulse force can be defined as:

$$Fi = m(V_i - V_f)/t \qquad (4.8)$$

Where V_i is initial velocity of coolant,V_f is final velocity of coolant and m/t is the mass flow rate. In vortex tube cold fraction is proportional to the mass flow rate. Hence, at higher cold fractions the m/t value is high which acts as higher impulse force on the tool based on equation 4.8. The second one is the cooling effect of CO_2 on the hot surface of the workpiece which causes strain hardening and increases the ultimate strength which demands higher cutting force to shear the material.

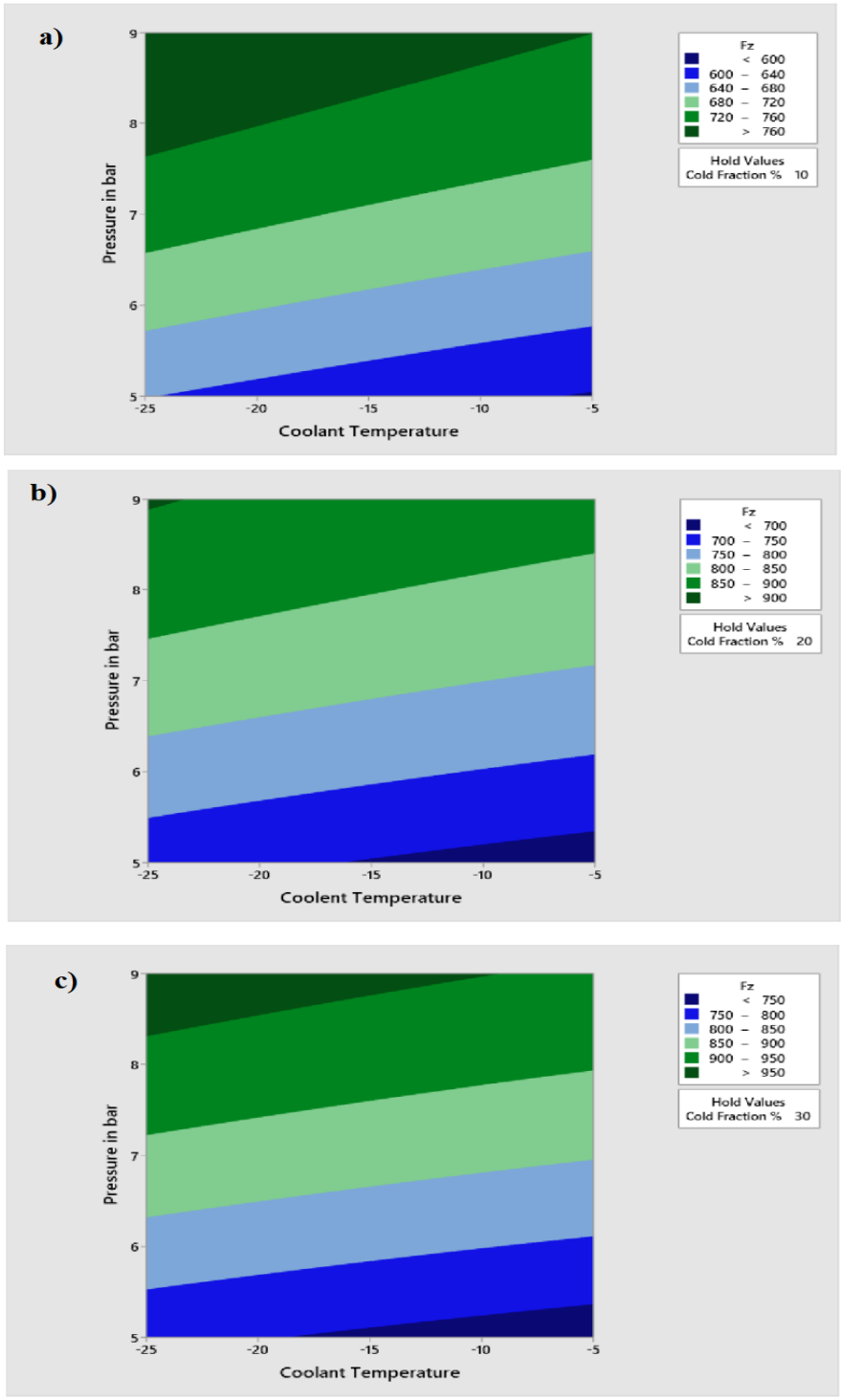

Figure 4.4*:* Variation of cutting force with coolant temperature and pressure at (a) 10% of cold fraction, (b) 20% of cold fraction (c) 30% of cold fraction

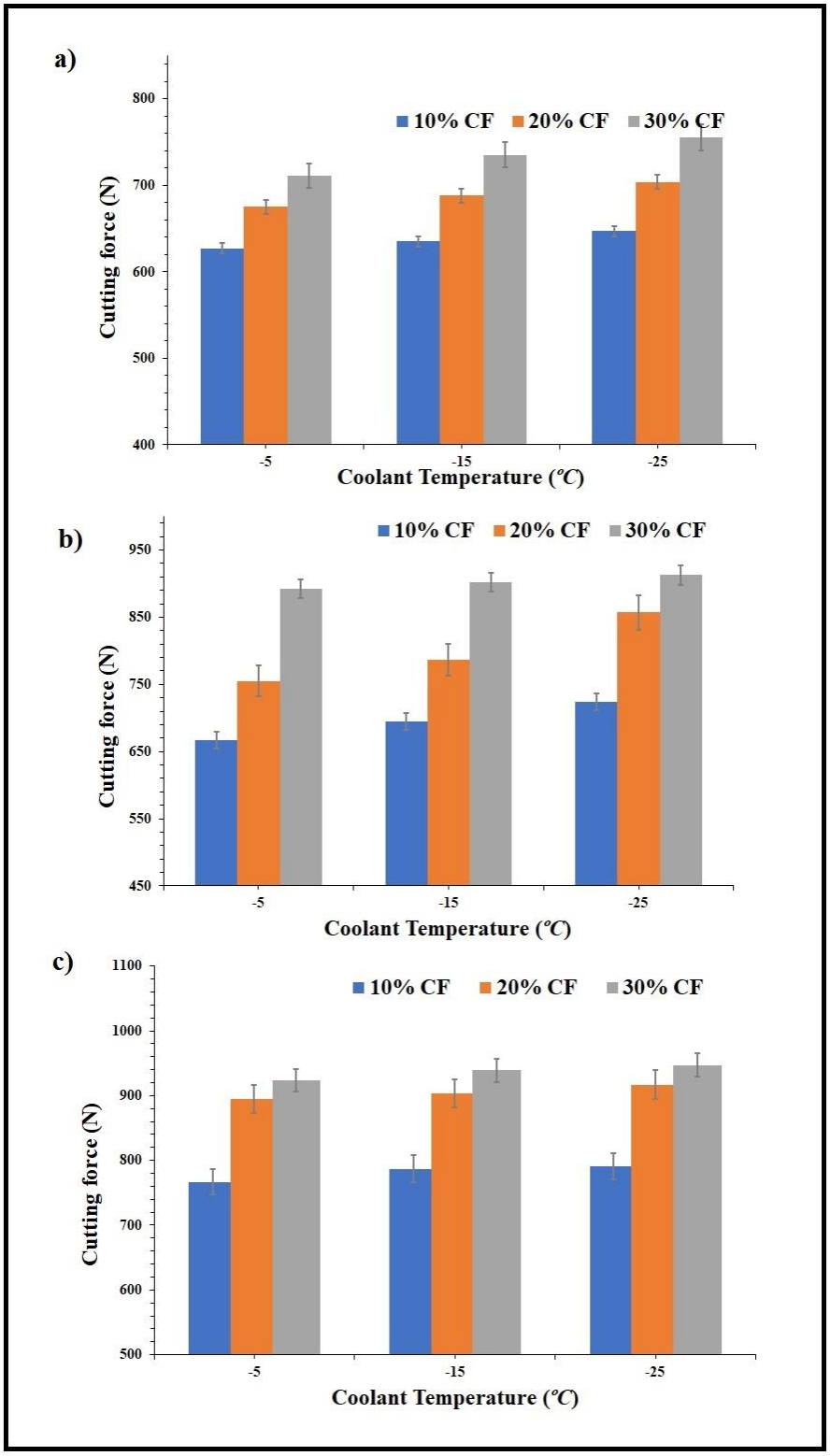

Figure 4.5: Variation of cutting force with coolant temperature and cold fraction at pressure of (a) 5 bar (b) 7 bar (c) 9 bar

4.2.5 Effect of flow parameters on surface roughness

Surface roughness is one of the vital parameters in any machining operation to ensure the quality of the machined surface. Hence, surface roughness is measured after machining at each condition. Figure 4.6 shows the effect of pressure and coolant temperature on surface roughness obtained during the turning operation for a cold fraction of 10%, 20%, and 30% respectively. It can be observed from Figure 4.7 that surface roughness value was high at lower cold fraction for all operating pressures. The reason for getting a better surface finish at high cold fraction is due to low coefficient of friction (μ) offered by CO_2 at tool-workpiece interface, which reduces the frictional force in machining. The reduced frictional force causes lower amount of rubbing action between the tool and the workpiece, which improves surface finish. The surface roughness obtained was 0.562 microns at -25^0C for a gas pressure of 9 bar with a 30% cold fraction. Similarly, at 5 bar of pressure, surface roughness obtained was 0.725 microns at the same cold fraction and coolant temperature. From the above, it is concluded that better surface finish occurs at high pressure because at high pressure CO_2 gas penetrates tool-workpiece interface effectively which enhances surface finish. The surface finish improved at lower coolant temperature because of reduction in generated heat at the tool chip interface [90]. Therefore, it can be concluded that pressure, cold fraction, and coolant temperature significantly affect surface roughness.

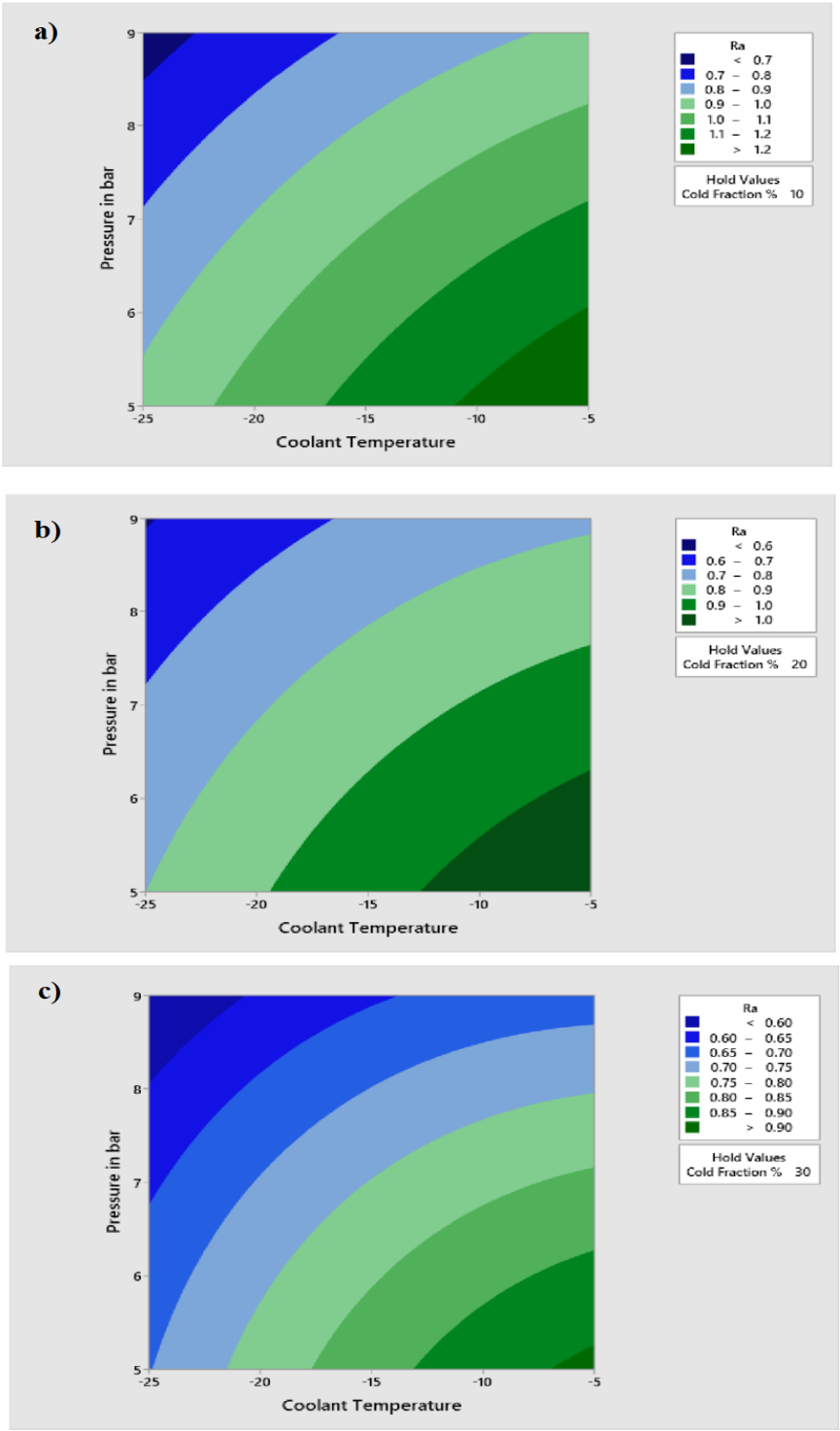

Figure 4.6: Variation of surface roughness with coolant temperature and pressures at (a) 10% of cold fraction, (b) 20% of cold fraction, (c) 30% of cold fraction

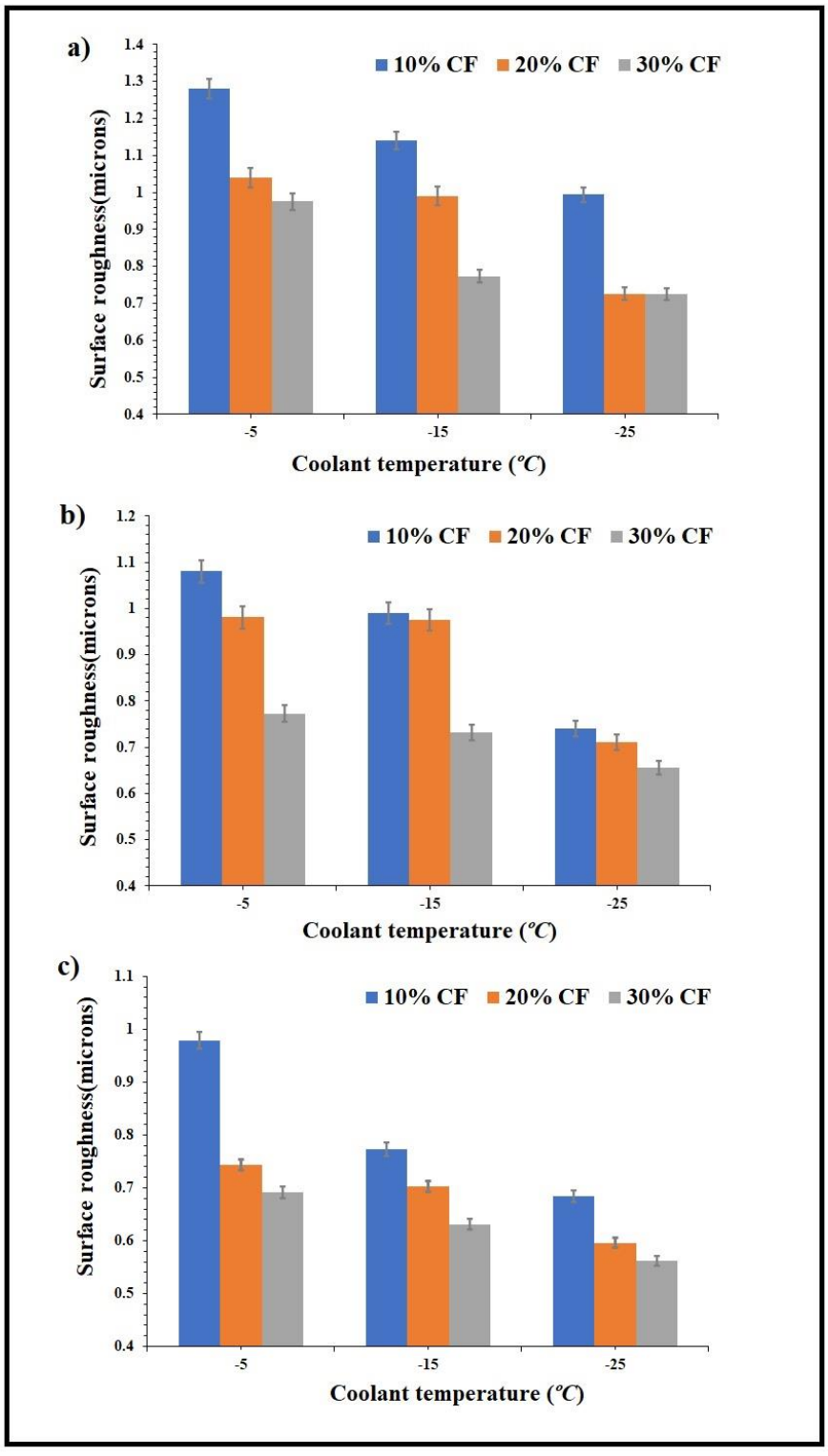

Figure 4.7: Variation of surface roughness with coolant temperature and cold fraction at a pressure of (a) 5 bar (b) 7 bar (c) 9 bar

4.3 Modelling

RSM was used to create a model by using experimental results data of VTCS assisted turning of Ti-6Al-4V. In this view, coolant temperature (T_c), pressure (P_c), and cold fraction (C_f) were selected as input parameters. The results obtained from experiments such as T_m, F_z, and Ra were used as output variables. MINITAB software was used to study RSM and perform analysis [91]. The levels and other constraints were selected and based on that experiments were performed. RSM was used to study the dependence of output variables on input parameters in the form a polynomial equation.

$$Z = a_0 + \sum_{i=1}^{k} a_i x_i + \sum_{i=1}^{k} a_{ii} x_i^2 + \sum_{i<j-2}^{2} a_{ij} \varkappa_i x_j \pm \epsilon_r \qquad (4.9)$$

where Z is the output response a0, ai, aii, and aij are coefficients, εr is the experimental error, and xiis the independent input parameters.

4.3.1 ANOVA for the fitted RSM model

To obtain practical (% contribution ≥ 10) and statistical significance ($p \leq 0.05$) of various machining parameters on output responses such as T_m, F_z, and *Ra,* ANOVA was performed at 95% confidence level. It is known that F (high) and P(low) values show the effectiveness of the output results. ANOVA for the fitted RSM model of output variables is shown in Table 4.3. Other parameters forms such as degree of freedom, sum of squares, and mean squares comprise ANOVA. ANOVA analysis was carried out for T_m, F_z, and *Ra* by taking pressure, coolant temperature, and cold fraction as input variables. The statistical data obtained from ANOVA analysis for T_m, F_z, and *Ra* are shown in Tables 4.3 to 4.6 respectively. The percentage contribution of individual factors is the ratio of individual SS (sum of squares) to the total SS multiplied by 100. From the ANOVA results, the percentage contribution of coolant temperature, pressure, and cold fraction on Tm were 6.8%, 84.28%, and 7.96% respectively (from Table 4.4), on cutting force they were 2.2%,54.96%, and 36.36% respectively (from Table 4.5), and on Ra, they were 28.7%,32.37%, and 28.52% respectively (from Table 4.6).

Table 4.3: The ANOVA for the fitted RSM model

Output	S	R-sq	R-sq(adj)	R-sq(pred)
T_m	3.13869	99.60%	99.38%	99.01%
F_z	26.8511	95.77%	93.54%	89.41%
Ra	0.0550292	94.23%	91.18%	84.81%

Table 4.4: The response ANOVA table for cutting temperature

Source	DF	Adj SS	Adj MS	F-Value	P-Value
Model	4	41310.9	10327.7	977.82	0.000
Linear	3	41176.9	13725.6	1299.53	0.000
T_C	1	2827.5	2827.5	267.71	0.000
P_C	1	35041.9	35041.9	3317.73	0.000
C_F	1	3307.6	3307.6	313.16	0.000
2-Way Interaction	1	134.0	134.0	12.69	0.002
T_C* C_F	1	134.0	134.0	12.69	0.002
Error	22	232.4	10.6		
Total	26	41543.3			

Table 4.5: The response ANOVA table for cutting force

Source	DF	Adj SS	Adj MS	F-Value	P-Value
Model	3	271416	90472	111.58	0.000
Linear	3	271416	90472	111.58	0.000
T_C	1	6498	6498	8.01	0.009
P_C	1	159424	159424	196.63	0.000
C_F	1	105494	105494	130.11	0.000
Error	23	18648	811		
Total	26	290064			

Table 4.6: The response ANOVA table for surface roughness

Source	DF	Adj SS	Adj MS	F-Value	P-Value
Model	3	0.80052	0.266840	66.49	0.000
Linear	3	0.80052	0.266840	66.49	0.000
T_C	1	0.25681	0.256806	63.99	0.000
P_C	1	0.28905	0.289053	72.03	0.000
C_F	1	0.25466	0.254660	63.46	0.000
Error	23	0.09230	0.004013		
Total	26	0.89282			

From experimental results and ANOVA analysis, it is observed that pressure had significant effect on Tm and Fz compared to other two parameters. The h value increases significantly with pressure which caused a higher rate of heat transfer leading to a reduction in Tm effectively (Figure 4.8). The velocity of the stream increases significantly with an increase in pressure which restricts the tool movement that leads to increase in Fz (Figure 4.9). All three parameters have a significant effect on surface roughness but the effect of cold fraction and coolant temperature was slightly lower than that of pressure. This was because of the combined effect of a lower coefficient of friction and lower cutting temperature (Figure 4.10). The main effect plots for cutting temperature, cutting force, and surface roughness are shown in Figure 4.11 respectively.

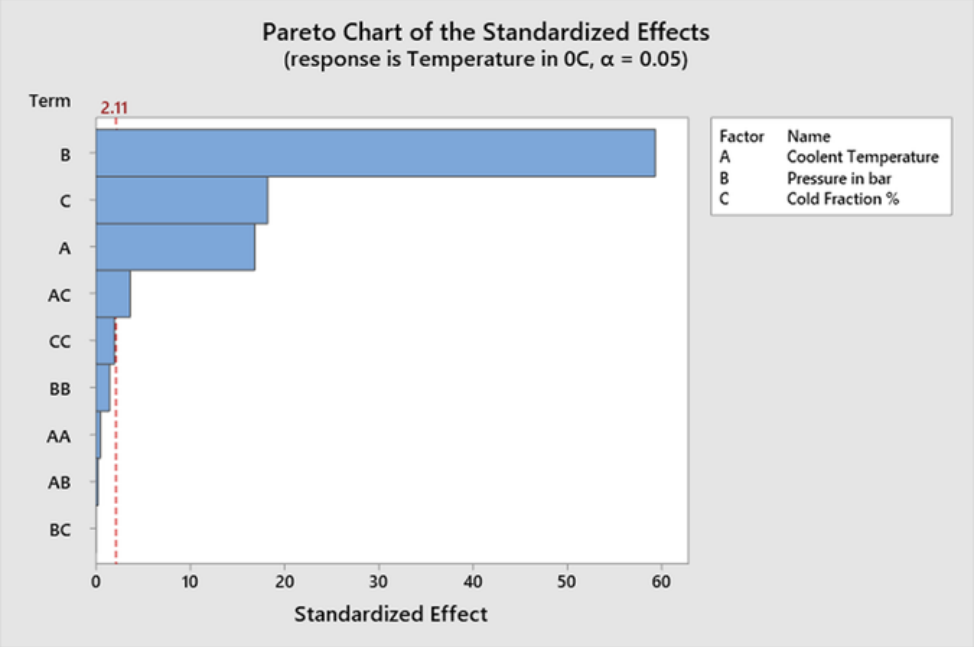

Figure 4.8: Interaction effects of input variables on cutting temperature

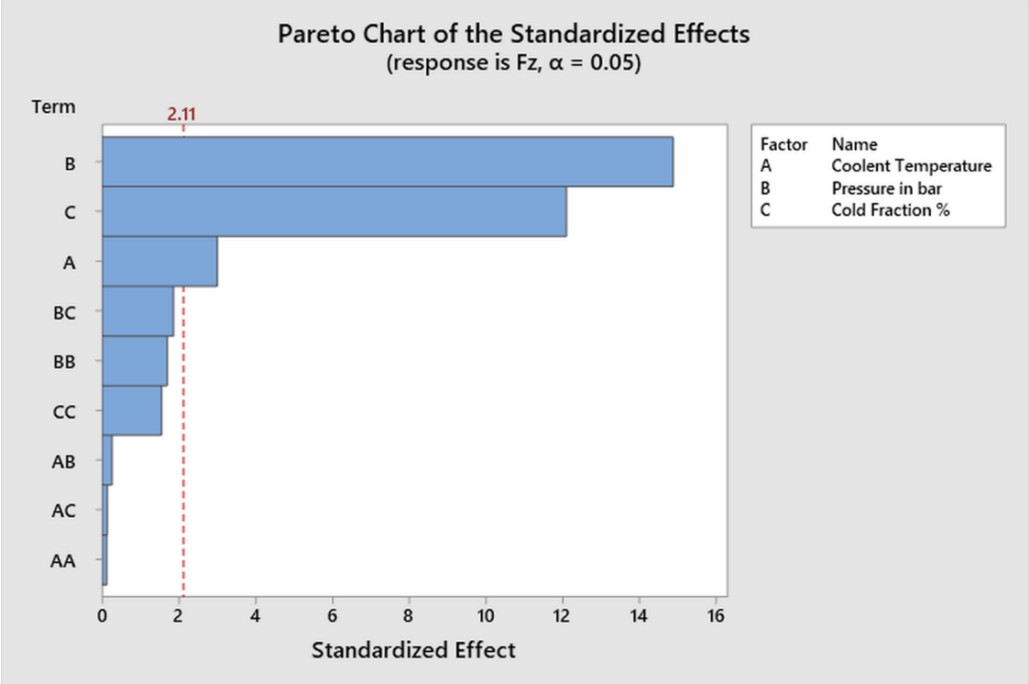

Figure 4.9: Interaction effects of input variables on cutting force

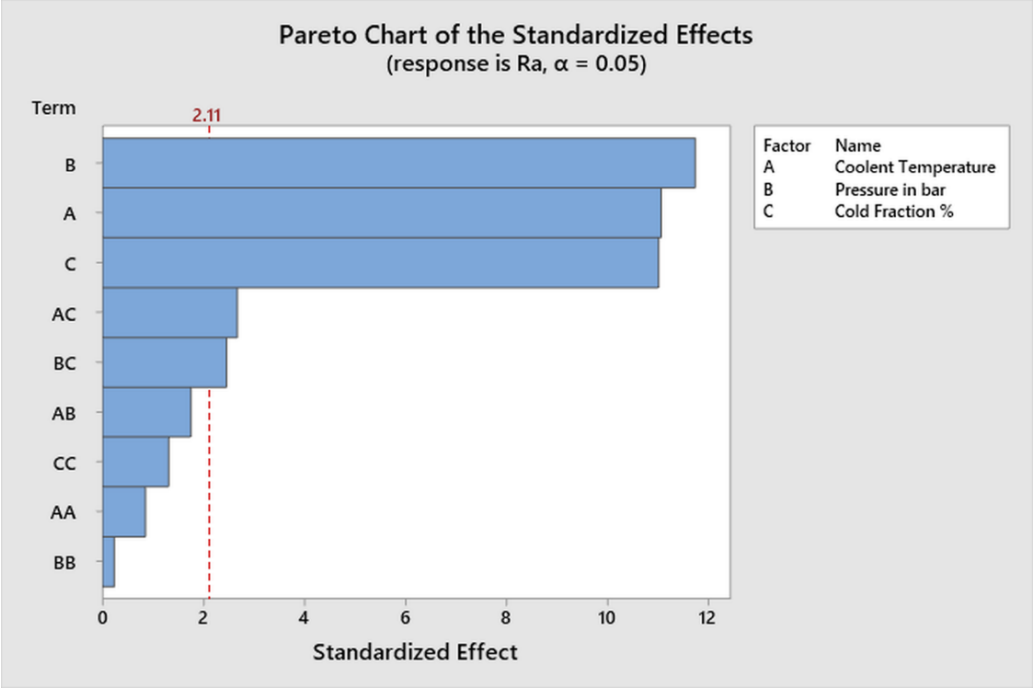

Figure 4.10**:** Interaction effects of input variables on surface roughness

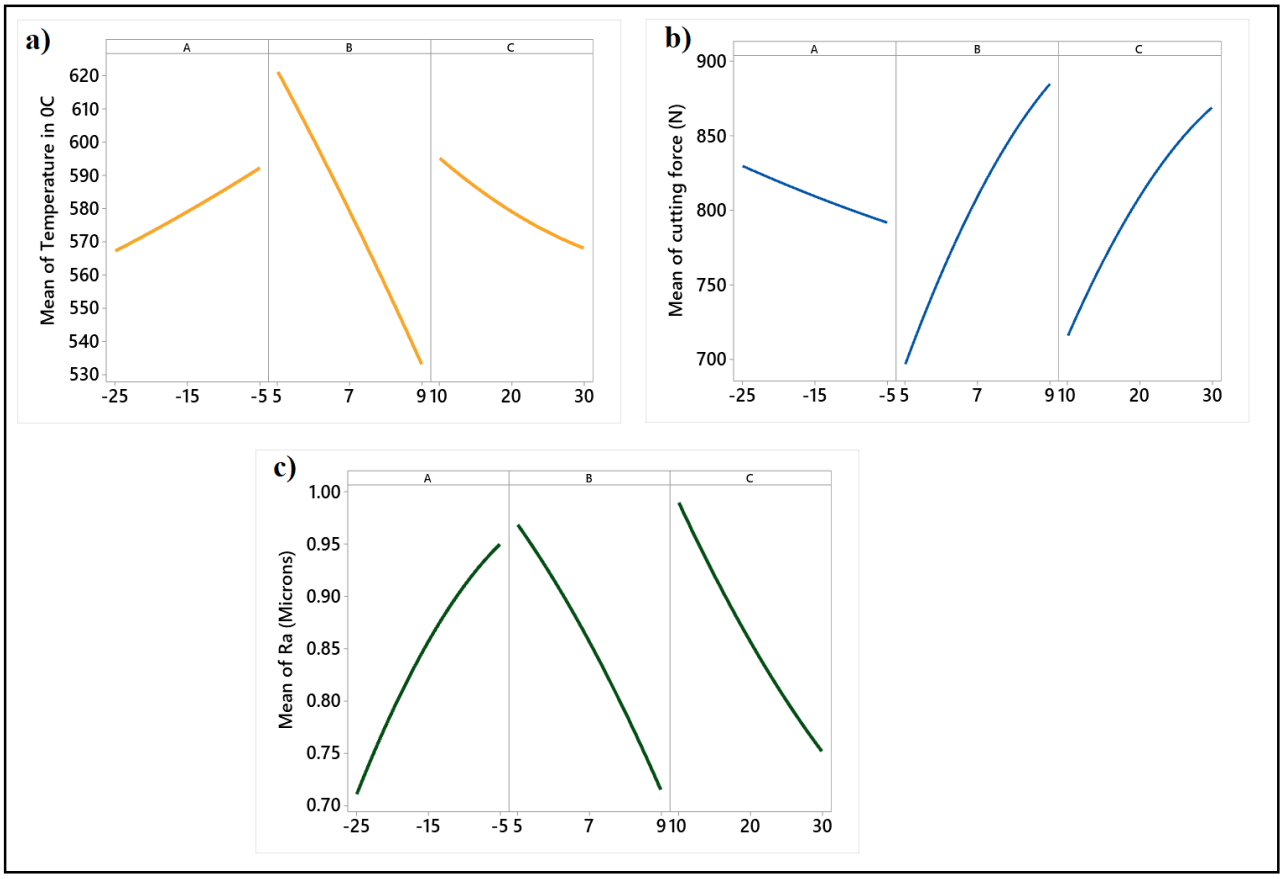

Figure 4.11: Main effect plots for (a) Cutting temperature (b) Cutting force (c) Surface roughness

4.3.2 Regression analysis

To establish the relation between the input and output variables, as mentioned earlier, regression analysis (ANOVA) was carried out at a confidence level of 95%. Three polynomial equations were obtained to predict the *Tm*, F_z, and *Ra* values based on the experimental results.

$$Tm = 756 + 0.700\,T_c - 15.06\,P_c - 1.875\,C_f + 0.0064\,T_c^2 - 0.489\,P_c^2 + 0.0254\,C_f^2 + .0112\,P_c{*}T_c + 0.03342\,C_f{*}T_c + 0.0004\,P_c{*}T_c \quad (4.10)$$

$$Ra = 1.986 + 0.01919\,T_c - 0.0609\,P_c - 0.0342\,C_f - 0.000264\,T_c^2 - 0.00374\,P_c^2 + 0.000141\,C_f^2 - 0.001158\,P_c{*}T_c - 0.000353\,C_f{*}T_c + 0.001625\,P_c{*}T_c \quad (4.11)$$

$$Fz = 592 - 2.42\,T_c + 99.5\,P_c + 9.57\,C_f + 0.013\,T_c^2 - 4.67\,P_c^2 - 0.170\,C_f^2 + 0.100\,P_c{*}T_c + 0.0108\,C_f{*}T_c + 0.721\,P_c{*}T_c \quad (4.12)$$

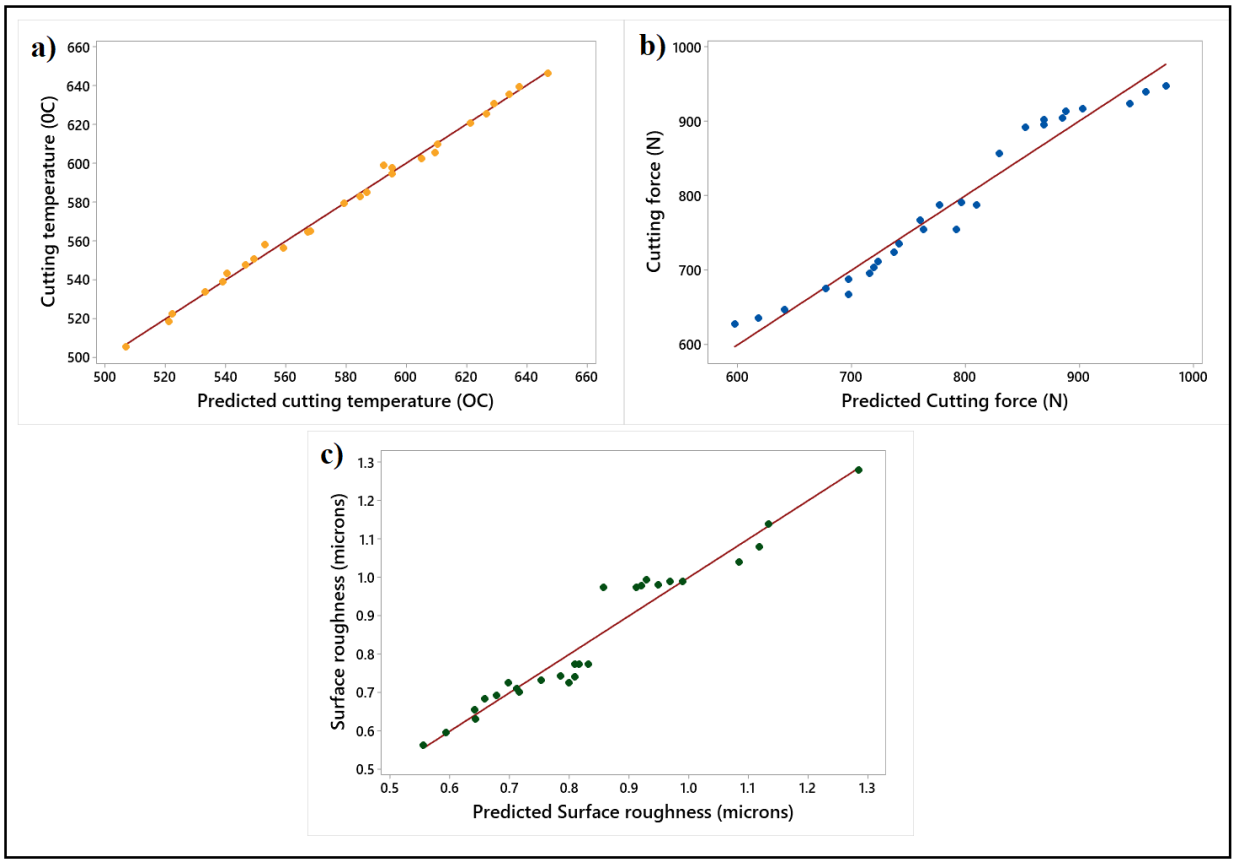

Figure 4.12: Regression fit for (a) Cutting temperature (b) Cutting force (c) Surface roughness

The values of cutting temperature, cutting force, and surface roughness obtained using the above equations were compared with experimental results. Figure 4.12 shows the comparison of the cutting temperature, cutting force, and surface roughness results found from the proposed model and experimental data. It can be observed that the predicted model and the experimental results show consistency with each other. Hence, this equation can be used to predict the values of cutting temperature, cutting force, and surface roughness under coolant temperature from -5 to -25 ºC, pressure from 5 to 9 bar, and cold fraction from 10% to 30%.

4.3.3 Response optimization

Optimization for the responses of the vortex tube cooling system was performed with RSM. The optimized results are shown in Table 4.7. The optimum response is shown at a coolant temperature of -25^0C, with a pressure of 9 bar and 13.8% of cold fraction. The composite desirability was found to be 0.915, which is acceptable for the optimum response. However, individual desirability for T_m, F_z, and *Ra* are 0.93,0.80, and 0.95 respectively as shown in Figure

4.13. Based on individual desirability, it is observed that optimized values wre significant. Responses are found in the model for the optimum conditions shown in Table 4.7.

Table 4.7: Optimum value of flow parameters and responses by composite desirability function

Solution	Coolant Temperature	Pressure in bar	Cold Fraction %	Temperature in ^{0}C Fit	F_z Fit	Ra Fit	Composite Desirability
1	-25	9	13.8384	532.355	841.493	0.629255	0.915657

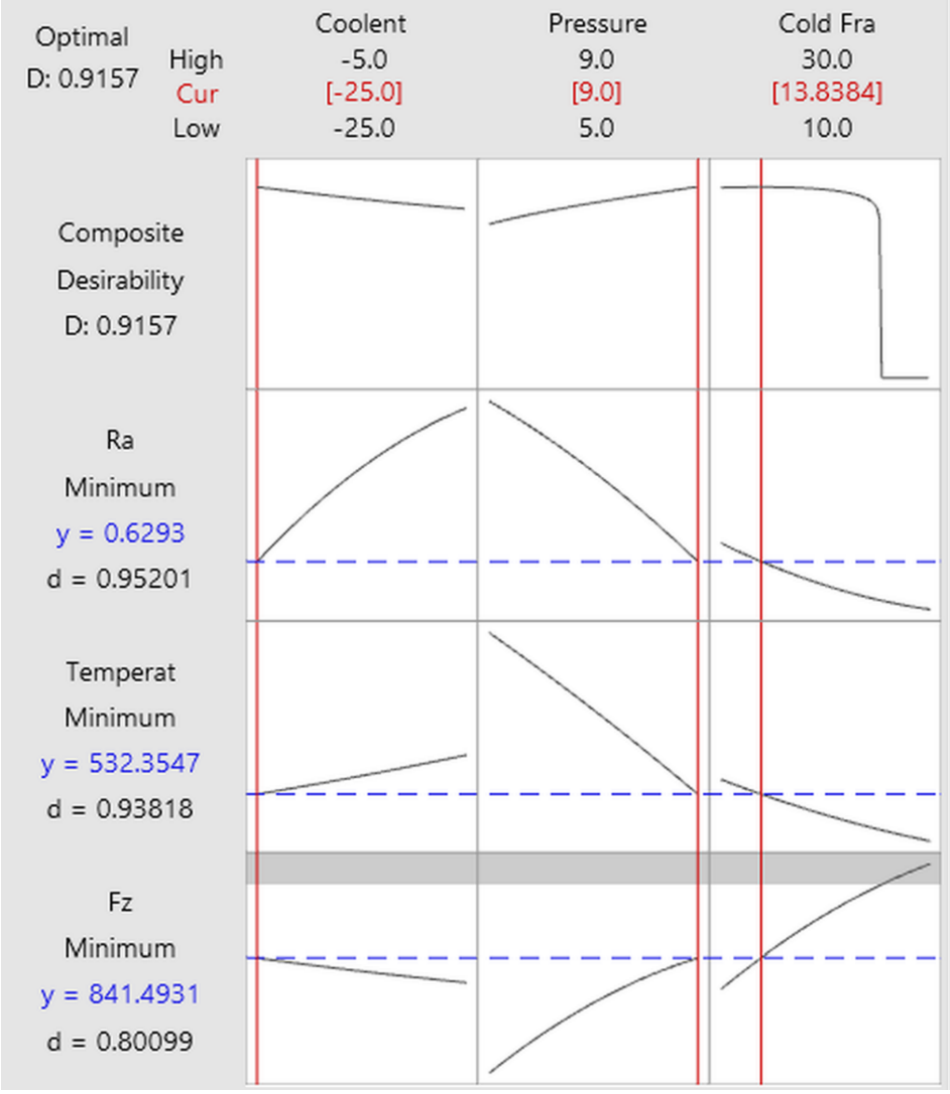

Figure 4.13: Optimization of Surface roughness, Cutting Temperature and Cutting force by composite desirability

4.3.4 Validation of the optimized model

The response obtained from RSM was validated with experimental results. For this purpose, the vortex tube was again calibrated for 13% of cold fraction. The turning operation was performed at optimum conditions by taking the same input parameter as taken earlier for the experiment. Output parameters were obtained as shown in Table 4.7. The experiential values were compared with output values given by the model. The percentage error obtained was less than 5% and hence the proposed model may well predict the results with low deviation.

Table 4.8 :Response in dry cutting condition and VTCS (experimental and RSM)

Output parameters	Dry cutting condition	VTC condition (experimental)	VTC condition (RSM Technique)	% of error
Cutting temperature (^{0}C)	785	541	532.22	3.3%
Cutting force (N)	610	828	841.4	1.57%
Surface roughness (microns)	2.17	0.661	0.629	4.8%

The response outcomes of RSM for dry cutting and VTCS at optimum conditions are given in Table 4.9. It is observed that VTCS provides better machining characteristics in terms of cutting temperature and surface roughness compared to dry cutting whereas cutting forces are higher in the case of VTCS. On the other hand, RSM provides an accurate prediction for optimized parameters.

4.4 Summary

The vortex tube cooling system was developed and experiments were performed by varying the coolant pressure, cold fraction, and coolant temperature. The individual effects and interaction effects of input parameters on responses were analyzed. The optimum combination of input parameters and most impacting parameters on the response were identified using RSM technique. At the optimum combination, the results of VTCS were compared with dry cutting. It was found that VTCS provided better results in terms of cutting temperature and surface roughness due to effective cooling of cold compressed CO_2 gas. However, higher cutting forces were observed under VTCS due to strain hardening of the workpiece and impulse force applied by the cold stream on the cutting tool. To overcome this limitation, the existing setup was modified and experiments were conducted at different parametric ranges discussed in detail in the succeeding chapter.

5 DUAL NOZZLE VORTEX TUBE COOLING SYSTEM

5.1 Introduction

This chapter discusses the machinability study of Ti-6Al-4V under dual nozzle vortex tube cooling system in which cold CO_2 gas was supplied using two similar nozzles. In dual nozzle VTCS, initially, the effect of nozzle configuration i.e nozzle angle, tip nozzle distance, and nozzle diameter on cutting force, cutting temperature, and surface roughness is discussed. Further, the effect of flow parameters and machining parameters on the responses are analyzed. The better combinations of flow and machining parameters were evaluated for performance improvement. To analyze the performance of dual nozzle VTCS, parameters such as cutting force, cutting temperature, surface roughness chip morphology, tool wear, and surface residual stress were evaluated. Further, the results obtained under dual nozzle VTCS were compared with other sustainable cooling methods at the same input conditions.

5.2 Dual nozzle vortex tube cooling system

A single nozzle vortex tube cooling system used as a cooling source in the machining of Ti-6Al-4V provided effective results in terms of cutting temperature, and surface roughness when compared to dry cutting. But the cutting force was significantly higher due to the strain hardening effect and impulse force. To overcome this limitation, the experimental setup was modified in which two nozzles were used for the supplied coolant. To find the advantages of dual nozzle, VTCS the results were compared with single nozzle VTCS under the same conditions (Optimum conditions evaluated in the previous chapter) presented in Table 5.1. The cutting force reduced by 15% whereas the rise in cutting temperature and surface roughness was less than 5 % in dual nozzle VTCS compared to single nozzle VTCS. From these experimental results, it is observed that the limitation of single nozzle VTCS was minimized to a certain extent with the use of dual nozzle VTCS.

Table 5.1: Single vs dual nozzle VTCS

Environment	Cutting Force (N)	Cutting Temperature(^{0}C)	Surface Roughness(µm)
Dual nozzle VTCS	703	538	0.692
Single nozzle VTCS	828	523	0.668

5.3 Effect of nozzle configuration on response parameters

The turning operation was performed on the lathe machine by attaching a dual nozzle VTCS setup. The nozzle angle, nozzle position from the cutting edge, and nozzle diameter were varied at different levels and the responses i.e cutting force, cutting temperature, and surface roughness were measured and analyzed. The cold fraction, coolant pressure, and machining parameters were maintained constant throughout the experiment. Their values are 7 bar, 20%,80 m/min,0.25 mm/rev, and 21 mm respectively.

5.3.1 Cutting force

Being a vital factor in increasing the specific cutting energy and power consumption, cutting force occurs mainly because of two major factors. The first one would be the resistance offered by deformation of Ti-6Al-4V and the other is the force generated by impulse-momentum of high speed gas stream flushing out of the nozzle. The force caused due to impulse-momentum of coolant is given by:

$$F = \rho a v^2 \ldots\ldots\ldots\ldots\ldots\ldots\ldots\ldots\ldots (5.1)$$

Where 'ρ' is density of the coolant, 'a' is the area of cross-section of the nozzle outlet and 'v' is the velocity of the coolant. The axis of the nozzle was maintained at an angle of θ to the horizontal plane.

From Figure 5.1, it is observed that the cutting force increased with nozzle angle (θ). The cold compressed gas with high velocity was focused on the cutting tool thus creating an impulse force equal to $\rho a v^2$ in the direction of the nozzle axis as shown in Figure 5.2. The force can be resolved in two components, vertical and horizontal. The vertical component ($2\rho a v^2 \sin\theta$) opposes the tool movement leading to an increase in cutting force and the horizontal component($\rho a v^2 \cos\theta$) of the two nozzles doesn't exhibit any significant effect since they oppose each other. Therefore, by increasing the nozzle angle, the vertical component increases which in turn leads to a rise in cutting force.

Figure 5.1 shows that the cutting force is mostly affected by the tip-nozzle distance i.e. increasing the tip-nozzle distance decreased the cutting force. This is because at higher distances the time of impact is more which reduces acceleration ($a = \frac{\Delta v}{\Delta t}$) of the coolant and therefore reduces the cutting force on the cutting tool. Along with this, the kinetic energy of the ejected fluid

depends on the velocity and the amount of the coolant. This energy gets diminished during the travel duration. Hence, this low energy coolant is responsible for generating low cutting force when the tip nozzle distance is high [92].

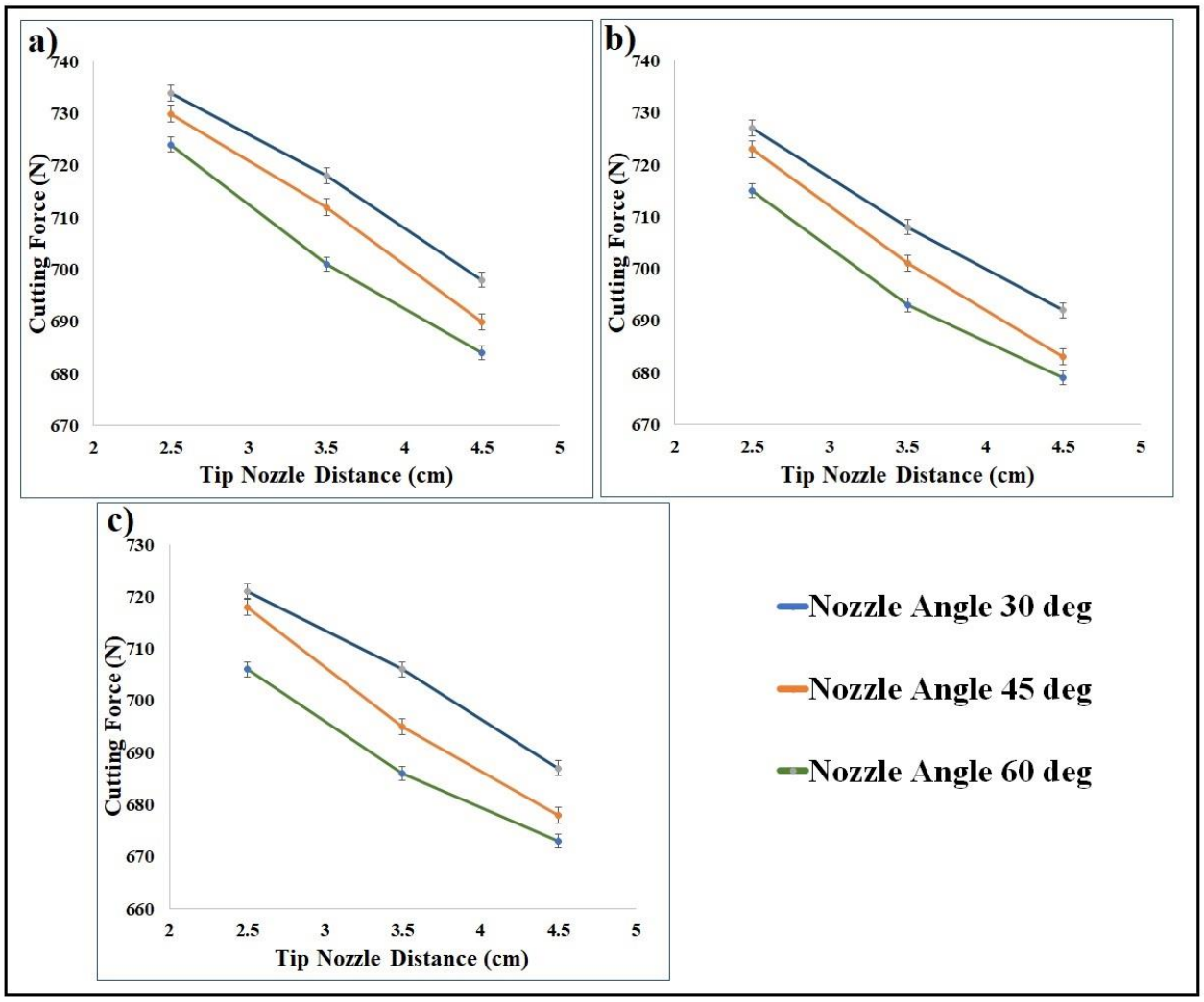

Figure 5.1: Variation of cutting force with tip nozzle distance at a) 5 mm b) 6 mm c) 7 mm of nozzle diameter

The cutting force increased with an increase in nozzle diameter during machining (figure 5.3). The machining operation was performed at a constant cold fraction which indicates that the amount of fluid available at the cold end of the vortex tube is maintained constant. For the same flow rate, the velocity of the fluid increased as the diameter decreased. When the coolant was supplied at a low diameter, it impinges at a higher velocity which in turn increases the impulse force that leads to an increase in cutting force during machining.

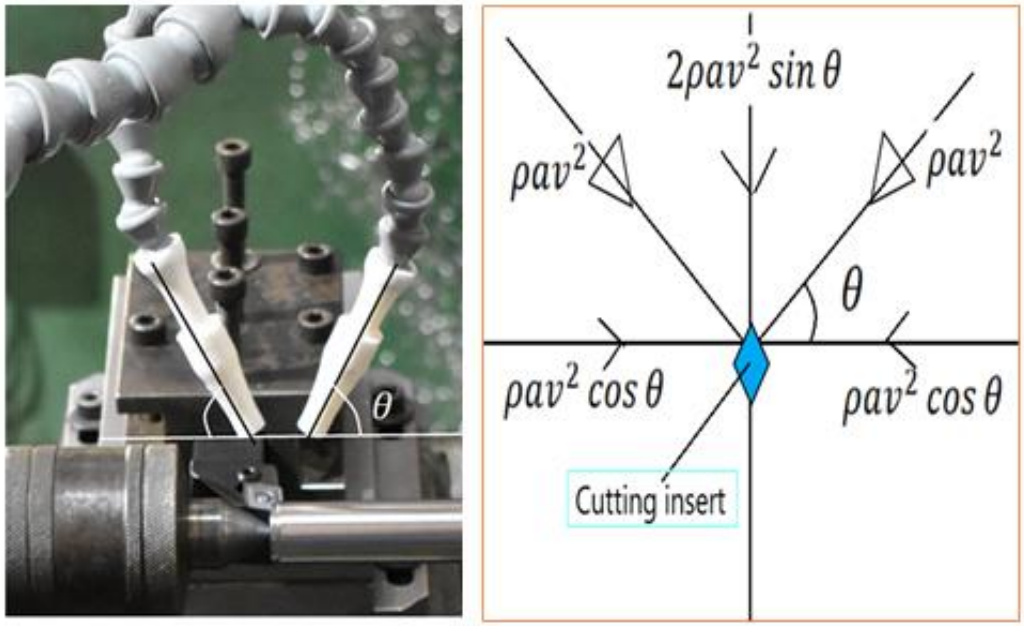

Figure 5.2: Nozzle setup and external forces on cutting insert

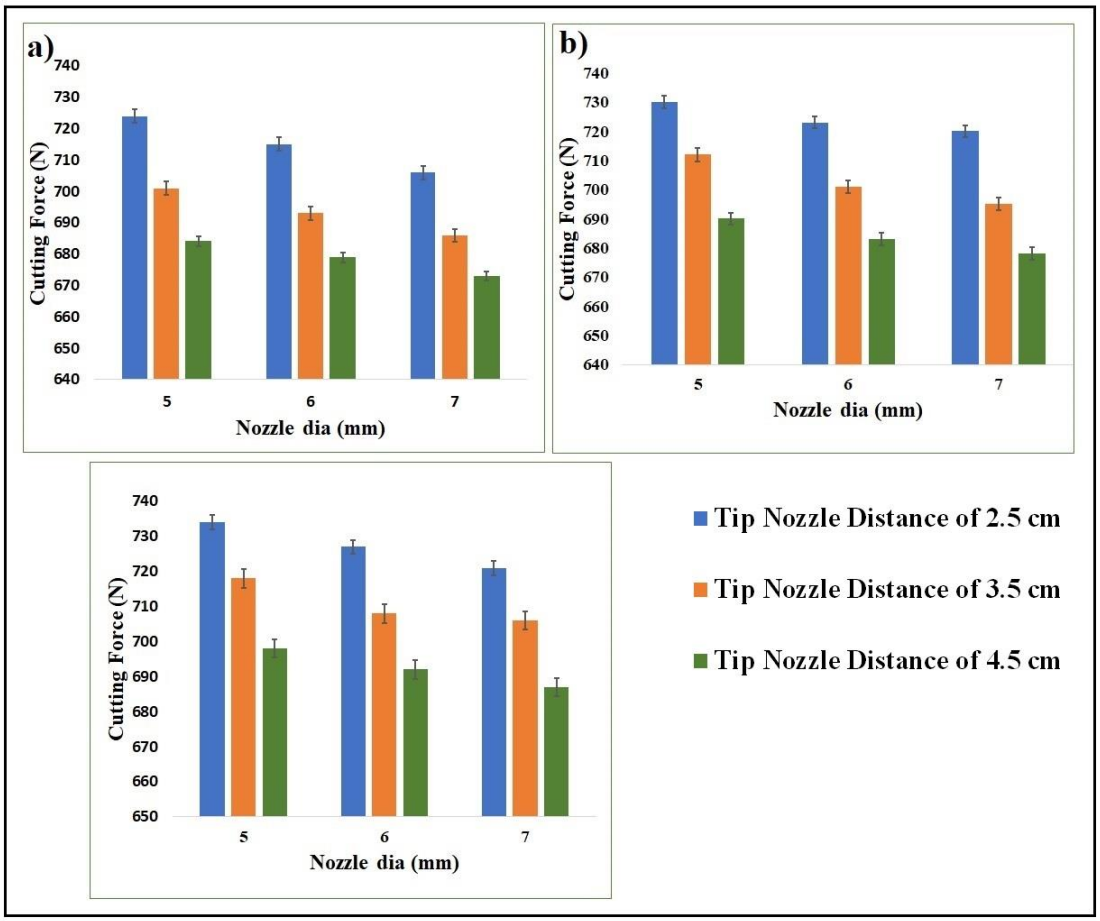

Figure 5.3: Variation of cutting force with nozzle diameter and tip nozzle distance at a) 30^0 b) A) 45^0 c) 60^0 Nozzle angle

5.3.2 Cutting temperature

Cutting temperature is the most influencing parameter for machining the Ti-6Al-4V as it influences the tool life and surface finish of the machined component. Heat generation and its transfer in the machining zone regulate the cutting temperature. The cutting temperature decreased with a rise in the nozzle angle as depicted in Figure 5.4. This may be due to reduction in the area focused by the coolant at higher angles. Such a drop in the area of coolant impact (for the same amount of coolant) increases the rate of heat transfer from the machining zone thereby causing a decrease in cutting temperature at higher nozzle angles. The heat transfer rate from the machining zone is given by the equation

$$Q = hA(T_m - T_c) \qquad \ldots\ldots\ldots\ldots\ldots\ldots\ldots \quad (5.2)$$

Where ‘h’ is heat transfer coefficient, ‘A’ is the surface area of the heat-affected zone, ‘Tm’ is the cutting temperature, and ‘Tc’ is the temperature of coolant supplied to the machining zone. The heat transfer coefficient is derived from the Nusselt number correlation which is given in equation 5.3.

$$Nu = K\,(Re^{a}\,Pr^{b}) \qquad \ldots\ldots\ldots\ldots\ldots\ldots\ldots\ldots\ldots\ldots\ldots\ldots\ldots\ldots\ldots\ldots\ldots(5.3)$$

Where Nu is Nusselt number, Re is Reynolds number, Pr is Prandtl number given by

$$Nu = \frac{hL}{k} \;\; , Re = \frac{\rho v L}{\mu} \;\; , Pr = \frac{\mu c_p}{k}$$

K, a, and b are constants depending on the type of flow and Re and Pr values, ‘k’ is thermal conductivity of the fluid, ‘L’ is the characteristic length, and ‘μ’ is the dynamic viscosity of the fluid. To minimize the cutting temperature, it is required to transfer more amount of heat and it is clear from the above equation that Q can be increased either by increasing the ‘h’ value or by decreasing ‘T_g’ value. The value of ‘h’ depends on the velocity of the fluid, its molecular weight and also on its specific heat.

As the tip nozzle distance increases, Figure 5.4 describes a pattern where cutting temperature first drops and then rises. Despite a higher heat transfer rate, cutting temperature is evidently more at a low tip nozzle distance. This may be because of the chip's adherence to the tool and workpiece in the machining zone, thereby triggering heat accumulation. The lower thermal conductivity of the chip material doesn’t allow heat flow and leads to soaring temperatures in the zone. But, even employing higher tip-nozzle distances seems to decrease the heat transfer rate due to loss in kinetic energy of the coolant. Since velocity is directly interlinked with the heat transfer coefficient, the after-effects of using a high tip nozzle also includes a reduction in heat removal from the machining zone. So, there must be a compromise between heat accumulation and heat transfer coefficient at both lower and higher tip-nozzle distances. Such a condition would lead to a minimum cutting temperature at a medium value of tip nozzle distance.

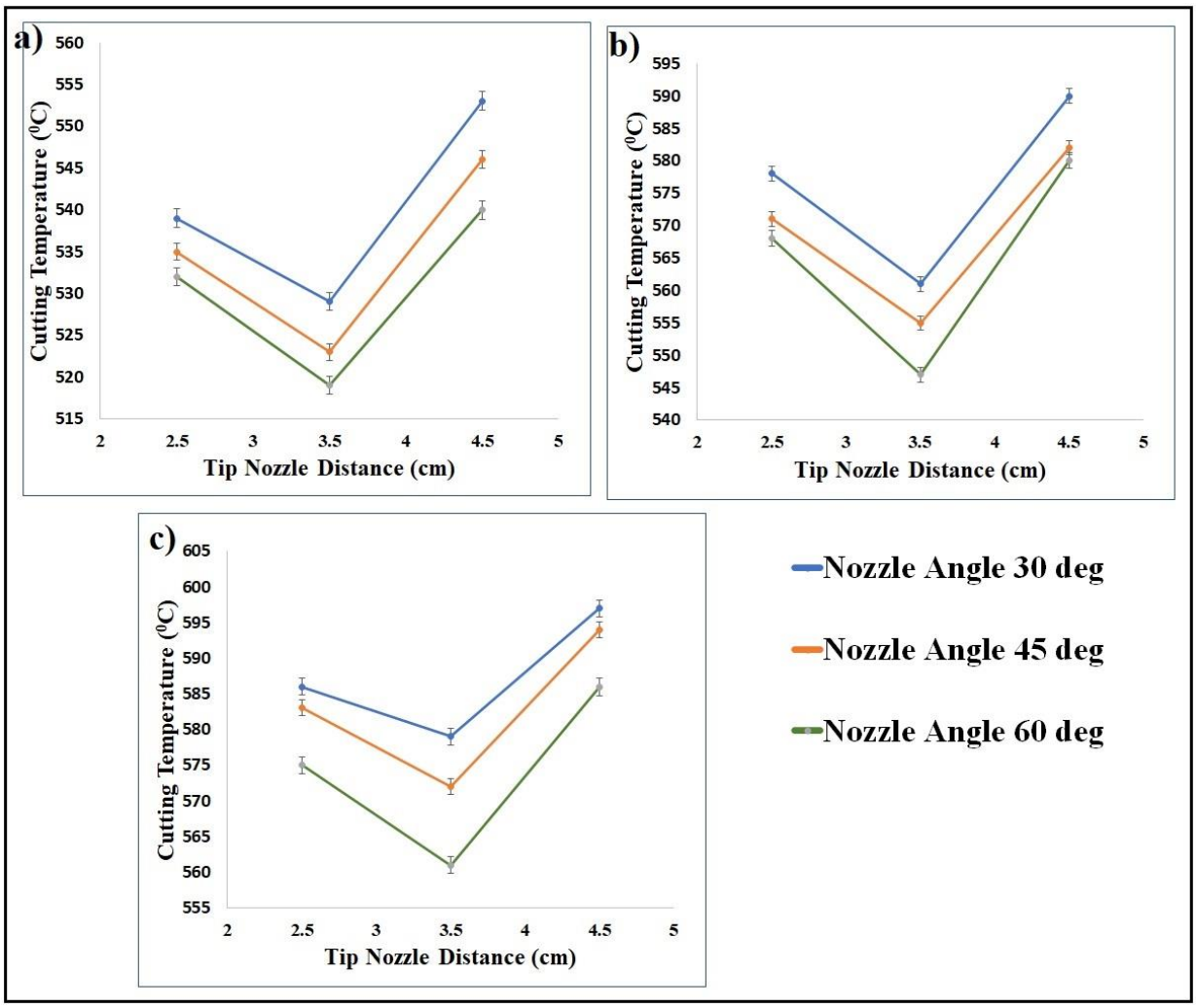

Figure 5.4: Variation of cutting Temperature with tip nozzle distance at a) 5 mm nozzle diameter b) 6 mm nozzle diameter c) 7 mm nozzle diameter

From figure 5.5, for a given tip nozzle distance, it was observed that cutting temperature rises with increasing nozzle diameter. Reduction in nozzle area increases the outlet velocity for the same flow rate, which in turn increases the heat transfer coefficient. The cumulative result of all these actions would increase the heat transfer rate from the machining zone. Hence, a decrease in cutting temperature is observed at lower diameters.

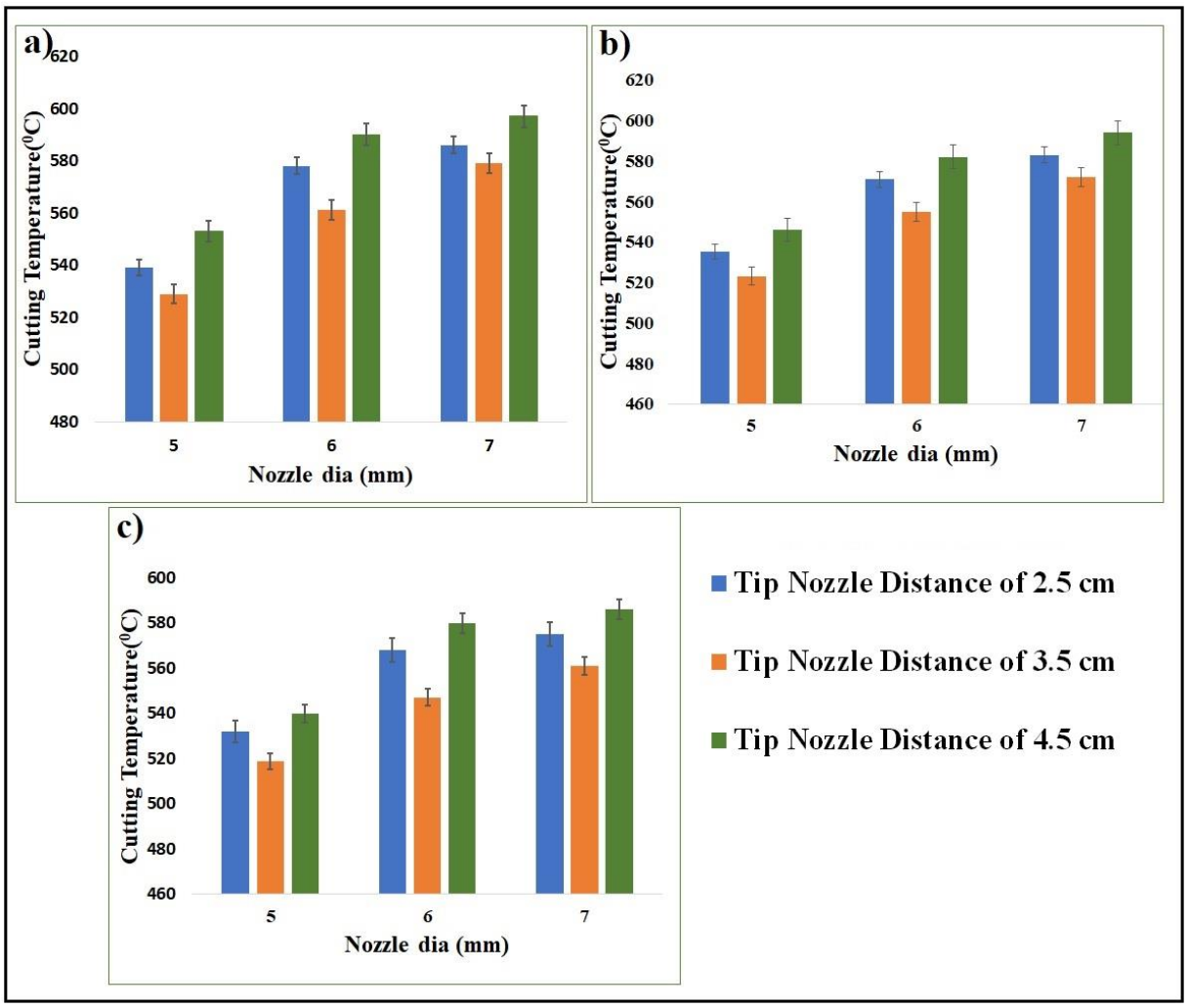

Figure 5.5: Variation of cutting temperature with nozzle diameter and tip nozzle distance at a) 30^0 b) 45^0 c) 60^0 nozzle angle

5.3.3 Surface roughness

Surface roughness is one of the critical factors in machining because it impacts fatigue strength, corrosion resistance, service life, and reliability of the component. A good surface finish improves the performance and durability of the component. Governing factors of surface finish include the penetrating ability of the coolant, the amount of fluid available, and the coefficient of friction of cutting fluid.

From figure 5.6 it is observed that the effect of nozzle angle on the surface finish was almost insignificant but there was a slight improvement in the surface finish with reduced nozzle angle. This was due to enhanced penetration capacity of the cutting fluid (at lower nozzle angles)

which in turn was responsible for the decrease in surface roughness. As depicted in Figure 5.6, the relation between surface roughness and tip nozzle distance is similar to that of cutting temperature and tip nozzle distance. At a lower distance, chips adhere to the surface thereby making their disposal difficult. Although coolant possesses a higher penetration ability at lower tip nozzle distances, chip adherence diminishes the surface finish. Similarly, at higher nozzle distances, higher surface roughness is observed due to the lack of effective coolant penetration. So, there must be a compromise between chip adherence and the penetration ability of the coolant. Therefore, a better surface finish is observed at medium ranges of tip nozzle distance of around 3.5 cm.

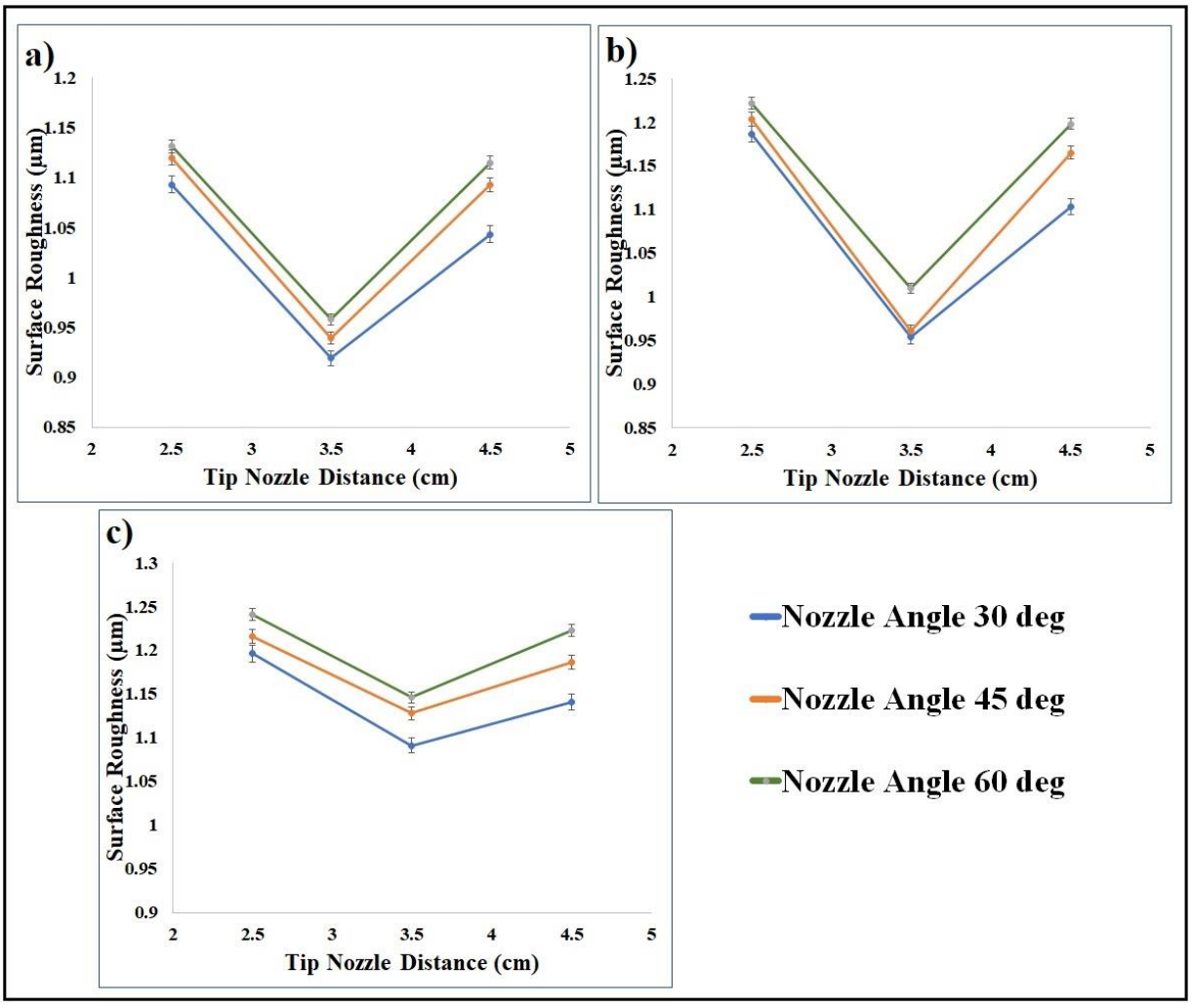

Figure 5.6: Variation of surface roughness with tip nozzle distance at a) 5 mm nozzle diameter b) 6 mm nozzle diameter c) 7 mm nozzle diameter

From Figure 5.7, it is observed that as the diameter decreased, surface roughness reduced. This may be because of the high coolant velocity which assists in effective chip removal, thereby minimizing the built-up edge formation. Along with this, higher velocity coolant can penetrate the mating zone effectively compared to that of low velocity which leads to a better surface finish at lower nozzle diameters.

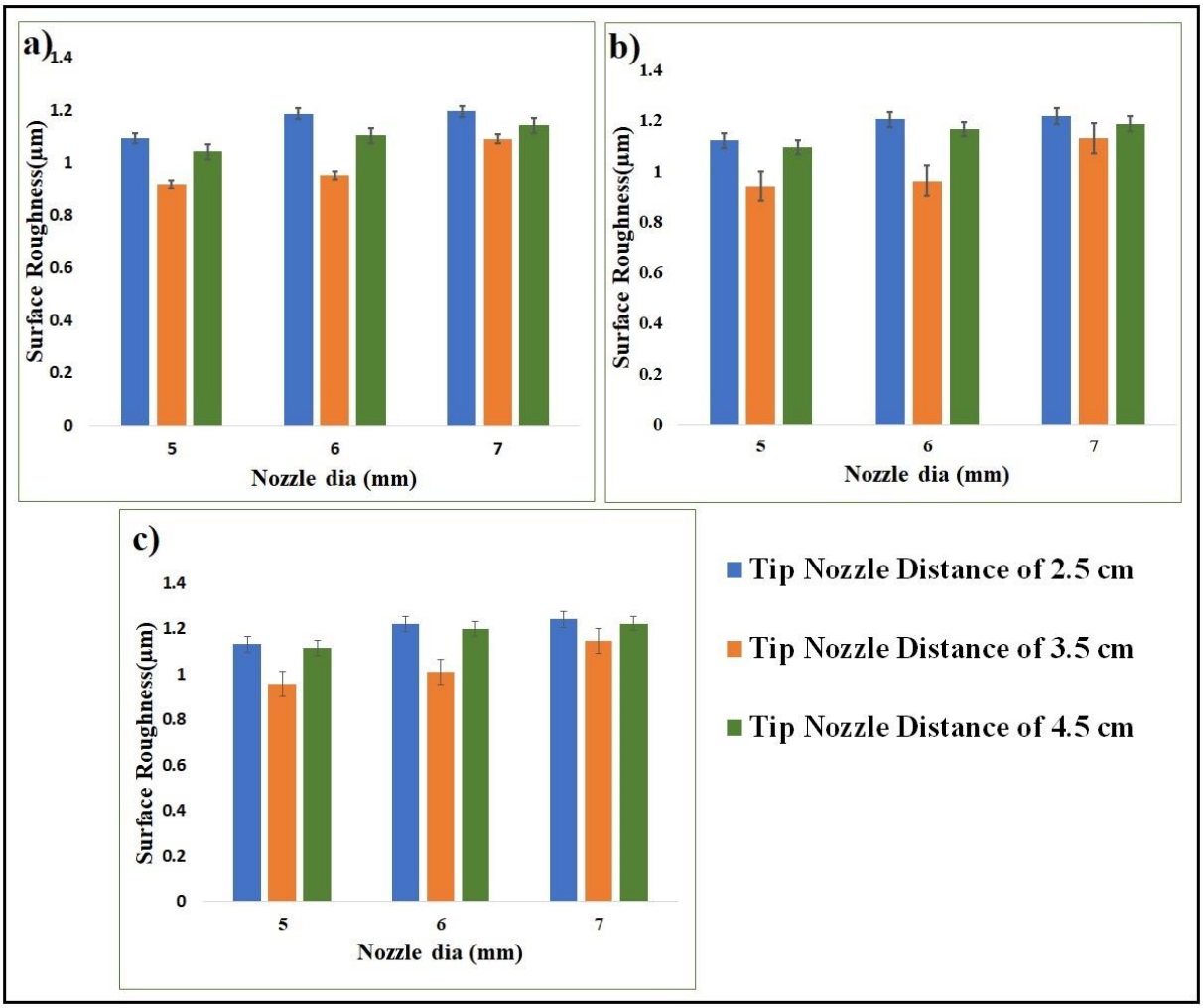

Figure 5.7: Variation of surface roughness with nozzle diameter and tip nozzle distance at a) 30^0b) 45^0c) 60^0 of Nozzle angle

5.4 Effect of flow parameters on response parameters

The turning operation is performed under VTCS environment at constant cutting conditions of speed, feed, and depth of cut (80 m/min, 0.25 mm/rev, 1mm) while cutting force, cutting temperature, and surface roughness were the responses. In VTCS, different levels of coolant

pressure, cold fraction, and nozzle diameter were used where nozzle angle (45^0) and, nozzle position (3.5 cm) are fixed throughout the experiment.

5.4.1 Cutting force

The cutting forces were analyzed by varying coolant pressure, cold fraction, and nozzle diameter in VTCS assisted turning and the variations are shown in Figure 5.8. The cutting forces increased with an increase in pressure at a particular cold fraction and nozzle diameter. The percentage increase in cutting force was 3.87%, 4.77%, 4.84%, and 5.43% respectively for each step of increase in pressure from 5 to 9 bar at a constant cold fraction and nozzle diameter of 20% and 6 mm respectively. The cutting force in the machining of Ti-6Al-4V under VTCS cooling environment is mainly influenced by (i) resistance offered by the material against shearing in the form of a chip, (ii) component of impulse force produced due to the high-pressure stream of gas, and (iii) strain hardening or thermal softening of the workpiece. In VTCS, the cool compressed gas having density 'ρ' is focused into the machining zone which acts at an angle 'θ' to the horizontal plane having area 'a' and velocity 'v'. The impulse force generated along the direction of the flow is given by;

$$F = \rho a v^2 \ldots\ldots\ldots\ldots\ldots \quad (5.4)$$

The vertical component of the force is acting in the direction of the main cutting force and is given by '$\rho a v^2 \sin\theta$'. During machining of Ti-6Al-4V, a large amount of heat is generated and it causes an increase in the temperature in the machining zone due to which the material becomes soft and requires low amount of force for machining. But the application of cool compressed gas on a high-temperature workpiece causes an increase in hardness of the surface known as strain hardening phenomena, that leads to an increase in cutting force. The impulse force can also be described as the product of mass flow rate and change in velocity which means an increase in mass flow rate or velocity increases the cutting force. According to the experimental setup, both the nozzles and the cutting tool move linearly with the same velocity and hence it is assumed as a stationary heat source with coolant.

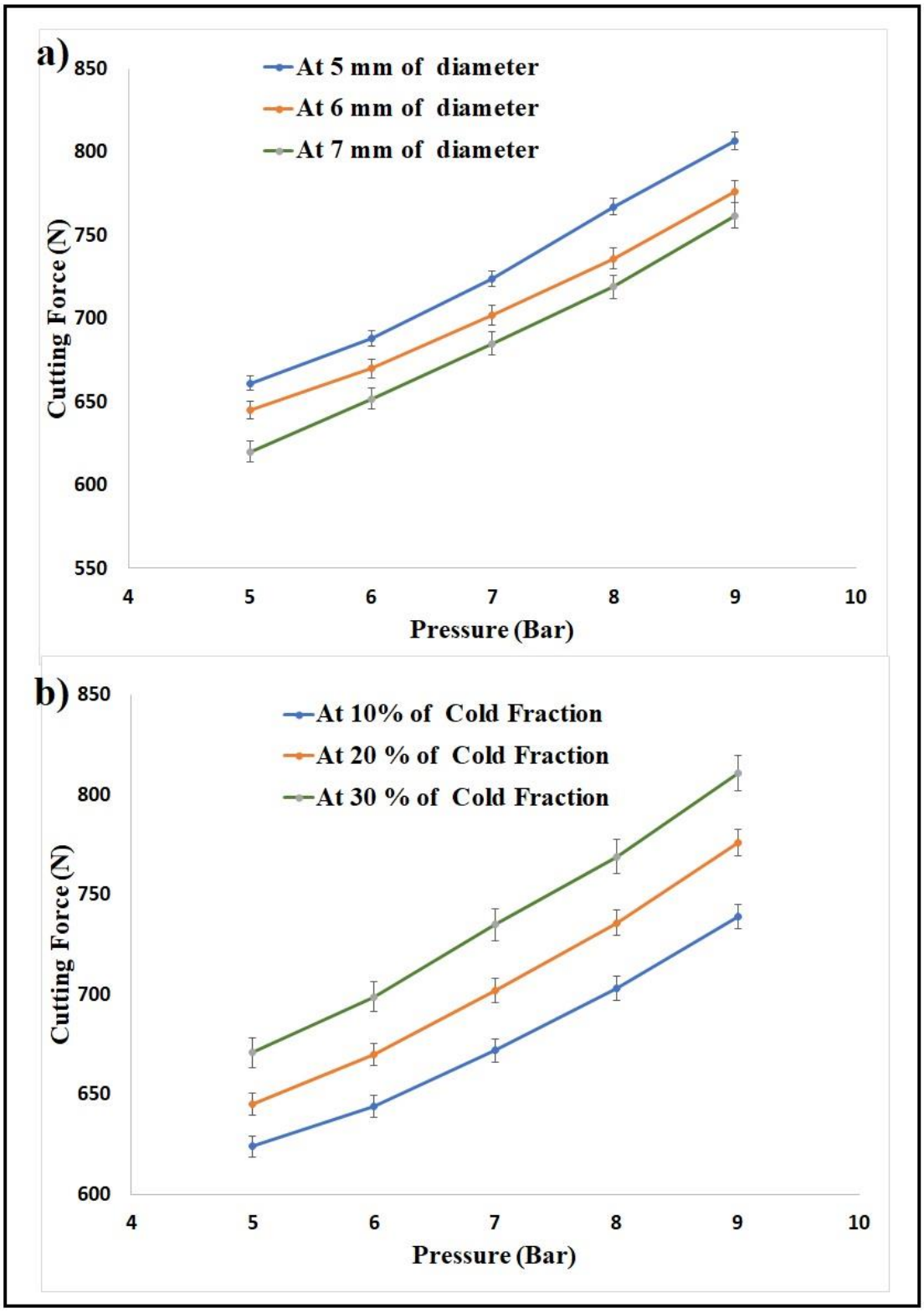

Figure 5.8: Variation of cutting force with a) pressure and nozzle diameter at a cold fraction of 20% b) Pressure and cold fraction at a nozzle diameter of 6 mm

It is observed that an increase in cutting force is significant at higher pressure due to the high velocity of the stream and high cooling effect (Figure 5.8). An increase in velocity of the coolant at high pressure may increase the vertical component of the impulse force actuated by the gas stream on the cutting tool. Along with this, a minimum coolant temperature is produced at high pressure in the vortex tube, so that the rate of strain hardening becomes so severe as to further increase the cutting forces.

The cutting force increased with a decrease in diameter for all cold fractions and pressures. Cutting force increased by 6.61 % for a change in diameter from 7 mm to 5 mm at a constant pressure and a cold fraction of 7 bar and 20% respectively (Figure 5.8 A). This is because 96% of the increment in velocity is due to the change in diameter which leads to an increase in the impulse force caused by the coolant stream on the cutting tool.

Cutting forces increased with an increase in cold fraction which is 9.37% following an increase in cold fraction from 10% to 30% at constant pressure and nozzle diameter of 7 bar and 6 mm respectively (Figure 5.8 B). This is because of an increase in the mass flow rate of cold compressed gas supplied through the nozzle with an increase in cold fraction at a constant nozzle diameter. Apart from this, more cooling effect is produced in the machining zone at a higher cold fraction thereby causing increased strain hardening of workpiece material. This in turn augments the hardness of the workpiece, leading to higher cutting force.

5.4.2 Cutting temperature

Machining of Ti-6Al-4V generates a large amount of heat in the machining zone because of its inherent properties, which increase the cutting temperature and deteriorate tool life and surface finish. From VTCS assisted turning, it is observed that the cutting temperature is decreased with an increase in pressure, as shown in Figure 5.9. The percentage decrease in cutting temperatures is 4.88%, 4.96%, 5.94%, and 7.47 % respectively for each step of increase in pressure from 5 bar to 9 bar at constant cold fraction and nozzle diameter of 20% and 6 mm respectively. Heat removal is necessary for effective machining and this mainly depends on convective heat transfer and heat absorption capacity of the coolant from the machining zone. The convection heat transfer is given by '$\boldsymbol{Qc = hA\Delta T}$' ,Where 'h' is the convective heat transfer coefficient, 'A' is the area exposing to the surrounding fluid, and ' $\boldsymbol{\Delta T}$ ' is the difference in temperature of the hot surface and the coolant supplied. In this study, heat transfer is considered as forced convection because the coolant is supplied by external aid. In forced convection, the heat transfer coefficient depends

on the velocity of the coolant, and its properties like molecular weight, density, kinematic viscosity, thermal conductivity, etc. It also depends on the nozzle configuration like the angle of the nozzle, diameter, and its position from the heat zone [71]. The heat absorbed by the coolant is given by ' $= \dot{m}c\Delta T$ ' Where $\dot{m}$ is the mass flow rate, and 'c' is the specific heat capacity of the coolant. The drop-in cutting temperature is higher at higher pressures because of high heat transfer coefficient which enhances the convective heat transfer from the machining zone. Apart from this, lower coolant temperature produced at higher pressures in the vortex tube increases ΔT value, and therefore increasing the heat transfer rate further.

The cutting temperature is reduced with a decrease in nozzle diameter for all cold fractions and pressures as shown in Figure 5.9. Cutting temperature decreased by 9.91% for a change in diameter from 7 mm to 5 mm at constant pressure and cold fractions of 7 bar and 20% respectively (Figure 5.9(a)). A reduction in diameter increases the velocity of the coolant thereby increasing the convective heat transfer coefficient that causes effective heat removal from the machining zone. Apart from this, the area focused is precise while using a lower diameter nozzle that resulted in minimizing the slippage of coolant. The maximum amount of gas focused on the mating zone and transfered heat effectively. The cutting temperature is reduced with an increase in cold fraction (Figure 5.9(b)). Around 11.34 % reduction in cutting temperature is obtained by varying cold fraction from 10% to 30% at a constant pressure and nozzle diameter of 7 bar and 6 mm respectively. This is due to an increase in the mass flow rate of the coolant with an increase in the cold fraction that absorbs a large amount of heat.

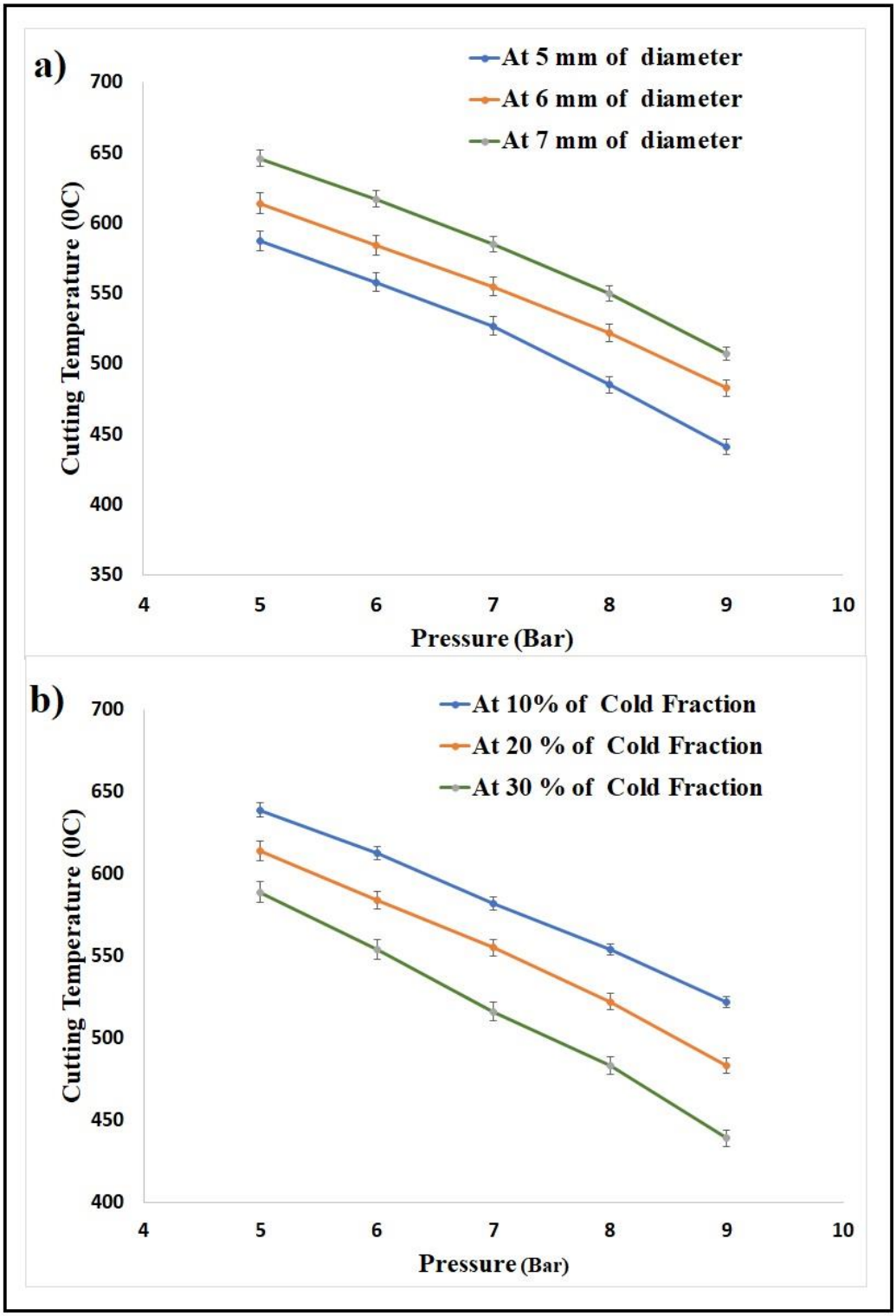

Figure 5.9: Variation of cutting temperature with a) pressure and nozzle diameter at a cold fraction of 20% b) Pressure and cold fraction at a nozzle diameter of 6 mm

5.4.3 Surface roughness

The surface roughness of the machined component mainly depends on the lubrication capacity between the mating parts, penetrating ability of the coolant, chip breakage facility in the machining zone, and evacuation of the chips. Cutting temperature also indirectly influences the surface quality i.e. lower cutting temperature helps to produce a better surface finish [90].

The surface roughness is reduced with an increase in pressure for all cold fractions and nozzle diameters as shown in Figure 5.10. The percentage reduction in surface roughness is 6.45%, 7.95%, 6.65%, and 11.4% respectively for each step increase in pressures from 5 to 9 bar at constant cold fraction and nozzle diameter of 20 % and 6 mm respectively. This is because of the high penetrating ability of coolant which reduces the coefficient of friction between the mating parts at higher pressure. Along with this, the braking and evacuation of chips are better at higher pressure, and lower cutting temperatures are observed at higher pressure, which further provide a better surface finish.

Surface roughness is reduced with a decrease in nozzle diameter for all cold fractions and pressures as shown in Figure 5.10. There is 15.29 % decrease in surface roughness for achange in diameter from 7 to 5 mm at constant pressure of 7 bar and cold fraction of 20% respectively (Figure 5.10(a)). The velocity of the stream is increased by 96% when 7 mm diameter is replaced by 5 mm diameter nozzle which can penetrate the matting parts and minimize surface roughness. Along with this, high velocity coolant can remove chips effectively and avoid built-up edges, further enhancing the surface quality effectively at lower diameters. The surface roughness is reduced with an increase in cold fraction (Figure 5.10(b)). Around 15.3 % reduction in surface roughness is obtained by varying cold fraction from 10% to 30% at constant pressure and nozzle diameter of 7 bar and 6 mm respectively. At higher cold fractions the amount of coolant available in the mating zone was higher, which provides a better lubricating effect compared to lower cold fractions. Along with this, the CO_2 gas as a coolant offers a lower friction coefficient between the mating parts, which further improves the surface finish.

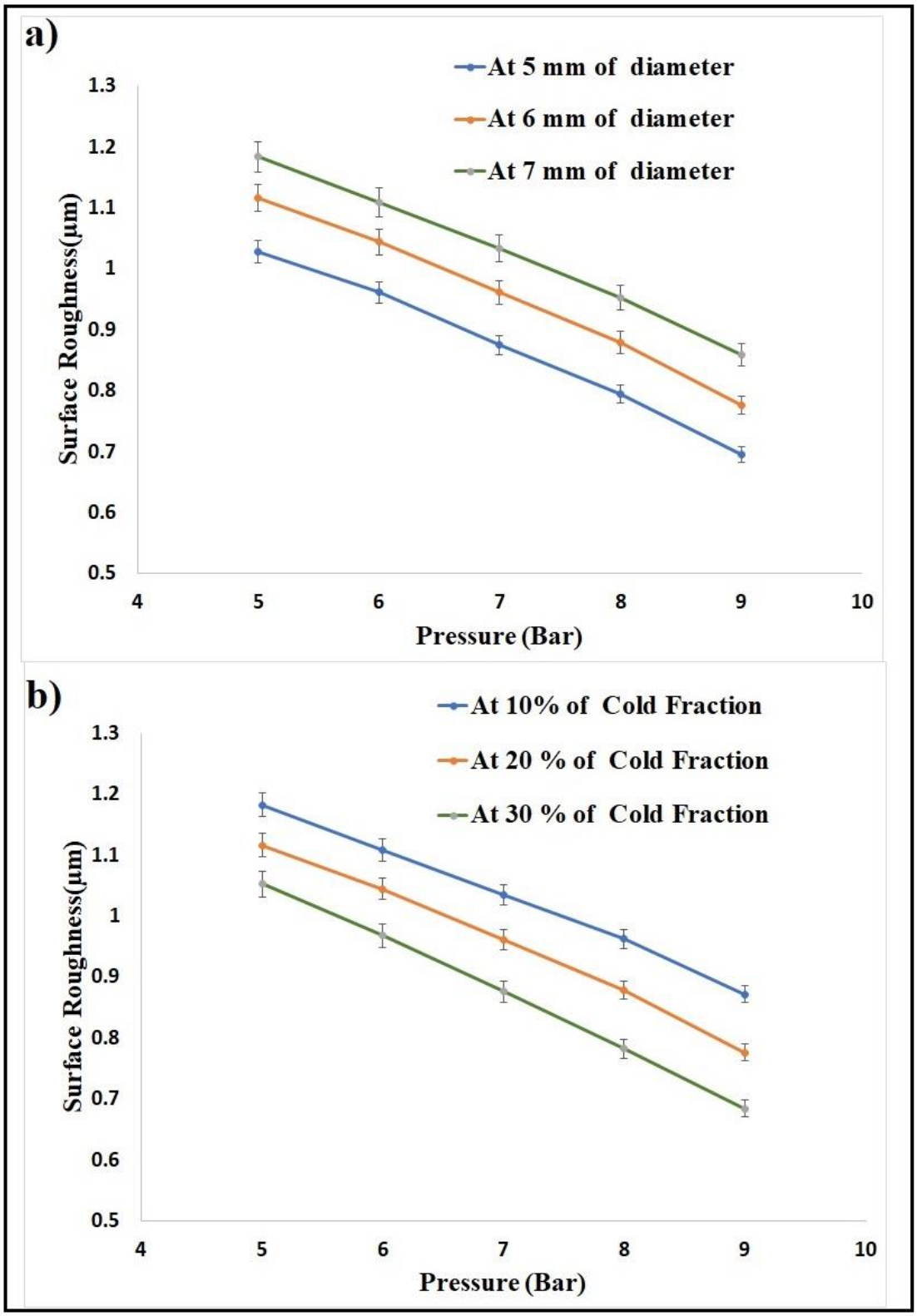

Figure 5.10: Variation of Ra value concerning a) pressure and nozzle diameter at a cold fraction of 20% b) Pressure and cold fraction at a nozzle diameter of 6 mm

5.5 Effect of machining parameters on response parameters

The turning operation is performed under VTCS environments by varying cutting conditions of speed, feed, and depth of cut while cutting force, cutting temperature, and surface roughness are responses. In VTCS, coolant pressure (7 bar), cold fraction (20%), and nozzle diameter (6 mm), nozzle angle (45^0) and, nozzle position (3.5 cm) are fixed throughout the experiment

5.5.1 Cutting Force

The cutting force is a vital parameter in machining which influences the power consumption, tool life, and rigidity requirement [22]. The cutting force is measured at different cutting speeds under different cooling media in VTCS assisted turning which is presented in Figure 5.11. The minimum cutting force is observed under dry cutting conditions, while the maximum cutting force occurred under compressed gas cooling conditions. In Ti-6Al-4V machining under dry cutting, the heat which is generated accumulates in the machining zone and the low thermal conductivity of the material prevents heat conduction to the atmosphere. This leads to high temperature in machining zone and the workpiece is subjected to thermal softening. Hence, low energy is required to perform the machining operation and low cutting force acts on the cutting tool. In the case of compressed air cooling, the heat generated is carried away by the pressurized gas and minimizes the thermal softening effect. Along with this, the gas-focused from the nozzle applies external impulse force on the cutting tool which increases the cutting force further. The impulse force acting due to high-velocity gas is given by $\rho a V^2$, where' ρ' is the density, 'a' is the area of the nozzle outlet and 'V' is the velocity of the gas leaving from the nozzle. The impulse force mainly depends on the flow rate and velocity of the coolant. In VTCS single nozzle, at 20% of the cold fraction, cutting force is lower compared to the compressed air because only 20% of the total flow rate is available. However, the low temperature coolant from the vortex tube produces a strain hardening effect in the workpiece and leads to higher cutting force compared to dry cutting. When the coolant is supplied using dual nozzle VTCS, the only vertical component of the impulse force ($2\rho a V^2 \sin\theta$) acts on the cutting tool and hence, the cutting force is lower compared to single nozzle VTCS.

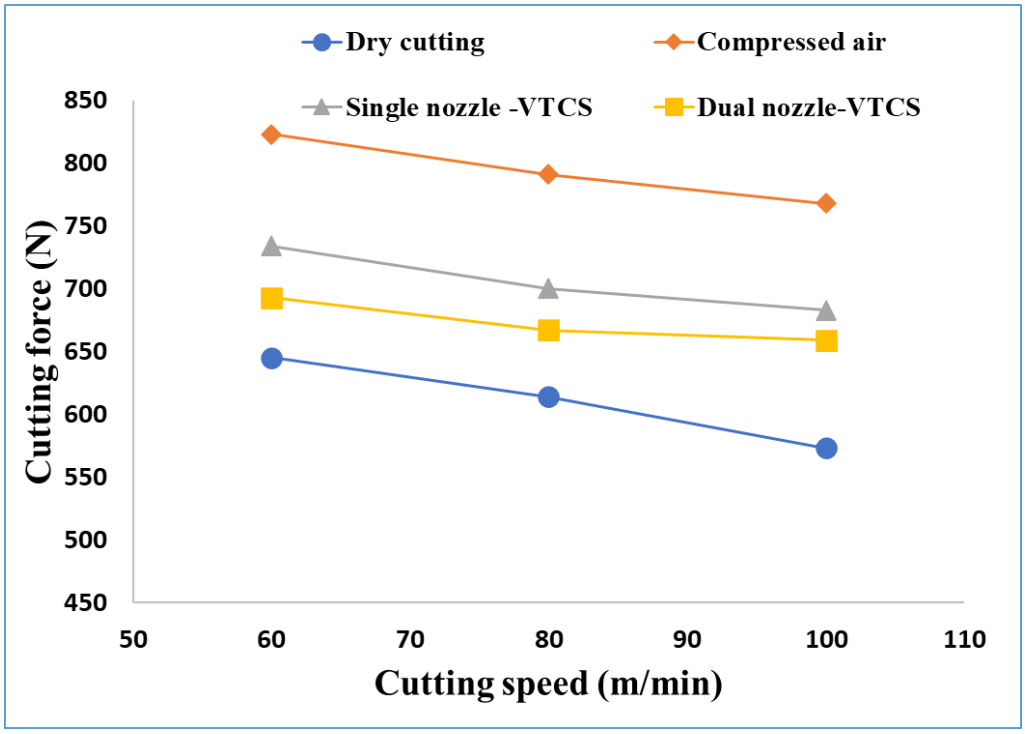

Figure 5.11: Influence of different cooling environments on cutting force

Figure 5.12 shows the influence of cutting velocity on cutting force in dual nozzle VTCS. From the Figure, it is identified that the cutting force reduced with velocity increment. It is reduced in the range of 9- 12 % based on the depth of cut when cutting speed increased from 60 to 10 m/min. The material removal rate increases with an increase in cutting velocity which requires more energy for machining. This energy is transformed into heat and increases the temperature in the machining zone which leads to thermal softening. In Ti-6Al-4V, beyond 25 m/min cutting speed, the thermal softening phenomenon dominates and reduces the cutting force [32]. Figure 5.13 shows the alteration of cutting force with depth of cut. It is increased in the range of 4 - 7% based on the cutting velocity when feed increased from 0.21 to 0.29 mm/ rev. The increase in feed increased the friction coefficient at the cutting zone which raised the rubbing force (friction force) and led to higher cutting force. Along with this, high feed rate increases MRR and requires more energy because of which more force is required for the shearing. The cutting force increased in the range of 6 – 10 % based on the cutting velocity when the depth of cut increased from 0.8 to 1.2 mm. MRR increases as depth of cut is increased and hence higher energy is required for machining which leads to an increase in cutting force.

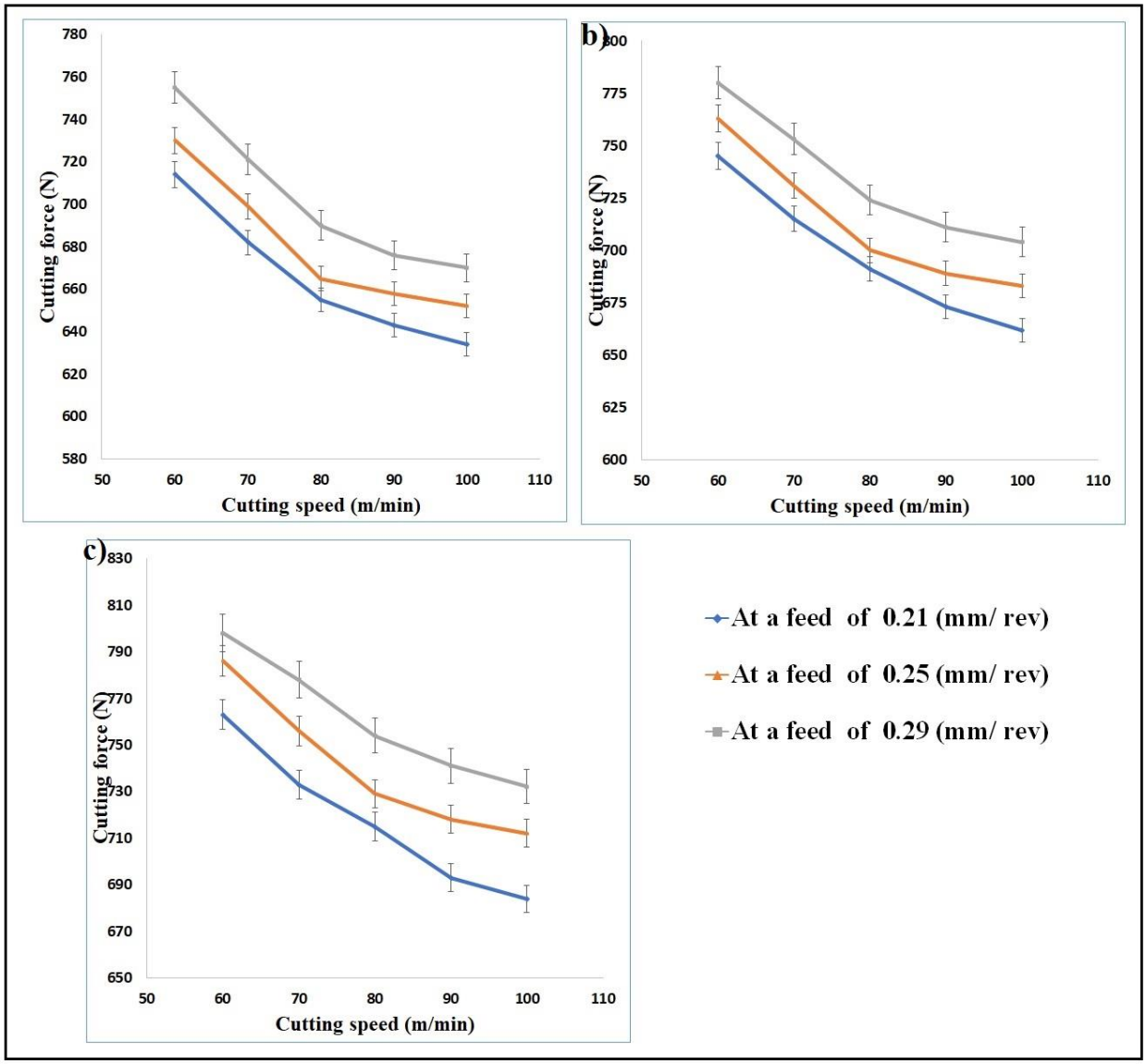

Figure 5.12: Variation of cutting force with cutting speed at depth of cut of (a) 0.8 mm,(b) 1 mm ,(c)1.2 mm

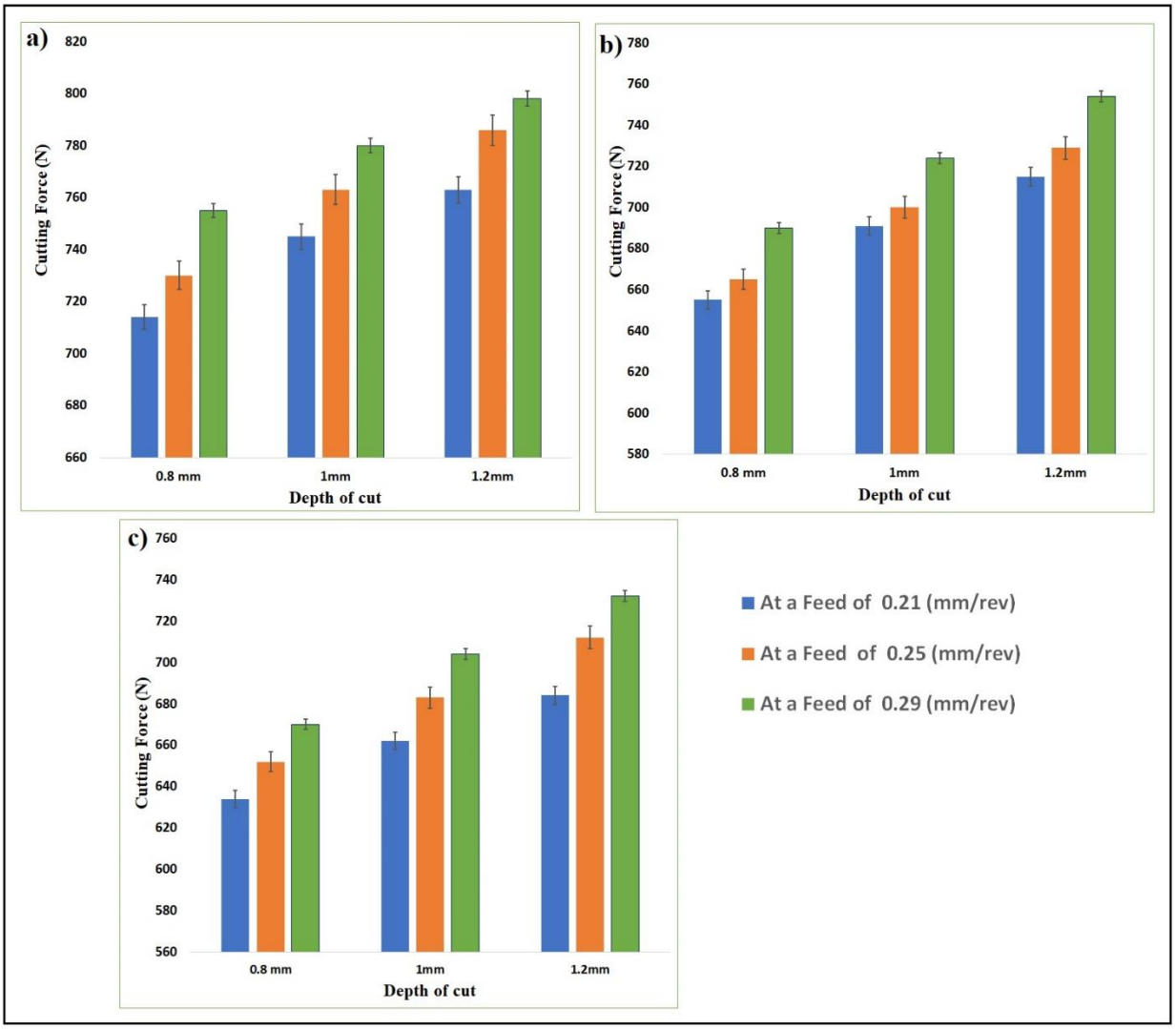

Figure 5.13: Variation of force with depth of cut and feed at cutting speed of (a) 60 m/min,, (b) 80 m/min , (c)100 m/min

5.5.2 Cutting Temperature

Cutting temperature is a crucial parameter in machining that directly influences the tool wear, surface quality, friction coefficient at the cutting zone. In the machining of Ti-6Al-4V, there is higher heat generation and the need to provide an effective heat removal mechanism to minimize tool failure and surface roughness that create a necessity to understand cutting temperature [34].

The cutting temperature measured by varying cutting speeds under different cooling media in VTCS assisted turning is presented in Figure 5.14. The maximum cutting temperature is obtained in dry environment due to lack of coolant. Hence the heat accumulation in the machining

zone is not carried away by any external means,leading to a rise in the temperature. Along with this, a high coefficient of friction between the chip tool interface (because of lack of lubricant) in dry cutting increased the cutting temperature. In compressed air cooling, pressurized air as a coolant increases heat transfer rate. It depends on heat transfer coefficient of the cooling medium and the temperature of the coolant. Supplying compressed air at a higher velocity enhances 'h' value and minimizes cutting temperature for all cutting speeds. In single nozzle VTCS, cold CO_2 gas is supplied which means the coolant temperature is in sub-zero value in the machining zone which increases the rate of heat transfer rate. Along with this, the positive Joule-Thomson coefficient of CO_2 gas generates refrigeration effect while expanding to lower pressures and reduces the heat which leads to lower temperature compared to dry and compressed air cooling. In Dual nozzle VTCS, the minimum temperature obtained is slightly lower than the cutting temperature obtained in single nozzle VTCS because of effective penetration of coolant when supplying coolant using two nozzles compared to a single nozzle.

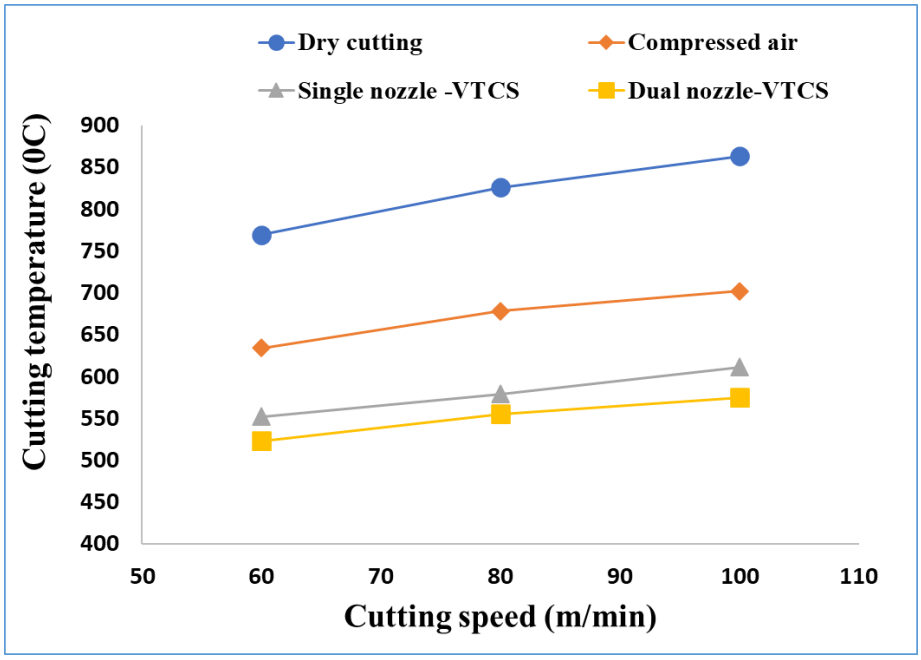

Figure 5.14: Influence of different cooling environments on cutting temperature

Figure 5.15 shows the impacting of cutting speed on cutting temperature. From the figure, it is identified that the cutting temperature increased as velocity increased. The cutting temperature increased in the range of 8- 10 % based on the depth of cut when cutting velocity increased from 60 to 100 m/min. This is because high speed leads to high MRR and consumes more energy in

machining. All the energy consumed is converted into heat and increases the cutting temperature. Along with this, the time of exposure of the machining zone to the coolant is lower at higher speeds which causes ineffective heat transfer that resulted in increased cutting temperature.

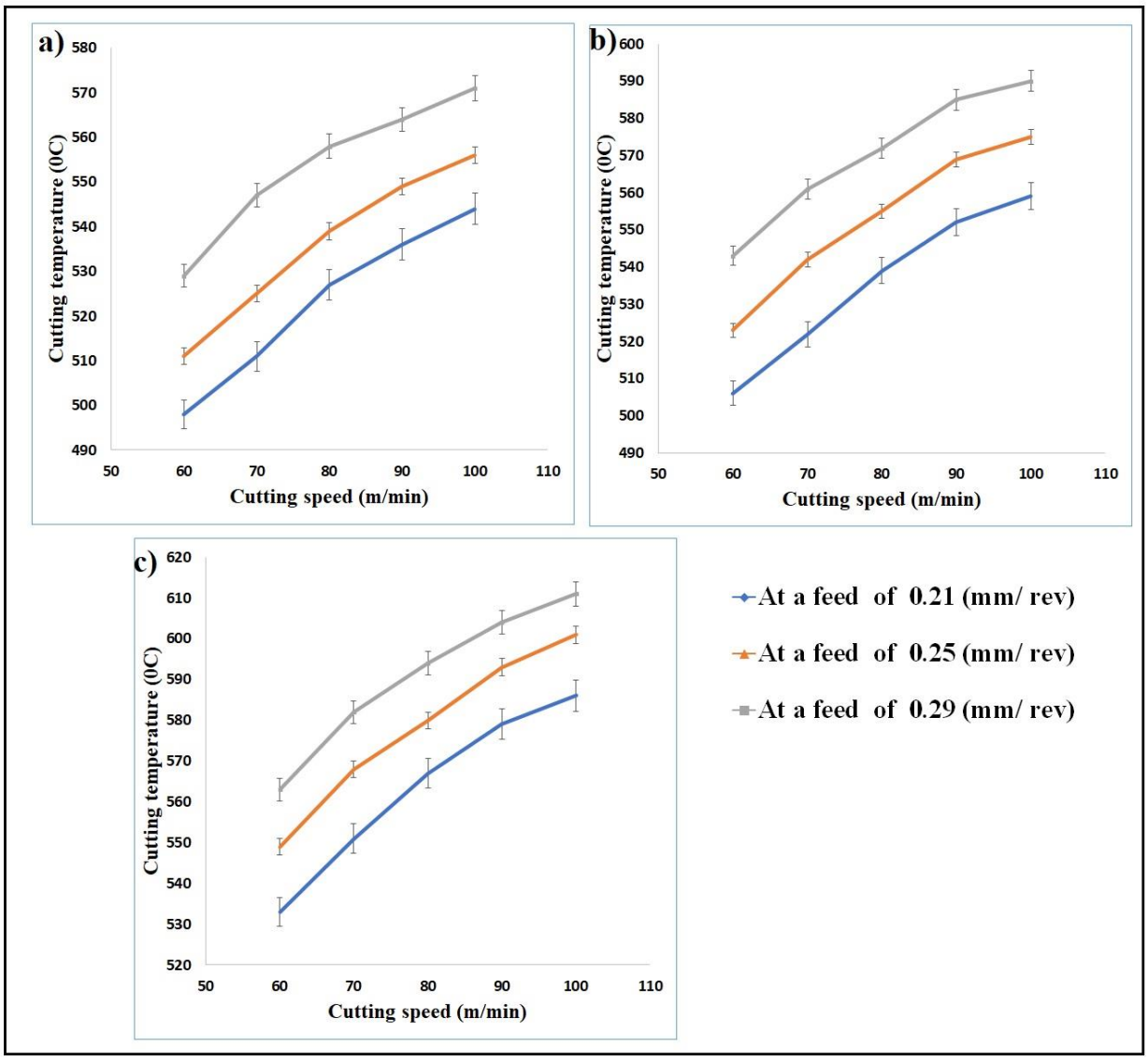

Figure 5.15: Variation of cutting temperature with cutting speed at depth of cut of (a) 0.8 mm,(b) 1 mm ,(c)1.2 mm

Figure 5.16 shows the variation of cutting temperature with feed rate and depth of cut. The cutting force increased in the range of 5 - 8% based on the cutting velocity when feed increased from 0.21 to 0.29 mm/ rev. The cutting temperature increased in the range of 7 - 8 % based on the cutting velocity when the depth of cut increased from 0.8 to 1.2 mm. The cutting temperature increased with feed as well as with the depth of cut at a particular speed. This is due to an increase

in MRR at higher feeds and depth of cuts where high energy was required for machining. This energy which converted into heat in the machining zone led to rise in cutting temperature.

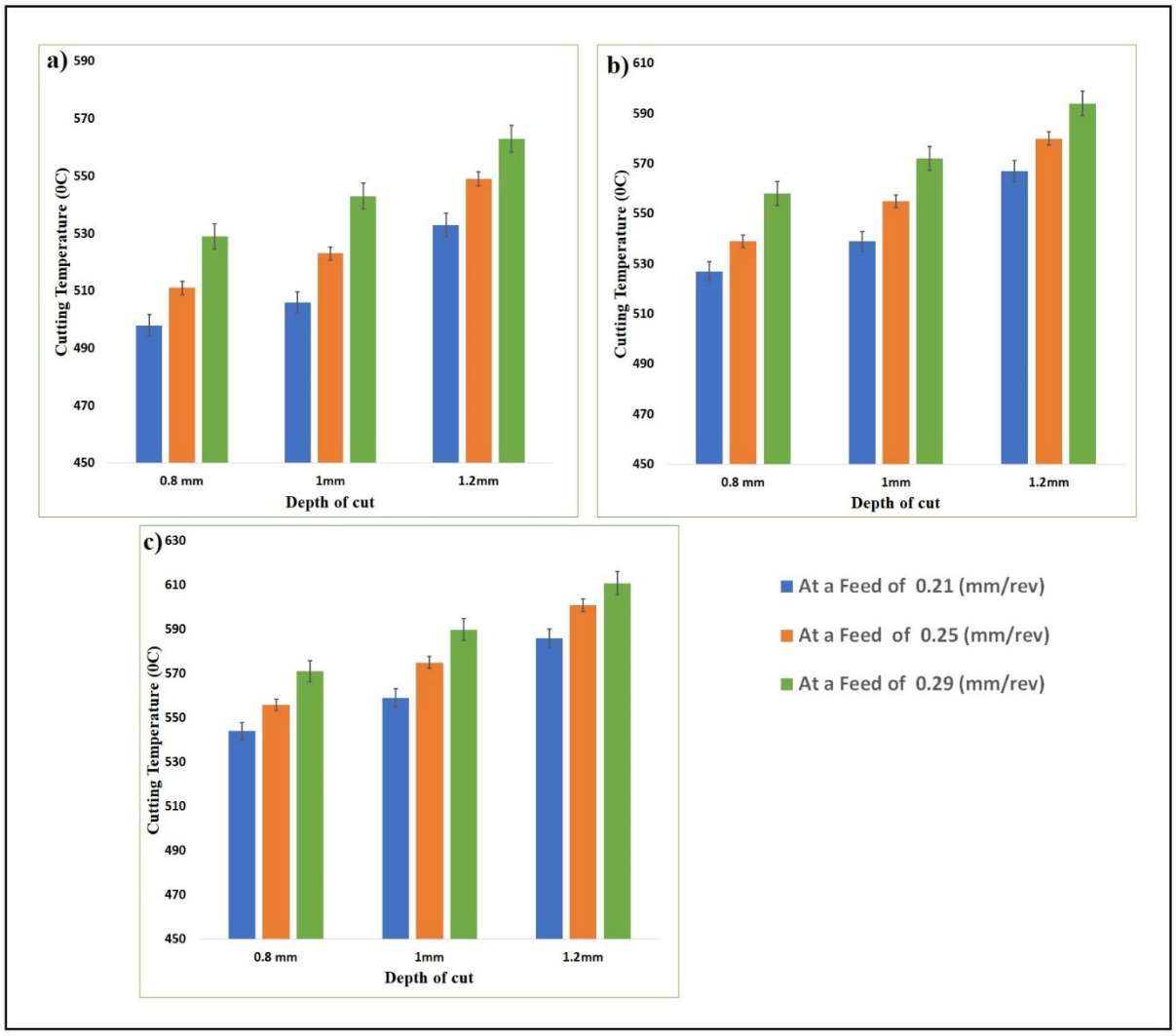

Figure 5.16: Variation of cutting temperature with depth of cut and feed at cutting speed of (a) 60 m/min,, (b) 80 m/min , (c)100 m/min

5.5.3 Surface roughness

Surface roughness influences the quality of the finished component and indirectly influences the fatigue life. In this study, the average roughness *(Ra)* is considered which is a widely accepted measure to evaluate the surface roughness.

The surface roughness is measured by varying cutting speeds under different cooling media in VTCS assisted turning is presented in Figure 5.17. The maximum surface roughness is observed

under the dry environment due to lack of coolant or lubricant in dry cutting causes large heat accumulation in the cutting zone which causes rapid tool wear and detoriated surface finish. A high friction coefficient is observed at the higher cutting temperature that further spoiled the finish. In compressed air cooling, the pressurized gas as a coolant removes heat accumulation to some extent. Along with this, high-pressure air can penetrate the mating zone and provide a lubricating effect and minimize friction coefficient, and reduce surface roughness compared to dry environment. In single nozzle VTCS, the removal of heat is effective and the friction coefficient is low at the cutting zone due to CO_2 gas. This improved the surface finish to a great extent compared to compressed air cooling. The penetrating ability of cold CO_2 gas and effective chip removal of high pressure coolant further improved the surface finish. Dual nozzle VTCS results in minimum surface roughness and it is slightly lower than surface roughness obtained in a single nozzle VTCS because of the effective penetration of coolant from using two nozzles compared to a single nozzle.

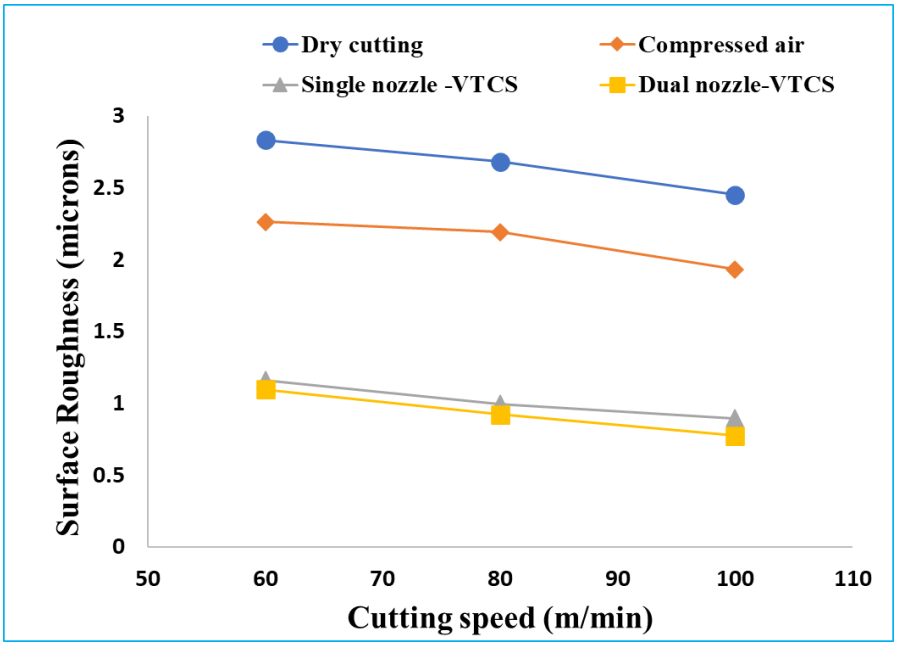

Figure 5.17: Influence of different cooling environments on surface roughness

Figure 5.18 represents the influence of cutting velocity on surface roughness. From the figure, it is evident that increment in velocity results in decrease in surface roughness. It is reduced in the range of 30- 32 % based on the depth of cut where cutting velocity increased from 60 to

100 m/min. At higher cutting speeds, the formation of chatter marks on the machined surface was lower and the time for BUE formation was low and hence improved the surface finish [57].

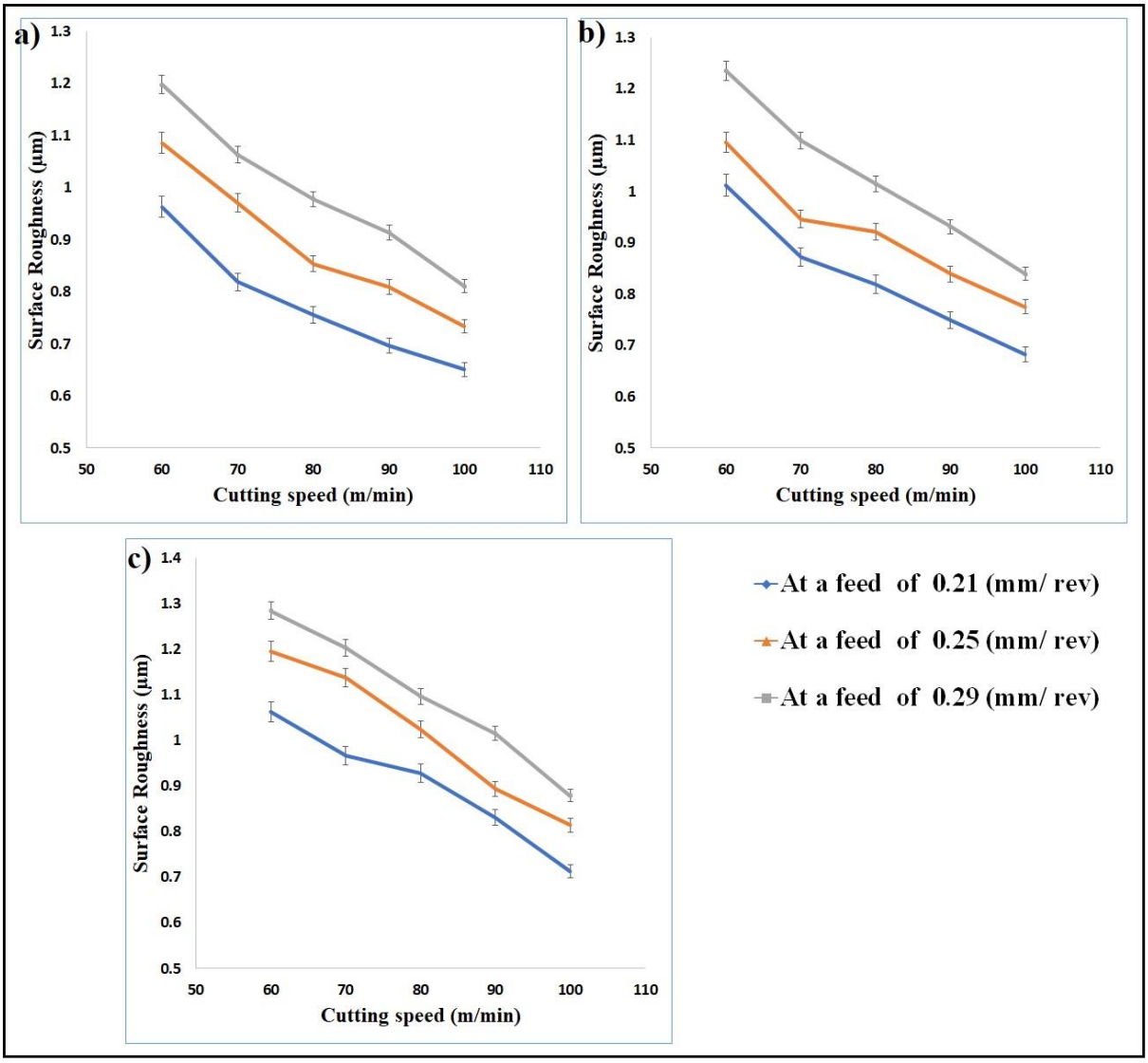

Figure 5.18: Variation of surface roughness with cutting speed at depth of cut of (a) 0.8 mm,(b) 1 mm ,(c)1.2 mm

Figure 5.19 indicates the influence of feed rate and depth of cut on surface roughness. It increased in the range of 11 - 24% based on the cutting velocity where feed increased from 0.21 to 0.29 mm/ rev. This is in line with the theoretical relationship $Ra=f^2/8r$ (f- feed rate, r- nose radius). The formation of chatter marks was higher at high feeds and distant feed marks also occured resulting in higher surface roughness [93]. The surface roughness increased in the range of 10 – 20 % based on the cutting velocity where depth of cut increased from 0.8 to 1.2 mm. This

is because of the high heat-affected zone, and a high shear angle that increases the friction coefficient at cutting zone and decreases the surface finish [23].

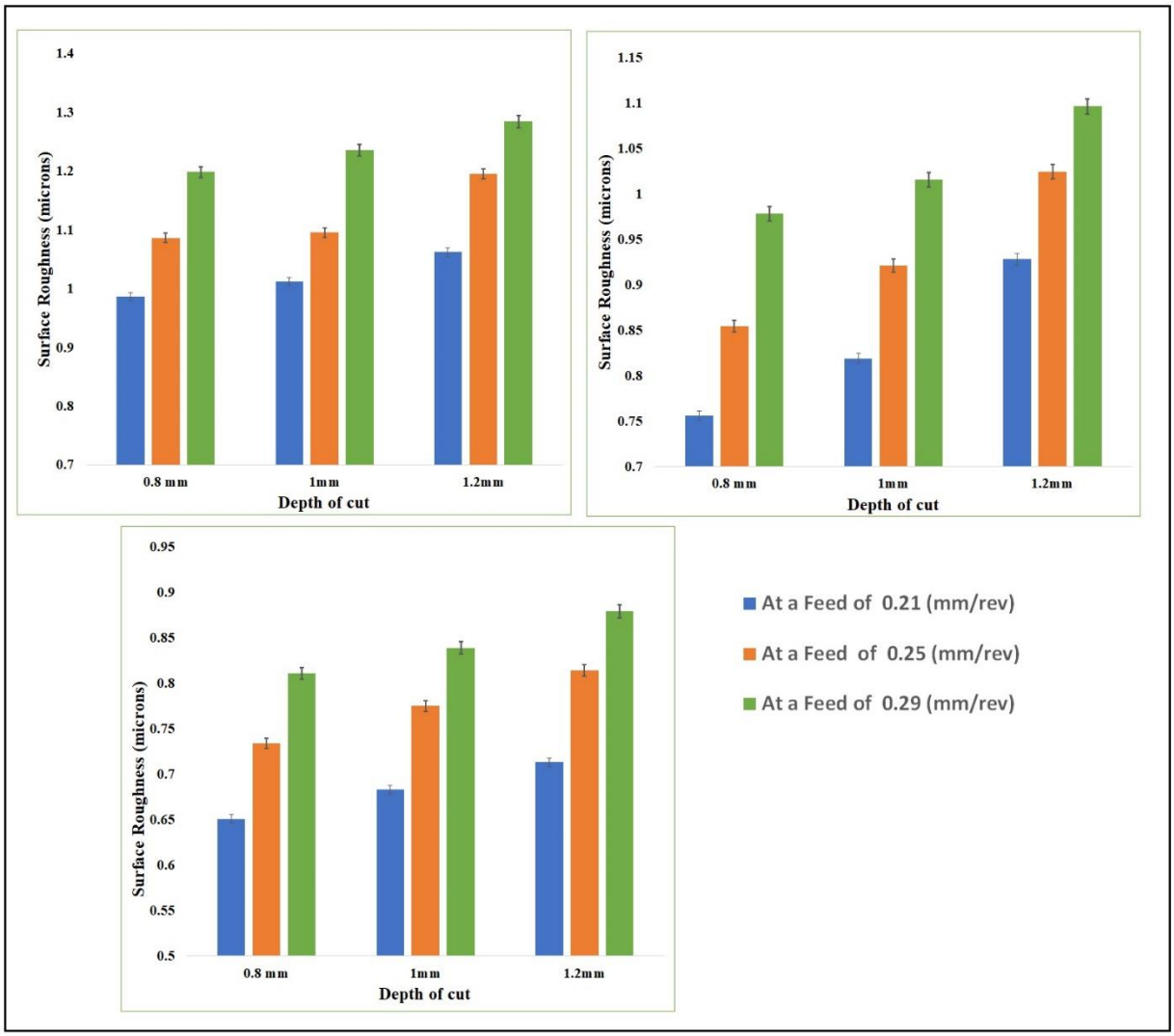

Figure 5.19 : Variation of surface roughness with depth of cut and feed at cutting velocity of (a) 60 m/min,, (b) 80 m/min , (c)100 m/min

5.6 Optimization

The experimental data was used to develop a model by using RSM technique individually for the nozzle, flow, and machining parameters. The significantly impacting parameters were determined from the model. Figure 5.20 shows the standardized effect of nozzle parameters on responses. It was found that the nozzle diameter is the most influential parameter for all the responses. Figure 5.21 shows the standardized effect of flow parameters on responses. It is observed that both coolant pressure and cold fractionsignificantly affect the responses. Similarly,

from Figure 5.22, it is observed that the cutting speed most impacts the responses. In VTCS system, the significantly influential parameters were considered for optimization. The best combination of parameters was determined by RSM optimization technique presented in Table 5.2.

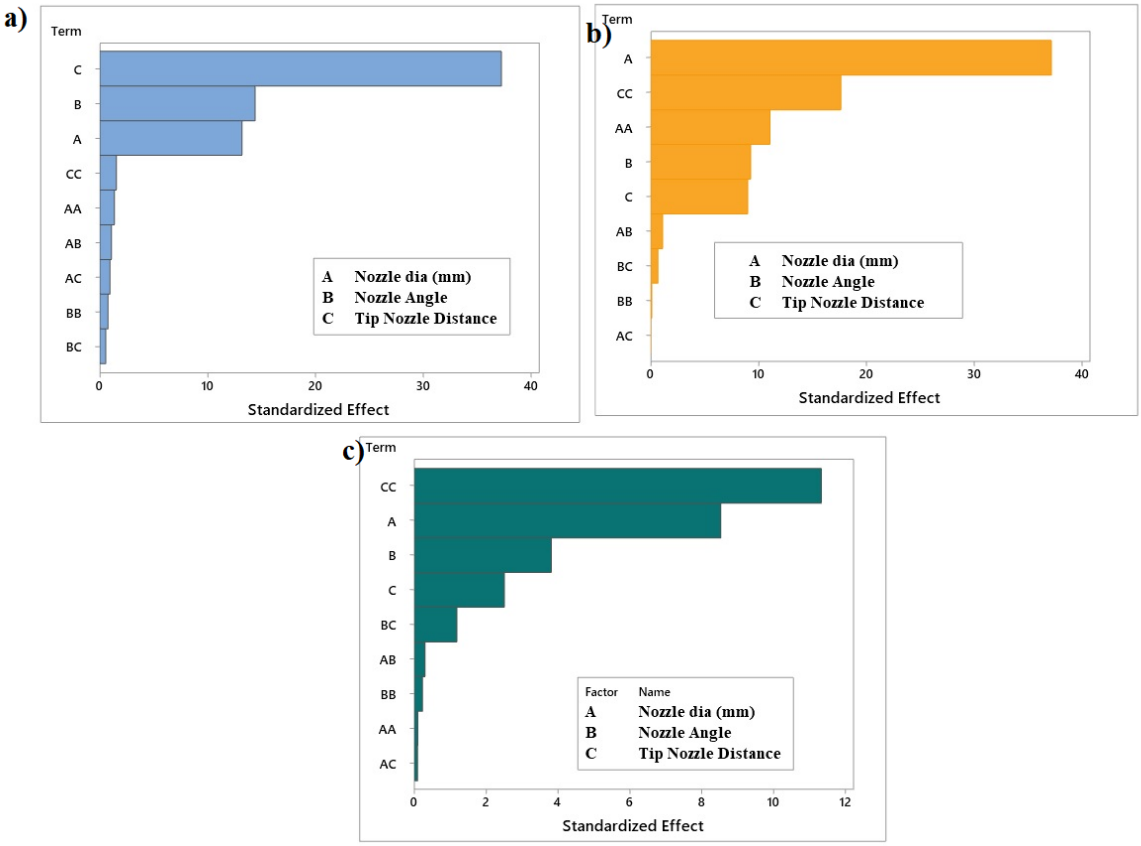

Figure 5.20: Standardized effects of nozzle parameters on A) Cutting force B) Cutting temperature C) Surface roughness

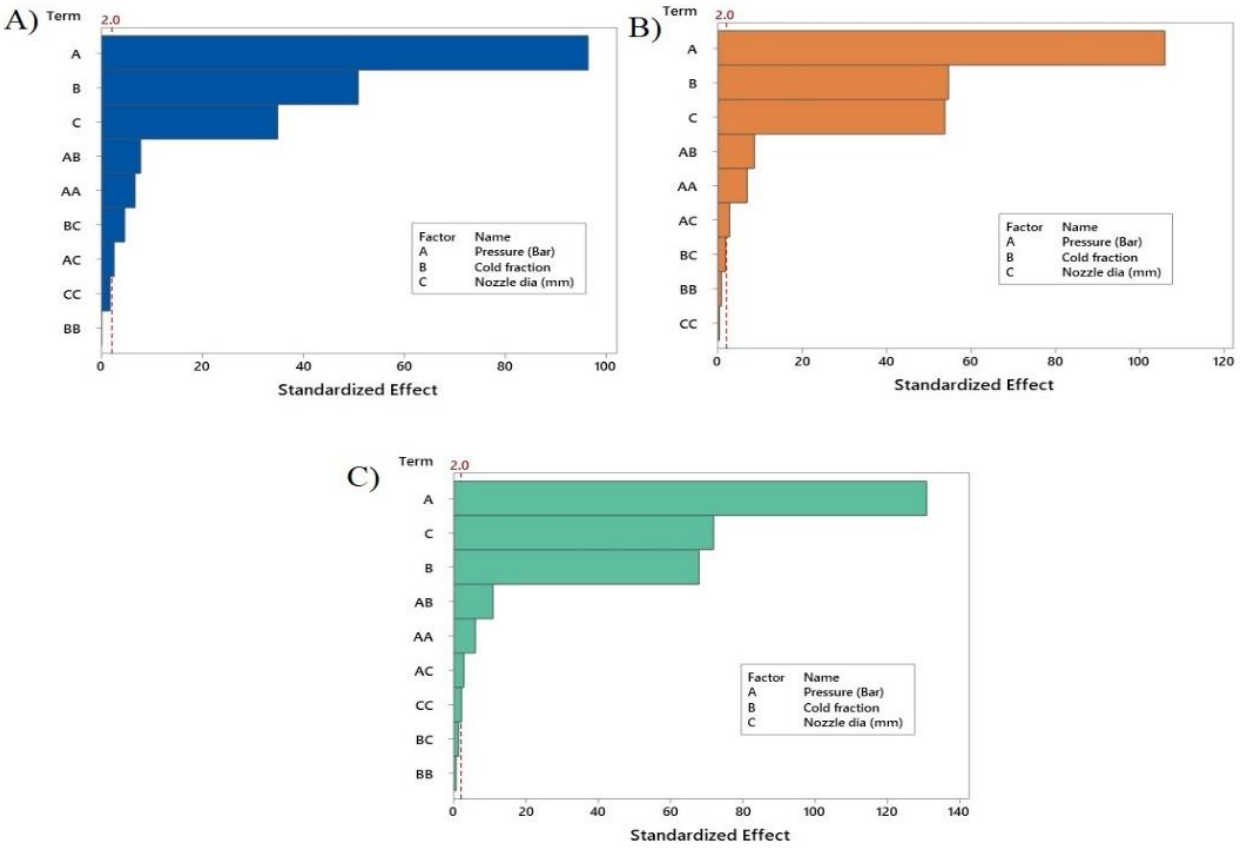

Figure 5.21: Standardized effects of flow parameters on A) Cutting force B) Cutting temperature C) Surface roughness

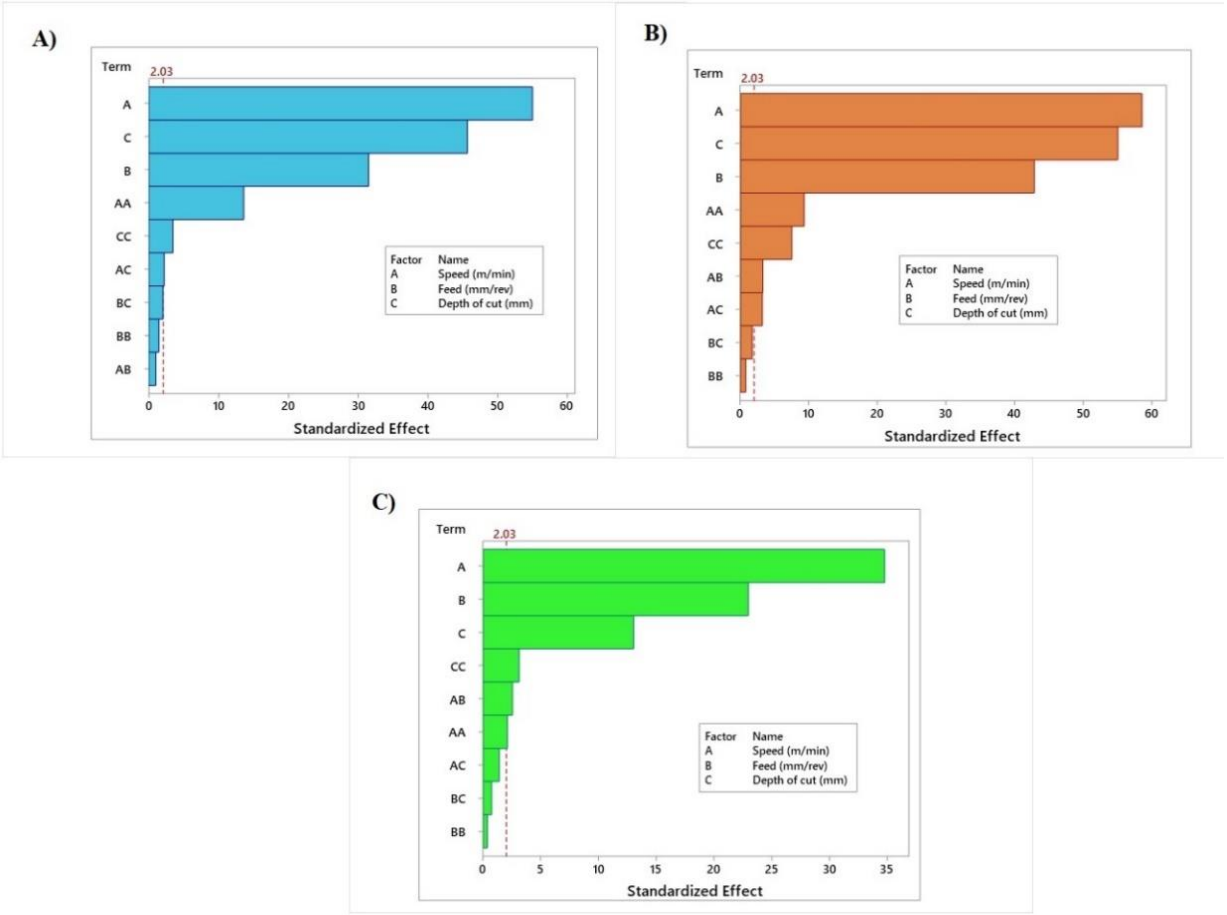

Figure 5.22: Standardized effects of machining parameters on A) Cutting force B) Cutting temperature C) Surface roughness

Table 5.2: Optimum combination of parameters

Input parameters	**Magnitude**
Nozzle angle	45^0
Nozzle diameter	5.89 mm
Coolant pressure	8.2 bar
Cold fraction	18.2%
Cutting speed	81.8 m/min

5.7 Performance evaluation

To evaluate the performance of the dual nozzle vortex tube cooling system while machining Ti-6Al-4V, it was compared with other cooling methods which use different cooling

media. For this, the turning experiments were performed under dry, compressed air, compressed CO_2 gas, air VTCS, and CO_2 VTCS environments by maintaining a constant speed, feed, and depth of cut. The input parameters considered are near round values of optimized results presented in Table 5.2 which were constant throughout the experiment. Feed and depth of cut values were 0.21 mm/ rev and 1 mm respectively, maintained and constant. The cutting temperature, cutting force, and surface roughness were compared with dry, compressed air, compressed CO_2 gas, and air VTCS. Chip morphology, surface morphology, and tool wear were compared only with dry cutting.

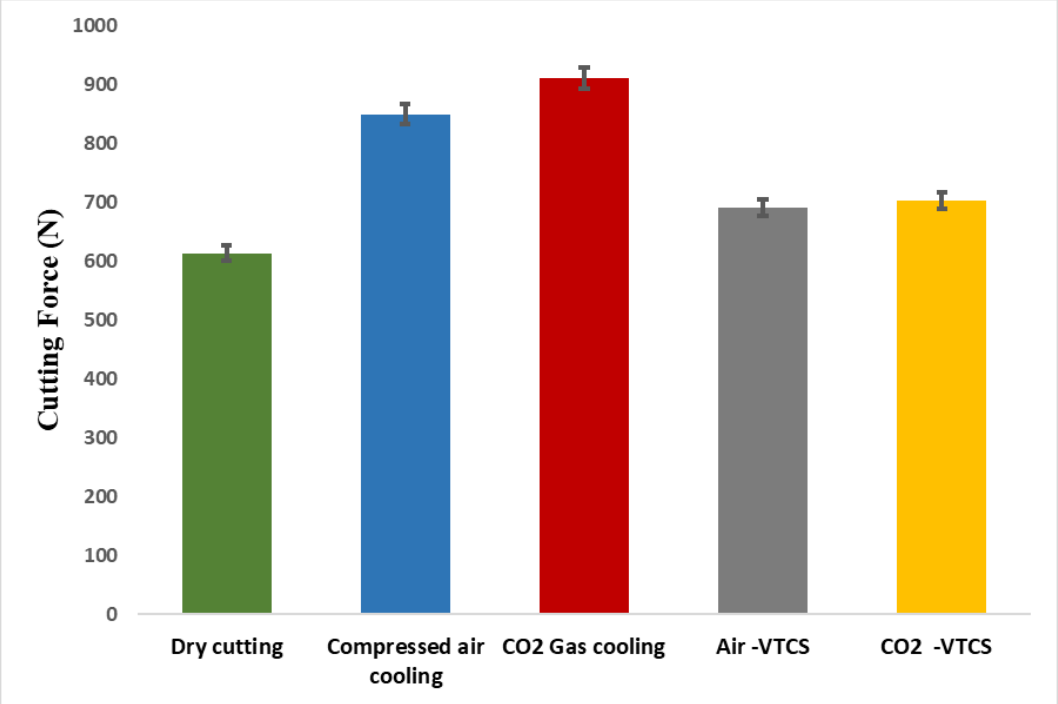

Figure 5.23: Variation of cutting force with respect to different cooling environments

Figure 5.23 shows the influence of different cooling media on cutting force. From the results, it is observed that dry cutting provides minimum cutting force while the CO_2 gas cooling process provides the maximum cutting force. The cutting force obtained in dry cutting is 12.6% less than CO_2 VTCS. This can be reasoned by the fact that a dry environment promotes thermal softening of the workpiece due to high temperature and the heat generated in the machining zone is not removed effectively facilitating easy deformation of the workpiece while machining. The force obtained through compressed air and compressed CO_2 gas is 13.7% and 29.7% more than that of VTCS. This is because of the impulse force generated by high pressure coolant jet on the

tool in both techniques. The amount of gas supplied into the machining zone in VTCS is only 20% of the inlet gas supplied in other methods. This can effectively reduce the momentum which in turn decreases the cutting force. The CO_2 VTCS produces a force that is slightly more than the air based system due to the higher cooling effect of CO_2 gas. This causes strain hardening and therefore increases the hardness of the workpiece.

Figure 5.24 shows the effect of the cooling environment on cutting temperature. From the results, it is observed that minimum cutting temperature is obtained while compressed CO_2 gas is used as a cooling medium and the maximum temperature is obtained in dry cutting. The cutting temperature obtained during compressed CO_2 is 5.35% lower than that of CO_2-VTCS while for dry cutting, compressed air, and Air-VTCS, it would be higher by 58.89%, 25.3%, and 16.8% respectively. The cutting temperature is dependent on heat transfer rate from the machining zone and also the thermal energy absorbed by the coolant. The heat transfer rate depends on the coolant temperature, coolant mass, its specific heat, and heat transfer coefficient (Equation 5.5).

$$Q=mc(T_m-T_g) \quad \ldots\ldots\ldots\ldots\ldots\ldots\ldots\ldots \quad (5.5)$$

Where m= mass of the coolant, c= specific heat of the coolant.

In dry cutting, coolant would be stagnant air, which possesses a very low heat transfer coefficient. Additionally, the inherent properties of Ti-6Al-4V cause the temperature to rise. To enhance the heat transfer from the machining zone, compressed air and CO_2 gas are supplied using a nozzle that reduced the machining temperature by 21.17% and 40.43% respectively. Use of CO_2 provided better results because of high Joule Thompson coefficient which can generate a significant cooling effect against expansion from 7 bar to atmospheric pressure. Although CO_2 gas assures lower temperature, its use is not recommended because of higher force and power consumption. By adopting VTCS, the cutting force can be reduced without much affecting the cooling effect. Hence, CO_2 based VTCS performed well in terms of reducing temperature as well as cutting force compared to CO_2.

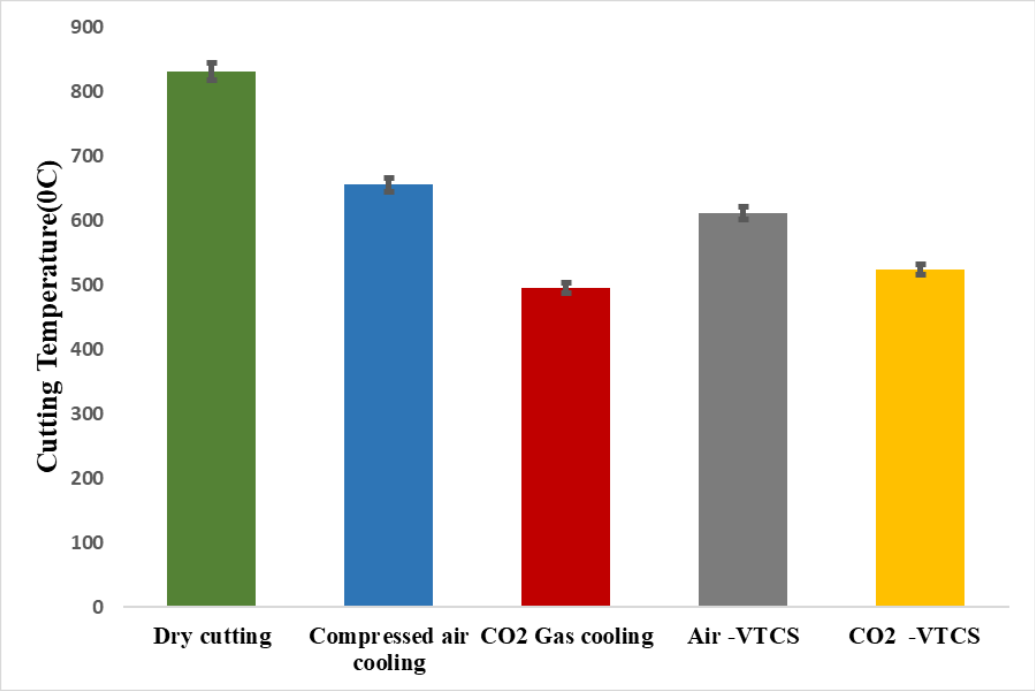

Figure 5.24: Variation of cutting temperature with respect to different cooling environments

Figure 5.25 shows the effect of different cooling environments on surface roughness. Apparently, maximum surface roughness is obtained at a dry environment and is minimum for CO_2-VTCS system. The surface roughness obtained in CO_2–VTCS system is lower by 66.7%, 58.23%, 42.31%, and 51.5% compared to dry cutting, compressed air, compressed CO_2 gas, and air-VTCS respectively. The surface roughness mainly depends on the penetration of coolant, coefficient of friction between the mating surfaces, and chip evacuation from the machining zone. In dry environment, absence of lubricant leads to higher coefficient of friction between mating surfaces. In addition to the above, high temperature in dry environment causes rapid tool wear which is responsible for deteriorating surface finish. Use of air or CO_2 gas as coolant medium would provide an opportunity for coolant penetration into the mating surfaces, an action that can reduce both friction and tool wear (by reducing cutting temperature). This improves the surface finish when compared to dry cutting. However, its use is not advisable as it generates chatter marks due to high cutting forces combined with low Young's modulus of Ti-6Al-4V. By employing CO_2 -VTCS system, better surface finish is obtained because of low coefficient of friction, high coolant penetration, and effective heat removal.

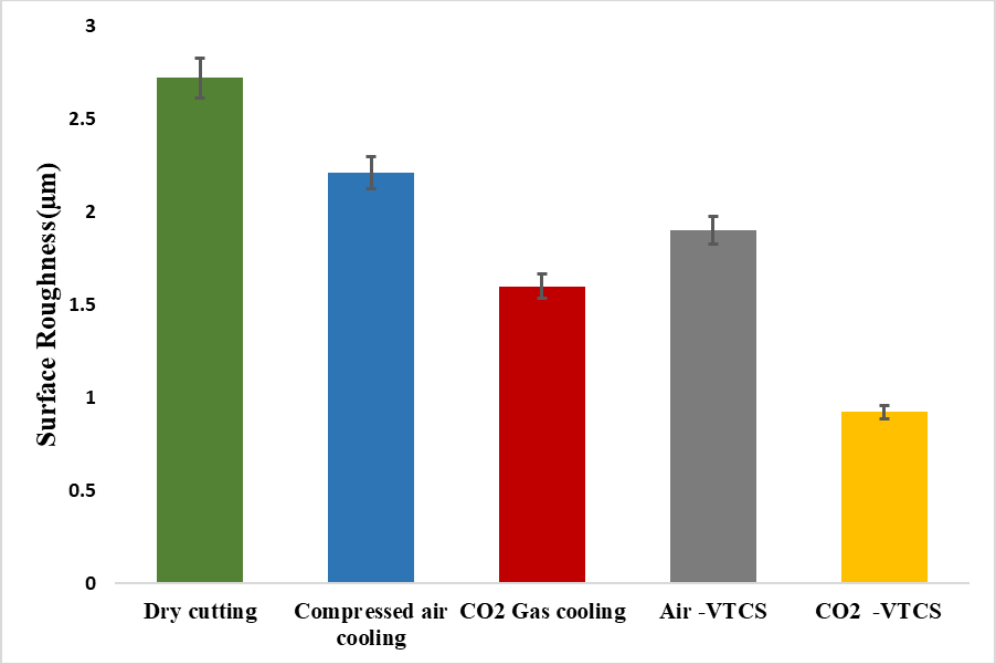

Figure 5.25: Variation of surface roughness with respect to different cooling environments

5.7.1 Chip morphology

In machining, cutting temperature, surface roughness, and tool wear are directly affected by chip formation. Chip morphology is closely related to machining efficiency and the surface integrity of the machined product. The chip geometry and chip-tool contact affect the response parameters. Entrapment of continuous or discontinuous chips at the flank and rake interface would generate vibrations. It may lead to poor surface quality, and chatter marks on the surface. The variables that mainly affect chip morphology are cutting speed, feed, depth of cut, lubrication, cooling conditions, and workpiece material properties.

Figure 5.26 shows the chips produced in machining Ti-6Al-4V in dry and VTCS environments. It is observed that continuous chips are obtained in dry cutting environment whereas discontinuous chips were obtained in VTCS. Disposal of continuous chips is a cumbersome task at elevated temperatures. Dry cutting operations are characterized by free convection mode of heat transfer with stagnant air as the medium. As most of the cutting operations require little time, this would limit heat transfer by free convection. Moreover, heat transfer is further hampered by the inherent low thermal conductivity of Ti-6Al-4V. As a result, temperatures increase at the cutting zone due to heat accumulation. The after-effects of this phenomenon include a rise in plasticity

and toughness, increased shear limit, and thermal softening of the chip material thereby increasing the energy required for chip breakage. All the these conditions would promote the formation of continuous chips as depicted in Figure 5.26 (a) [20].

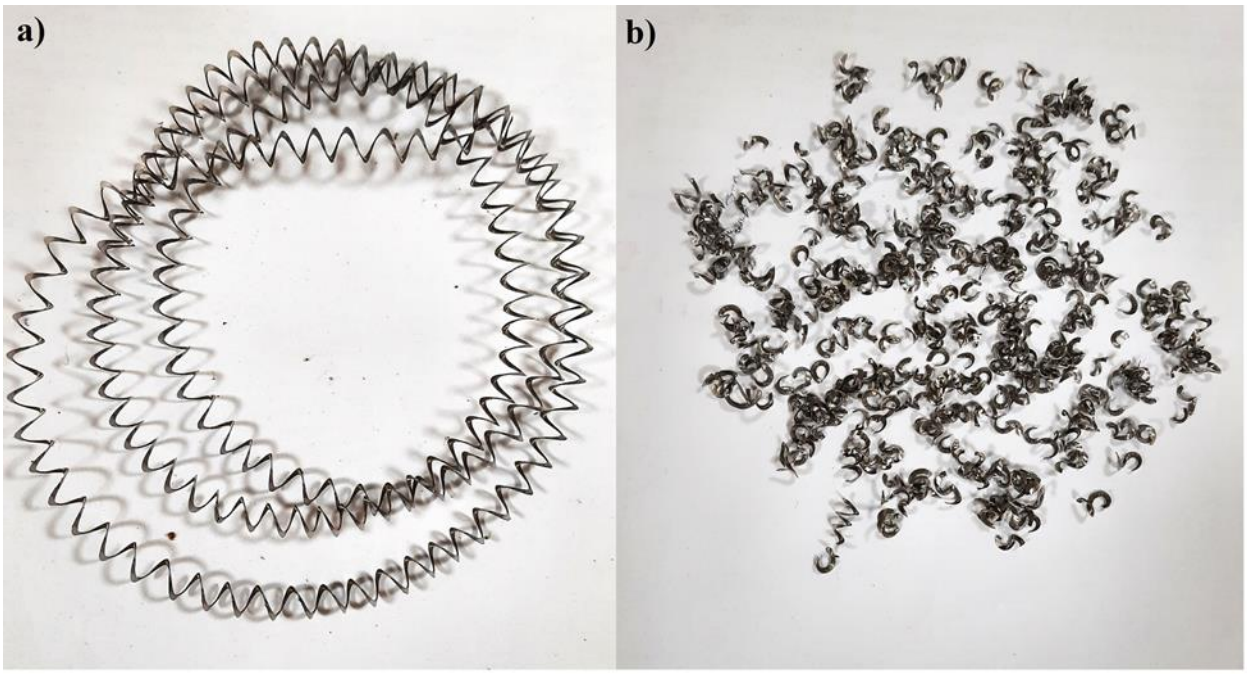

Figure 5.26: Chips produced in a) dry machining b) VTCS conditions

VTCS environment implements forced convection that facilitates improved heat transfer thereby reducing cutting temperatures. As a result, toughness of chips decreases since it is directly proportional to temperature. Impingement of cold gas quenches the chips, making them brittle for easy breaking. The CO_2 gas moreover reduces friction and adhesion, and also effectively penetrates into the chip-tool interface. This leads to low chip thickness and produces discontinuous chips as evident from Figure 5.27(b) [10]. High pressure gas assists in effective evacuation of chips from the machininig zone. Figure 5.27 shows the SEM images of chips under dry and VTCS environments. It is observed that segmented chips are produced when machining Ti-6Al-4V under both dry conditions and VTCS. The observations indicate a shorter chip segment in the case of VTCS envirornments. The geometry of segmented chips mainly depends upon the work hardening and thermal softening phenomenon. The crack produced on the segmented zone propagates and breaks the segmented portion. When the thermal softening dominates, the cracks observed on the chip segments are smaller in size because of the plasticity of the chip material and hence rander crack propagation difficult. When the strain hardening phenomenon dominates, the propagation of

crack is easier due to the brittleness of the segmented portion, leading to breakage. In dry cutting, due to higher cutting temperature, thermal softening dominates strain hardening and produces segmented chips. However, in VTCS, the impingement of cold and compressed gas leads to strain hardening which in turn helps the propagation of the crack. Due to this, the length of the segmented portion is relatively lower compared to dry cutting [94].

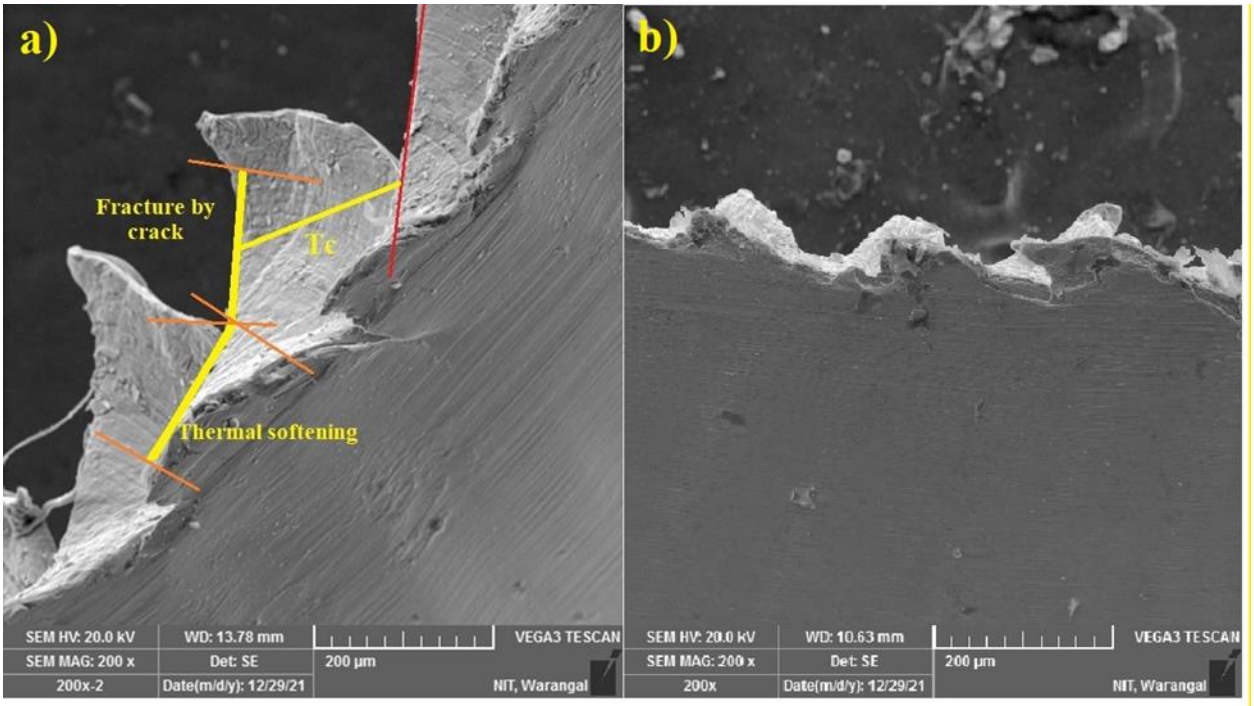

Figure 5.27: SEM images of chips produced under a) dry cutting b) VTCS

Figure 5.28 shows the SEM images of the machined surface under dry cutting and VTCS conditions. The conditions during machining are responsible for heating the chip fragments and workpiece. The rise in temperatures is also due to the conversion of shear energy into thermal energy. These high temperatures initiate a bond between the workpiece and the chip fragments thus creating BUE, which breaks and ends up sticking to the machined surface. The factors responsible for the formation of BUE droplets as depicted in Figure 5.28 (a) are high temperature and rubbing friction between chip, tool, and workpiece. Evidently, this situation is encountered in the case of dry cutting conditions due to thermal softening, high temperatures and also ineffective heat removal mechanism. Manifestation of feed marks on the machined surface is an indication of the deteriorating surface finish of the machined component. VTCS system enables effective heat removal, leading to reduced cutting temperatures. Low temperatures inadvertently hamper thermal

softening and hence limit the tendency of sticking chips. Additionally, CO_2 gas reduces friction and facilitates easy chip removal from machining zone. Even the feed marks are no longer visible which is a consequence of an improved surface finish. This entire explanation seems to be in line with the observation in Figure 5.28 (b).

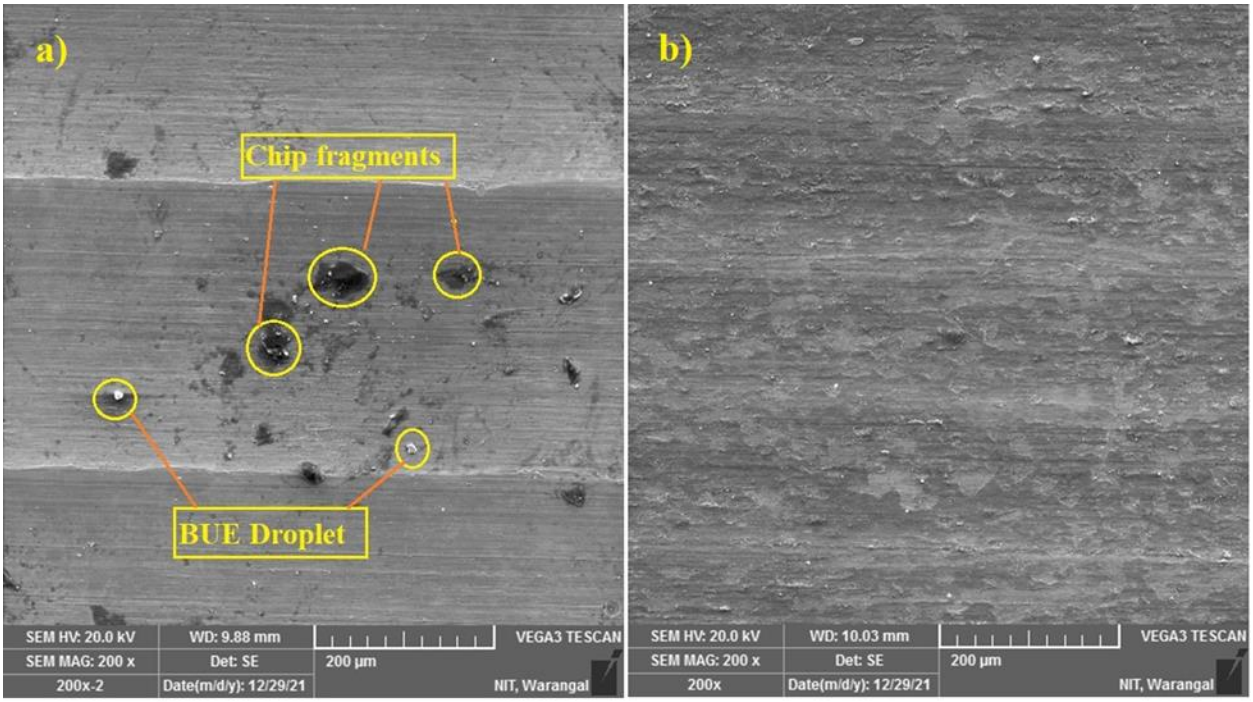

Figure 5.28: SEM images of the workpiece after machining under a) dry cutting and b) VTCS

5.7.2 Tool wear

The machinability of the material is directly evaluated by tool wear, so it is important to analyze and understand the different mechanisms of tool wear. Chipping, notching, and catastrophic failure are the main failure mechanisms for machining titanium alloys. The tool wear is influenced by shear zone temperature as it is directly proportional to tool wear [95].

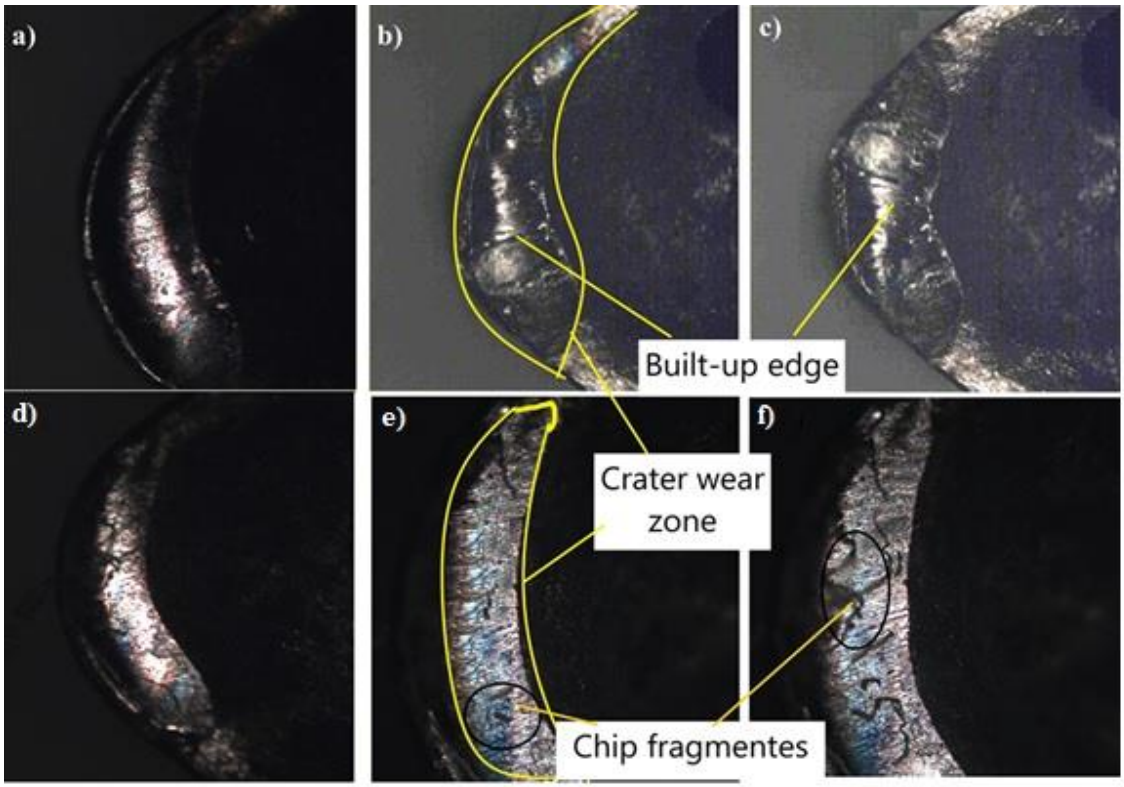

Figure 5.29: Images of cutting insert captured by microscope after 5, 10 and 15 minutes of machining respectively under dry cutting (a, b, c) and VTCS (d, e, f)

Figure 5.29 shows the cutting insert images under the optical microscope after 5,10, and 15 minutes of machining time under dry and VTCS environments. For a 5-minute duration, not much variation is visible in both cases 5.29(a) and 5.29(d). As time progresses, built up edge formation on the insert rapidly occurs as depicted in Figure 5.29(b) and is increased further, as illustrated in Figure 5.29(c). Cutting temperature and friction coefficient are the prime culprits that promote BUE formation in dry cutting conditions. However, in VTCS condition, BUE is non-existent from microscope images as reported in Figures 5.29(e) and 5.29(f). Such a phinomenon can be accounted for because of minimized cutting temperature and reduced coefficient of friction obtained by the use of cold compressed CO_2 gas. Interestingly, Figures 5.29(e) and 5.29(f) expose the presence of chip fragments in meager quantity on the rake face of the tool. This can be attributed to the fact that some of the chip fragments that were relatively hotter than others got welded to the rake face due to the application of high pressure gas on them. Though, crater wear exists in both cases, its width is slightly less in VTCS condition. The occurrence of crater wear

can be credited to chemical reactivity of Ti-6Al-4V. Wear zone is slightly wider in dry cutting condition since reactivity is more at high temperatures.

Figure 5.30 represents the SEM images of the tool flank face after 15 minutes of machining under dry and VTCS environments. It is evident from the figure that flank wear is high in dry cutting compared to the VTCS environment. The area of the wear is measured by using Image -J software and is found to be 0.261 mm^2 and 0.136 mm^2 under dry and VTCS conditions respectively. The main reason for flank wear is the temperature associated with diffusion. In dry cutting, the cutting temperature is high and heat accumulates due to lower thermal conductivity of Ti-6Al-4V. Additionally, Ti-6Al-4V tends to chemically react with tool materials. Although both these conditions favor flank wear, it is significant in the case of dry cutting conditions. Employing the VTCS system resulted in relatively lower flank wear due to its ability to minimize cutting temperature by facilitating forced convective heat transfer.

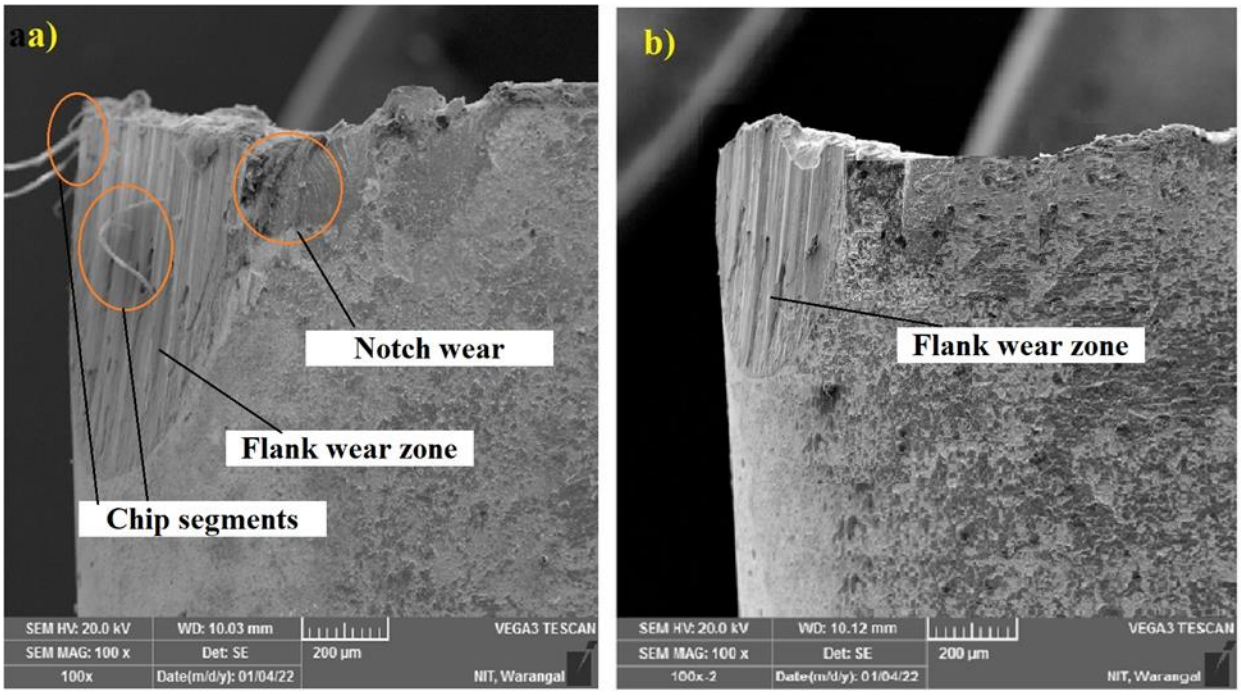

Figure 5.30: SEM images for the flank face of the tool after machining for 15 minutes under a) dry cutting and b) VTCS

Figure 5.30(a) displays the adhesion of chip segments on the flank face of the cutting tool. This is due to plastic deformation and thermal softening of the chips arising from high cutting temperatures. Even notch wear was observed in dry cutting due to the adhesion of the workpiece

and chip material at higher temperature. VTCS system eliminates all these issues due to the effective control of cutting temperature in Ti-6Al-4V machining. The use of CO_2 gas as a coolant in VTCS minimized the notch wear [62].

5.7.3 Surface residual stress

Surface residual stress primarily influences the integrity of the surface, functionality, and fatigue life of the machined component. The cutting temperature (thermal load) and cutting force (mechanical load) are the prime reasons for generation of residual stresses. These stresses may be compressive or tensile based on the quantity of themal and mechanical loads. Compressive stresses improve product life, improve corrosion resistance and fatigue life, and minimize premature failure regardless of material [17]. Mechanical load generates compressive residual stresses while thermal load gives rise to tensile residual stresses. The surface residual stress on the specimen is measured using $\sin^2\psi$ method.

Figure 5.31 shows the plot of d-spacing versus $\sin^2\psi$ for the surface machined under dry cutting. It is observed that d-spacing increased with an increase in ψ value, indicating the development of tensile residual stress on the surface. The rise of cutting temperature in dry cutting makes the thermal load dominate mechanical load, leading to tensile residual stresses on the surface [16]. The thermal softening of the workpiece leads to reduced cutting forces which in turn are responsible for developing surface residual tensile stress on the machined component as seen in Figure 5.31. The residual stress tensor under dry cutting is given below.

$$\begin{bmatrix} 304.8 & 0 & 15.5 \\ 0 & 334.2 & 69.7 \\ 15.5 & 69.7 & 0 \end{bmatrix}$$

Figure 5.32 displays the plot of d-spacing versus $\sin^2\psi$ for the surface machined with the VTCS. It is observed that the d-spacing reduced with increased ψ value indicating the development of compressive residual stress on the surface. This is due to the minimization of the thermal loads achieved by reducing the cutting temperature. Employing a cold, compressed and high velocity stream of CO_2 gas facilitates better heat transfer and lower coefficient of friction. Table 5.3 shows the principal residual stresses generated on the machined surface [16]. The stress Tensor on the specimen under the VTCS environment is given by (MPa).

$$\begin{bmatrix} -187.9 & 0 & 11.6 \\ 0 & -124.3 & 30.5 \\ 11.6 & 30.5 & 0 \end{bmatrix}$$

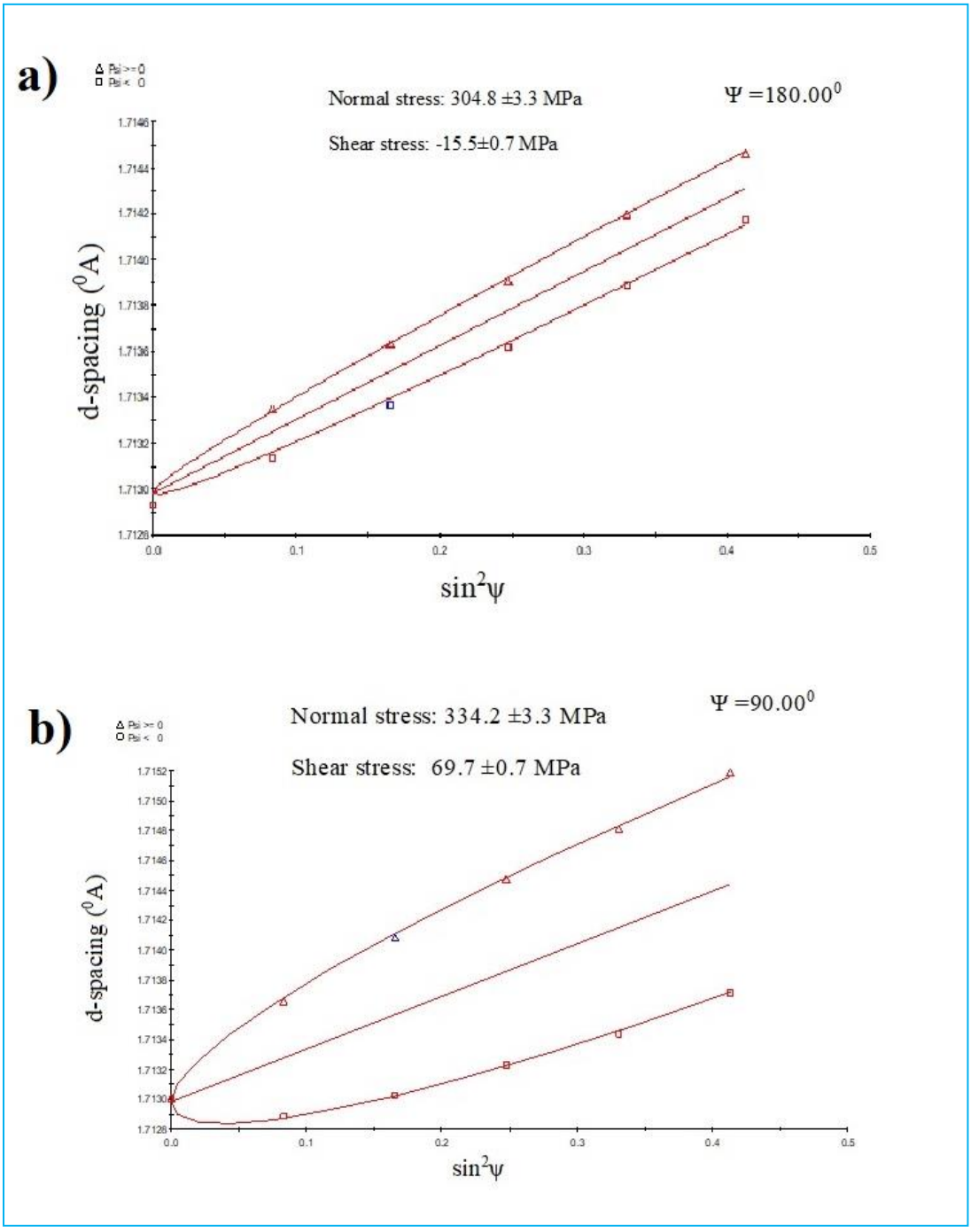

Figure 5.31: Surface residual stresses developed under dry condition

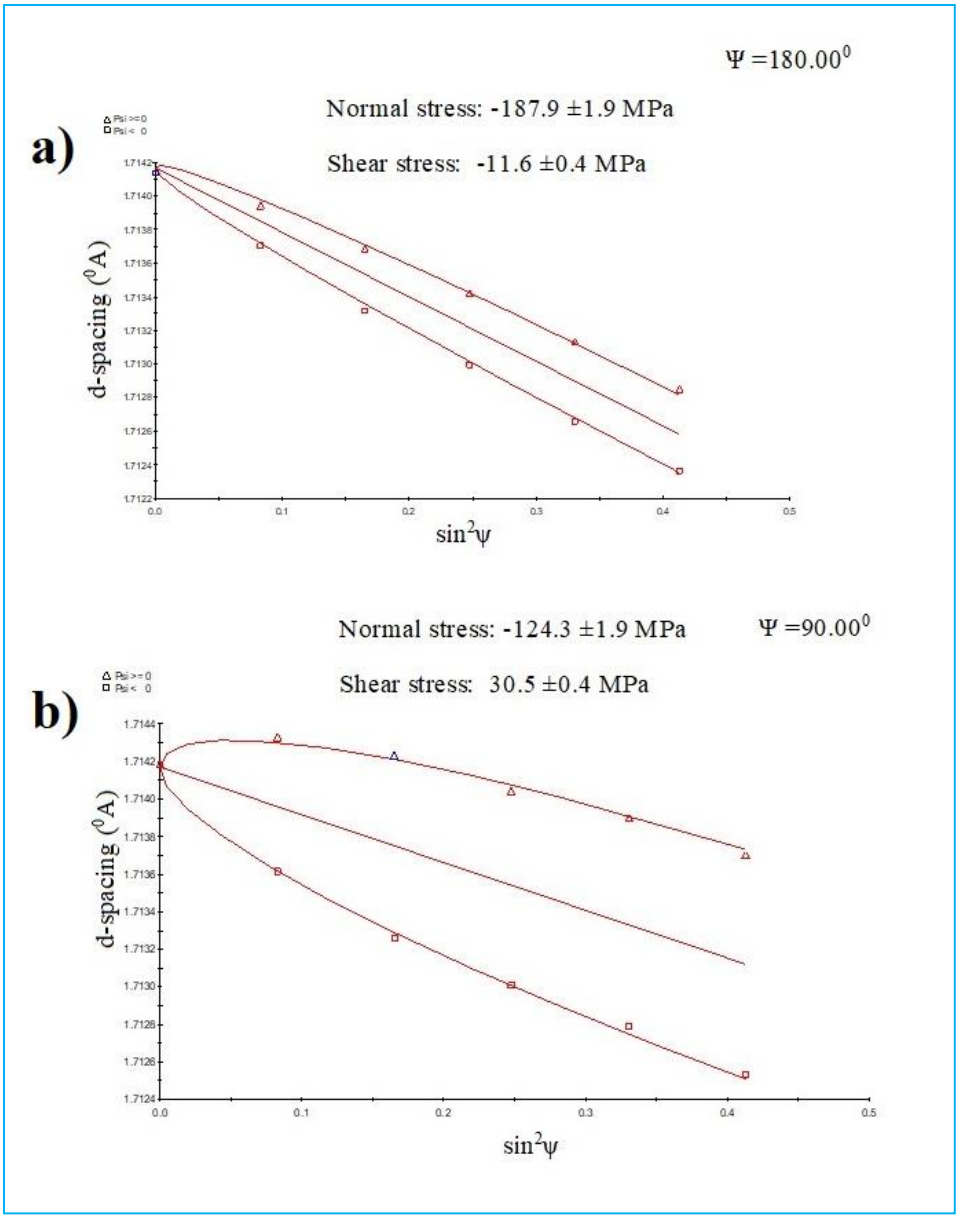

Figure 5.32: Surface residual stresses developed under VTCS

Table 5.3: Principal residual stress on the machined surface

Environment	σ_1 (MPa)	σ_2 (MPa)	σ_3 (MPa)
Dry cutting	304.8	190	306.3
VTCS	-187.9	7.1	0.66

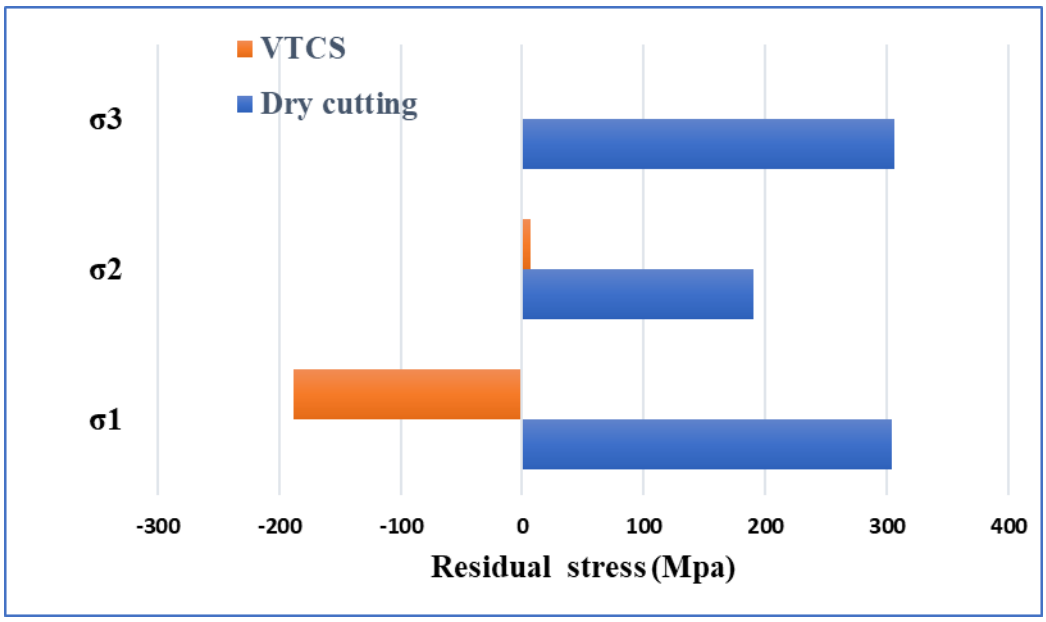

Figure 5.33: Graphical representation of principle surface residual stresses under dry and VTCS environments.

Figure 5.33 represents the principal residual stress in three dimensions. It is observed that compressive residual stresses developed on the specimen under VTCS environment. At higher cutting forces, residual compressive stresses are obtained and their magnitude decreases by reducing the cutting force [96]. In dry cutting, residual tensile stresses are developed due to low cutting forces. This is because of thermal softening of the workpiece. VTCS condition is characterized by compressive residual stress in z-direction and almost negligible stress in other two directions. This is because of improved heat transfer rate and lubrication provided by cold compressed CO_2 gas. The penetrating ability of the compressed gas also reduced coefficient of friction resulting in reduced heat generation due to friction and rubbing. High heat transfer coefficient of cold compressed gas would rapidly cool the material thereby leading to sudden quenching and subsequent hardening of the surface. All these actions would limit cutting temperature and thermal softening Ti-6Al-4V. So higher cutting forces are needed due to reduced thermal softening effect which leads to higher mechanical loads and hence induces compressive residual stresses on the surface.

Summary

This chapter discussed the dual nozzle vortex tube cooling system in the machining of Ti-6Al-4V. The effects of nozzle angle, nozzle position, nozzle diameter, coolant pressure, cold

fraction, cutting speed, feed, and depth of cut on the responses were studied initially. In this case, cutting force, cutting temperature, and surface roughness were considered as responses. The best combination was selected based on optimum values and the responses along with chip morphology, tool wear, and surface integrity were analyzed under optimum conditions. These outcomes were compared to dry cutting results to analyze the effectiveness of the dual nozzle vortex tube cooling system with CO_2 gas.

6 CONCLUSIONS AND FUTURE SCOPE

6.1 Introduction

In the machining process, a large amount of heat is generated which increases the cutting temperature and reduces the dimensional accuracy and quality of the machined surface. This investigation looked at an innovative methodology to design a CO_2 based vortex tube cooling system for the machining of Ti-6Al-4V using uncoated carbide tools. A single nozzle vortex tube cooling system was developed and the experiments were performed by varying the flow parameters. The optimum combination of flow parameters is obtained and the results were compared with dry cutting. It was found that this system provided better results in terms of cutting temperature and surface roughness but cutting forces are increased compared to dry cutting. Hence attempts were made to reduce cutting forces by replacing the single nozzle with dual nozzle. The effect of nozzle parameters on responses were analyzed. The experiments were performed by varying flow parameters and machining parameters individually and their effects on responses were also analyzed. An optimum combination of nozzle configuration, flow parameters, and machining parameters was identified. At optimum condition, the cutting force, cutting temperature, surface roughness, chip morphology, tool wear, and surface residual stresses were analyzed and compared with the dry cutting results. All the above-discussed evaluations collectively let to the following conclusions.

6.2 Conclusions

The machining operation of Ti-6Al-4V was performed by using uncoated carbite tool. TCO_2 gas used as coolant. The experimental analysis led to the following observations:

- In single nozzle VTCS, the cutting temperature and surface roughness were reduced with an increase in coolant pressure and cold fraction, with a decrease in coolant temperature. Cutting force increased with a rise in pressure, cold fraction, and decrease in temperature of the coolant.
- The cutting temperature reduced by 31.1% in VTCS compared to dry cutting due to a lot of heat removal from the machining zone because of high heat transfer coefficient of cold compressed CO_2 gas. Coolant pressure has a significant effect on cutting temperature compared to coolant temperature and cold fraction.

- The cutting force increased by 35.7% in VTCS compared to dry cutting because of the impingement of high pressure jet of CO_2 gas on the cutting tool and strain hardening effect of Ti–6Al–4V. Cutting force is predominantly affected by cold fraction and coolant pressure
- The surface roughness reduced by 69.5% due to low coefficient of friction offered by CO_2 gas at interfaces. Surface roughness is significantly affected by all three parameters coolant temperature, coolant pressure, and cold fraction.

In VTCS, to minimize the cutting force, the experimental setup was modified to dual nozzle system where two similar nozzles were used to supply the coolant. The machining operation of Ti-6Al-4V was performed by using uncoated carbite tool and this system reduced the cutting force by 15 % compared to single nozzle VTCS under the same conditions.

- In dual nozzle VTCS, cutting force increased by increasing nozzle angle and decreased with larger tip nozzle distance. A decrease in nozzle diameter led to rise in cutting force.
- The cutting temperature increased with an increase in nozzle angle. As tip nozzle distance is made larger, cutting temperature would first begin to drop and then rise after reaching a minimum value. It is also found to be low when smaller nozzles were used.
- Surface finish would improve with reduction in nozzle angle. Increasing tip nozzle distance would enable surface roughness to reduce first and then to rise after attaining the least value. The finish of the component seemed to deteriorate with the use of larger nozzles.
- Cutting forces reduced with a decrease in coolant pressure and cold fraction, and an increase in nozzle diameter. Cutting temperature and surface roughness decreased with an increase in coolant pressure, cold fraction, and decrease in nozzle diameter.
- Coolant pressure shows the most significant effect on all response parameters followed by cold fraction and nozzle diameter.
- RSM was performed to identify the most influencing parameters of all nozzle, flow and machining parameters. To obtain the effectiveness of dual nozzle VTCS, the responses were compared with other alternative cooling methods.
- The minimum cutting temperature was obtained in compressed CO_2 gas cooling followed by VTCS-CO_2 and dry cutting. There is a 37 % reduction in cutting temperature in VTCS environment compared to the dry cutting. A better surface finish is obtained while using

CO_2-VTCS which can be reflected in the 66% reduction of surface roughness relative to dry cutting.

- However, the minimum cutting force is obtained in dry machining because of thermal softening phenomena and the absence of additional force generated by impulse-momentum of coolant. VTCS system encounters forces that are 14 % higher to the dry cutting conditions.
- VTCS system facilitates discontinuous chip formation whose disposal becomes easier with the use of cold compressed CO_2 gas. The presence of an effective cooling mechanism reduced the temperature of chip fragments henceforth minimized the chip fragment adherence.
- SEM micrographs revealed the formation of segmented chips for both dry and VTCS environments. However, VTCS conditions favor relatively short chip segments in Ti-6Al-4V machining.
- The chip fragments, BUE segments, and feed marks are observed on the machined surface for dry cutting. But, the VTCS system maintains negligible fragments because of effective chip disposal and tool wear minimization.
- Flank wear is reduced by 48% and notch wear is almost eliminated in VTCS condition with the supply of cold CO_2 gas into the machining zone. However, the reduction of crater wear is insignificant due to the reactive nature of Ti-6Al-4V alloy.
- Compressive surface residual stresses are observed in VTCS conditions whereas the surface residual stresses are tensile in dry cutting conditions due to high thermal loads.

6.3 Future scope

The VTCS discussed in this study can be used as an alternative to conventional cutting fluids which need to replace due to their negative effect on the environment and workers' health. In VTCS, there are no other power-consuming devices and no moving parts which create consistency in machining. In the present study, many challenges are treated successfully, yet some research points can be achieved to expand the current study. Thus, some further research is recommended for both experimentation and finite element simulation. In the current study, VTCS is used to supply the coolant in the machining of Ti-6Al-4V only this be extended for other hard to cut materials like nickel alloys. The coolant used was CO_2 can be replaced with other fluids like

air, nitrogen, and helium depending on application and requirements. VTCS performance may be improved by incorporating MQL setup into the system.

7 References

[1] N. L. Bhirud R R Gawande Chetan R Patil, "'Alternative Techniques for Reducing the Use of Cutting Fluids,'" *Sci. Technol.*, no. 03, 2016.

[2] Amitabha Bhattacharya, *Metal Cutting*. 2012.

[3] M. C. Shaw, . *"The theory of metal cutting."* Proc. Twenty-fifth int. Mach. Tool des. Res. Conf. London: Macmillan Education UK.

[4] E. M. Rubio, B. Agustina, M. Marín, and A. Bericua, "Cooling Systems Based on Cold Compressed Air: A Review of the Applications in Machining Processes," *Procedia Eng.*, vol. 132, pp. 413–418, 2015, doi: 10.1016/j.proeng.2015.12.513.

[5] E. O. Ezugwu and Z. M. Wang, "Titanium alloys and their machinability - A review," *J. Mater. Process. Technol.*, vol. 68, no. 3, pp. 262–274, 1997, doi: 10.1016/S0924-0136(96)00030-1.

[6] A. Shokrani, I. Al-Samarrai, and S. T. Newman, "Hybrid cryogenic MQL for improving tool life in machining of Ti-6Al-4V titanium alloy," *J. Manuf. Process.*, vol. 43, no. September 2018, pp. 229–243, 2019, doi: 10.1016/j.jmapro.2019.05.006.

[7] V. S. Sharma, M. Dogra, and N. M. Suri, "Cooling techniques for improved productivity in turning," *Int. J. Mach. Tools Manuf.*, vol. 49, no. 6, pp. 435–453, 2009, doi: 10.1016/j.ijmachtools.2008.12.010.

[8] S. E. Oraby and D. R. Hayhurst, "Tool life determination based on the measurement of wear and tool force ratio variation," *Int. J. Mach. Tools Manuf.*, vol. 44, no. 12–13, pp. 1261–1269, 2004, doi: 10.1016/j.ijmachtools.2004.04.018.

[9] S. Thamizhmanii and S. Hasan, "Relationship between flank wear and cutting force on the machining of hard martensitic stainless steel by super hard tools," *WCE 2010 - World Congr. Eng. 2010*, vol. 3, pp. 2185–2190, 2010.

[10] B. Dilip Jerold and M. Pradeep Kumar, "The influence of cryogenic coolants in machining of Ti-6Al-4V," *J. Manuf. Sci. Eng. Trans. ASME*, vol. 135, no. 3, 2013, doi: 10.1115/1.4024058.

[11] X. Yang and C. R. Liu, *Machining titanium and its alloys*, vol. 3, no. 1. 1999.

[12] E.M. Trent, *Metal Cutting*. Elsevier Science, 2013.

[13] P N Rao, *Manufacturing Technology—Metal Cutting and Machine Tools*. McGraw-Hill Education, 2018.

[14] N. Buyurgan, *Analysis of the Effects of Coolant/lubricant Aiming in Machining Operations*. University of Missouri--Rolla, 2000.

[15] P. J. Arrazola, A. Garay, L. M. Iriarte, M. Armendia, S. Marya, and F. Le Maître, "Machinability of titanium alloys (Ti6Al4V and Ti555.3)," *Journal of Materials Processing Technology*. 2009, doi: 10.1016/j.jmatprotec.2008.06.020.

[16] N. P. Pasam Vamsi Krishna, “Effect of Vegetable Oil–Based Hybrid Nano-Cutting Fluids on Surface Integrity of Titanium Alloy in Machining Process,” *ASTM Int.*, pp. 1–18, 2020, doi: 10.1520/SSMS20190050.

[17] J. C. Outeiro, J. C. Pina, R. M’Saoubi, F. Pusavec, and I. S. Jawahir, “Analysis of residual stresses induced by dry turning of difficult-to-machine materials,” *CIRP Ann. - Manuf. Technol.*, vol. 57, no. 1, pp. 77–80, 2008, doi: 10.1016/j.cirp.2008.03.076.

[18] A. Aramcharoen, “Influence of Cryogenic Cooling on Tool Wear and Chip Formation in Turning of Titanium Alloy,” *Procedia CIRP*, vol. 46, pp. 83–86, 2016, doi: 10.1016/j.procir.2016.03.184.

[19] S. Sun, M. Brandt, and M. S. Dargusch, “Characteristics of cutting forces and chip formation in machining of titanium alloys,” *Int. J. Mach. Tools Manuf.*, vol. 49, no. 7–8, pp. 561–568, 2009, doi: 10.1016/j.ijmachtools.2009.02.008.

[20] Y. S. Hernández, F. J. T. Vilches, C. B. Gamboa, and L. S. Hurtado, “Experimental parametric relationships for chip geometry in dry machining of the Ti6Al4V alloy,” *Materials (Basel).*, vol. 10, no. 7, 2018, doi: 10.3390/ma11071260.

[21] S. Debnath, M. M. Reddy, and Q. S. Yi, “Environmental friendly cutting fluids and cooling techniques in machining: A review,” *J. Clean. Prod.*, vol. 83, pp. 33–47, 2014, doi: 10.1016/j.jclepro.2014.07.071.

[22] A. Shokrani, V. Dhokia, and S. T. Newman, “Environmentally conscious machining of difficult-to-machine materials with regard to cutting fluids,” *Int. J. Mach. Tools Manuf.*, vol. 57, pp. 83–101, 2012, doi: 10.1016/j.ijmachtools.2012.02.002.

[23] D. Y. Pimenov *et al.*, “Improvement of machinability of Ti and its alloys using cooling-lubrication techniques: A review and future prospect,” *J. Mater. Res. Technol.*, vol. 11, pp. 719–753, 2021, doi: 10.1016/j.jmrt.2021.01.031.

[24] M. Jamil *et al.*, “Sustainable milling of Ti–6Al–4V: A trade-off between energy efficiency, carbon emissions and machining characteristics under MQL and cryogenic environment,” *J. Clean. Prod.*, vol. 281, 2021, doi: 10.1016/j.jclepro.2020.125374.

[25] M. A. Suhaimi, G. D. Yang, K. H. Park, M. J. Hisam, S. Sharif, and D. W. Kim, “Effect of Cryogenic Machining for Titanium Alloy Based on Indirect, Internal and External Spray System,” *Procedia Manuf.*, vol. 17, pp. 158–165, 2018, doi: 10.1016/j.promfg.2018.10.031.

[26] S. Khandekar, M. R. Sankar, V. Agnihotri, and J. Ramkumar, “Nano-cutting fluid for enhancement of metal cutting performance,” *Mater. Manuf. Process.*, vol. 27, no. 9, pp. 963–967, 2012, doi: 10.1080/10426914.2011.610078.

[27] Y. Su *et al.*, “Refrigerated cooling air cutting of difficult-to-cut materials,” *Int. J. Mach. Tools Manuf.*, vol. 47, no. 6, pp. 927–933, 2007, doi: 10.1016/j.ijmachtools.2006.07.005.

[28] Exair, “Adjustable Spot Cooler (SystemsVortex Tubes).” [Online]. Available: https://web.archive.org/web/20200709020350/https://www.vivekengineers.net/catalog/VortexTubesAndSpotCooling/AdjustableSpotCooler.pdf.

[29] E. O. Ezugwu, R. B. Da Silva, J. Bonney, and Á. R. MacHado, “Evaluation of the

performance of CBN tools when turning Ti-6Al-4V alloy with high pressure coolant supplies," *Int. J. Mach. Tools Manuf.*, vol. 45, no. 9, pp. 1009–1014, 2005, doi: 10.1016/j.ijmachtools.2004.11.027.

[30] A. K. Parida and K. Maity, "FEM and experimental analysis of thermal assisted machining of titanium base alloys," *Meas. J. Int. Meas. Confed.*, vol. 152, p. 107292, 2020, doi: 10.1016/j.measurement.2019.107292.

[31] A. Olleak and T. Özel, "3D Finite Element Modeling Based Investigations of Micro-textured Tool Designs in Machining Titanium Alloy Ti-6Al-4V," *Procedia Manuf.*, vol. 10, pp. 536–545, 2017, doi: 10.1016/j.promfg.2017.07.042.

[32] R. A. Rahman Rashid, S. Sun, G. Wang, and M. S. Dargusch, "An investigation of cutting forces and cutting temperatures during laser-assisted machining of the Ti-6Cr-5Mo-5V-4Al beta titanium alloy," *Int. J. Mach. Tools Manuf.*, vol. 63, pp. 58–69, 2012, doi: 10.1016/j.ijmachtools.2012.06.004.

[33] C. R. Dandekar, Y. C. Shin, and J. Barnes, "Machinability improvement of titanium alloy (Ti-6Al-4V) via LAM and hybrid machining," *Int. J. Mach. Tools Manuf.*, vol. 50, no. 2, pp. 174–182, 2010, doi: 10.1016/j.ijmachtools.2009.10.013.

[34] K. Busch, C. Hochmuth, B. Pause, A. Stoll, and R. Wertheim, "Investigation of Cooling and Lubrication Strategies for Machining High-temperature Alloys," *Procedia CIRP*, vol. 41, pp. 835–840, 2016, doi: 10.1016/j.procir.2015.10.005.

[35] P. J. Liew, A. Shaaroni, N. A. C. Sidik, and J. Yan, "An overview of current status of cutting fluids and cooling techniques of turning hard steel," *Int. J. Heat Mass Transf.*, vol. 114, pp. 380–394, 2017, doi: 10.1016/j.ijheatmasstransfer.2017.06.077.

[36] S. Debnath, M. M. Reddy, and Q. S. Yi, "Environmental friendly cutting fluids and cooling techniques in machining: A review," *Journal of Cleaner Production*. 2014, doi: 10.1016/j.jclepro.2014.07.071.

[37] A. Shokrani, V. Dhokia, and S. T. Newman, "Energy conscious cryogenic machining of Ti-6Al-4V titanium alloy," *Proc. Inst. Mech. Eng. Part B J. Eng. Manuf.*, vol. 232, no. 10, pp. 1690–1706, 2018, doi: 10.1177/0954405416668923.

[38] C. H. Che-Haron and A. Jawaid, "The effect of machining on surface integrity of titanium alloy Ti-6% Al-4% v," *J. Mater. Process. Technol.*, vol. 166, no. 2, pp. 188–192, 2005, doi: 10.1016/j.jmatprotec.2004.08.012.

[39] G. Singh *et al.*, "Investigations of machining characteristics in the upgraded MQL-assisted turning of pure titanium alloys using evolutionary algorithms," *Materials (Basel).*, vol. 12, no. 6, pp. 1–17, 2019, doi: 10.3390/ma12060999.

[40] M. K. Gupta, P. K. Sood, G. Singh, and V. S. Sharma, "Sustainable machining of aerospace material – Ti (grade-2) alloy: Modeling and optimization," *J. Clean. Prod.*, vol. 147, pp. 614–627, 2017, doi: 10.1016/j.jclepro.2017.01.133.

[41] O. Pereira, A. Celaya, G. Urbikaín, A. Rodríguez, A. Fernández-Valdivielso, and L. N. L. de Lacalle, "CO2 cryogenic milling of Inconel 718: cutting forces and tool wear," *J. Mater. Res. Technol.*, vol. 9, no. 4, pp. 8459–8468, 2020, doi: 10.1016/j.jmrt.2020.05.118.

[42] R. W. Maruda *et al.*, "Evaluation of turning with different cooling-lubricating techniques in terms of surface integrity and tribologic properties," *Tribol. Int.*, vol. 148, p. 106334, 2020, doi: 10.1016/j.triboint.2020.106334.

[43] A. M. Adam Race, Iwona Zwierzak,Jack Secker ,Julia Carrell ,Tom Slatter, "Environmentally sustainable cooling strategies in milling of SA516: Effects on surface integrity of dry, flood and MQL machining," *J. Clean. Prod.*, vol. 288, no. 15, 2021, doi: https://doi.org/10.1016/j.jclepro.2020.125580.

[44] M. Jamil, N. He, L. Li, and A. M. Khan, "Clean manufacturing of Ti-6Al-4V under CO2-snow and hybrid nanofluids," *Procedia Manuf.*, vol. 48, pp. 131–140, 2020, doi: 10.1016/j.promfg.2020.05.029.

[45] A. K. Nandy, M. C. Gowrishankar, and S. Paul, "Some studies on high-pressure cooling in turning of Ti-6Al-4V," *Int. J. Mach. Tools Manuf.*, vol. 49, no. 2, pp. 182–198, 2009, doi: 10.1016/j.ijmachtools.2008.08.008.

[46] S. Palanisamy, S. D. McDonald, and M. S. Dargusch, "Effects of coolant pressure on chip formation while turning Ti6Al4V alloy," *Int. J. Mach. Tools Manuf.*, vol. 49, no. 9, pp. 739–743, 2009, doi: 10.1016/j.ijmachtools.2009.02.010.

[47] R. Kumar, A. K. Sahoo, P. C. Mishra, and R. K. Das, "Measurement and machinability study under environmentally conscious spray impingement cooling assisted machining," *Meas. J. Int. Meas. Confed.*, vol. 135, pp. 913–927, 2019, doi: 10.1016/j.measurement.2018.12.037.

[48] G. Rotella, O. W. Dillon, D. Umbrello, L. Settineri, and I. S. Jawahir, "The effects of cooling conditions on surface integrity in machining of Ti6Al4V alloy," *Int. J. Adv. Manuf. Technol.*, vol. 71, no. 1–4, pp. 47–55, 2014, doi: 10.1007/s00170-013-5477-9.

[49] S. Sun, M. Brandt, and M. S. Dargusch, "Machining Ti-6Al-4V alloy with cryogenic compressed air cooling," *Int. J. Mach. Tools Manuf.*, vol. 50, no. 11, pp. 933–942, 2010, doi: 10.1016/j.ijmachtools.2010.08.003.

[50] S. Sartori, A. Ghiotti, and S. Bruschi, "Temperature effects on the Ti6Al4V machinability using cooled gaseous nitrogen in semi-finishing turning," *J. Manuf. Process.*, vol. 30, pp. 187–194, 2017, doi: 10.1016/j.jmapro.2017.09.025.

[51] M. Mia *et al.*, "Multi-objective optimization and life cycle assessment of eco-friendly cryogenic N2 assisted turning of Ti-6Al-4V," *J. Clean. Prod.*, vol. 210, pp. 121–133, 2019, doi: 10.1016/j.jclepro.2018.10.334.

[52] S. Y. Hong, Y. Ding, and W. cheol Jeong, "Friction and cutting forces in cryogenic machining of Ti-6Al-4V," *Int. J. Mach. Tools Manuf.*, vol. 41, no. 15, pp. 2271–2285, 2001, doi: 10.1016/S0890-6955(01)00029-3.

[53] P. Shah, N. Khanna, and Chetan, "Comprehensive machining analysis to establish cryogenic LN2 and LCO2 as sustainable cooling and lubrication techniques," *Tribol. Int.*, vol. 148, no. January, p. 106314, 2020, doi: 10.1016/j.triboint.2020.106314.

[54] B. Dilip Jerold and M. Pradeep Kumar, "Experimental comparison of carbon-dioxide and liquid nitrogen cryogenic coolants in turning of AISI 1045 steel," *Cryogenics (Guildf).*,

2012, doi: 10.1016/j.cryogenics.2012.07.009.

[55] A. Shokrani, V. Dhokia, and S. T. Newman, “Comparative investigation on using cryogenic machining in CNC milling of Ti-6Al-4V titanium alloy,” *Mach. Sci. Technol.*, vol. 20, no. 3, pp. 475–494, 2016, doi: 10.1080/10910344.2016.1191953.

[56] K. A. Venugopal, S. Paul, and A. B. Chattopadhyay, “Tool wear in cryogenic turning of Ti-6Al-4V alloy,” *Cryogenics (Guildf).*, vol. 47, no. 1, pp. 12–18, 2007, doi: 10.1016/j.cryogenics.2006.08.011.

[57] M. Mia and N. R. Dhar, “Influence of single and dual cryogenic jets on machinability characteristics in turning of Ti-6Al-4V,” *Proc. Inst. Mech. Eng. Part B J. Eng. Manuf.*, vol. 233, no. 3, pp. 711–726, 2019, doi: 10.1177/0954405417737581.

[58] M. Jamil, A. M. Khan, N. He, L. Li, A. Iqbal, and M. Mia, “Evaluation of machinability and economic performance in cryogenic-assisted hard turning of α-β titanium: a step towards sustainable manufacturing,” *Mach. Sci. Technol.*, vol. 23, no. 6, pp. 1022–1046, 2019, doi: 10.1080/10910344.2019.1652312.

[59] S. Y. Hong, I. Markus, and W. cheol Jeong, “New cooling approach and tool life improvement in cryogenic machining of titanium alloy Ti-6Al-4V,” *Int. J. Mach. Tools Manuf.*, vol. 41, no. 15, pp. 2245–2260, 2001, doi: 10.1016/S0890-6955(01)00041-4.

[60] P. Sivaiah and D. Chakradhar, “Effect of cryogenic coolant on turning performance characteristics during machining of 17-4 PH stainless steel: A comparison with MQL, wet, dry machining,” *CIRP J. Manuf. Sci. Technol.*, vol. 21, pp. 86–96, 2018, doi: 10.1016/j.cirpj.2018.02.004.

[61] C. MacHai and D. Biermann, “Machining of β-titanium-alloy Ti-10V-2Fe-3Al under cryogenic conditions: Cooling with carbon dioxide snow,” *J. Mater. Process. Technol.*, vol. 211, no. 6, pp. 1175–1183, 2011, doi: 10.1016/j.jmatprotec.2011.01.022.

[62] M. I. Sadik, S. Isakson, A. Malakizadi, and L. Nyborg, “Influence of Coolant Flow Rate on Tool Life and Wear Development in Cryogenic and Wet Milling of Ti-6Al-4V,” *Procedia CIRP*, vol. 46, pp. 91–94, 2016, doi: 10.1016/j.procir.2016.02.014.

[63] D. A. Stephenson, S. J. Skerlos, A. S. King, and S. D. Supekar, “Rough turning Inconel 750 with supercritical CO2-based minimum quantity lubrication,” *J. Mater. Process. Technol.*, vol. 214, no. 3, pp. 673–680, 2014, doi: 10.1016/j.jmatprotec.2013.10.003.

[64] E. A. Rahim, A. A. Rahim, M. R. Ibrahim, and Z. Mohid, “Experimental Investigation of Supercritical Carbon Dioxide (SCCO2) Performance as a Sustainable Cooling Technique,” *Procedia CIRP*, vol. 40. pp. 637–641, 2016, doi: 10.1016/j.procir.2016.01.147.

[65] M. Jamil *et al.*, “Heat Transfer Efficiency of Cryogenic-LN2 and CO2-snow and their application in the Turning of Ti-6AL-4V,” *Int. J. Heat Mass Transf.*, vol. 166, 2021, doi: 10.1016/j.ijheatmasstransfer.2020.120716.

[66] A. Iqbal, D. Biermann, H. Abbas, K. A. Al-Ghamdi, and M. Metzger, “Machining β-titanium alloy under carbon dioxide snow and micro-lubrication: a study on tool deflection, energy consumption, and tool damage,” *International Journal of Advanced Manufacturing Technology*, vol. 97, no. 9–12. pp. 4195–4208, 2018, doi: 10.1007/s00170-018-2267-4.

[67] S. Sartori, A. Ghiotti, and S. Bruschi, “Hybrid lubricating/cooling strategies to reduce the tool wear in finishing turning of difficult-to-cut alloys,” *Wear*, vol. 376–377, pp. 107–114, 2017, doi: 10.1016/j.wear.2016.12.047.

[68] S. Yüksel and A. Onat, “Investigation of CNC turning parameters by using a vortex tube cooling system,” in *Acta Physica Polonica A*, 2015, doi: 10.12693/APhysPolA.127.881.

[69] Z. Taha, H. A. Salaam, T. M. Y. S. Tuan Ya, S. Y. Phoon, C. F. Tan, and M. A. Akiah, “Vortex tube air cooling: The effect on surface roughness and power consumption in dry turning,” *Int. J. Automot. Mech. Eng.*, vol. 8, no. 1, pp. 1478–1486, 2013, doi: 10.15282/ijame.8.2013.34.0122.

[70] M. Mia, G. R. Singh, M. K. Gupta, and V. S. Sharma, “Influence of Ranque-Hilsch vortex tube and nitrogen gas assisted MQL in precision turning of Al 6061-T6,” *Precis. Eng.*, vol. 53, no. April, pp. 289–299, 2018, doi: 10.1016/j.precisioneng.2018.04.011.

[71] H. Khazaei, A. R. Teymourtash, and M. Malek-Jafarian, “Effects of gas properties and geometrical parameters on performance of a vortex tube,” *Sci. Iran.*, vol. 19, no. 3, pp. 454–462, 2012, doi: 10.1016/j.scient.2012.03.003.

[72] V. Kirmaci, “Exergy analysis and performance of a counter flow Ranque-Hilsch vortex tube having various nozzle numbers at different inlet pressures of oxygen and air,” *Int. J. Refrig.*, vol. 32, no. 7, pp. 1626–1633, 2009, doi: 10.1016/j.ijrefrig.2009.04.007.

[73] J. D. Golhar, B. R. Rathod, and A. N. Pawar, “Experimental Investigation and Optimization of Vortex Tube with Regard to Nozzle Diameter,” *Int. Conf. Benchmarks Eng. Sci. Technol. ICBEST Int. J. Comput. Appl.*, pp. 32–36, 2012.

[74] J. Liu and Y. Kevin Chou, “On temperatures and tool wear in machining hypereutectic Al-Si alloys with vortex-tube cooling,” *Int. J. Mach. Tools Manuf.*, vol. 47, no. 3–4, pp. 635–645, 2007, doi: 10.1016/j.ijmachtools.2006.04.008.

[75] B. Zhang and X. Guo, “Prospective applications of Ranque–Hilsch vortex tubes to sustainable energy utilization and energy efficiency improvement with energy and mass separation,” *Renew. Sustain. Energy Rev.*, vol. 89, no. April, pp. 135–150, 2018, doi: 10.1016/j.rser.2018.02.026.

[76] N. Agrawal, S. S. Naik, and Y. P. Gawale, “Experimental investigation of vortex tube using natural substances,” *Int. Commun. Heat Mass Transf.*, vol. 52, pp. 51–55, 2014, doi: 10.1016/j.icheatmasstransfer.2014.01.009.

[77] M. Attalla, H. Ahmed, M. S. Ahmed, and A. A. El-Wafa, “Experimental investigation for thermal performance of series and parallel Ranque-Hilsch vortex tube systems,” *Appl. Therm. Eng.*, vol. 123, pp. 327–339, 2017, doi: 10.1016/j.applthermaleng.2017.05.084.

[78] M. Attalla, H. Ahmed, M. S. Ahmed, and A. A. El–Wafa, “Experimental investigation of the effect of nozzle numbers on Ranque–Hilsch vortex tube performance,” *Exp. Heat Transf.*, vol. 30, no. 3, pp. 253–265, 2017, doi: 10.1080/08916152.2016.1233150.

[79] O. Aydin and M. Baki, “An experimental study on the design parameters of a counterflow vortex tube,” *Energy*, vol. 31, no. 14, pp. 2763–2772, 2006, doi: 10.1016/j.energy.2005.11.017.

[80] K. Dincer, “Experimental investigation of the effects of threefold type Ranque-Hilsch vortex tube and six cascade type Ranque-Hilsch vortex tube on the performance of counter flow Ranque-Hilsch vortex tubes,” *Int. J. Refrig.*, vol. 34, no. 6, pp. 1366–1371, 2011, doi: 10.1016/j.ijrefrig.2011.05.008.

[81] M. K. Gupta, M. Mia, G. R. Singh, D. Y. Pimenov, M. Sarikaya, and V. S. Sharma, “Hybrid cooling-lubrication strategies to improve surface topography and tool wear in sustainable turning of Al 7075-T6 alloy,” *Int. J. Adv. Manuf. Technol.*, vol. 101, no. 1–4, pp. 55–69, 2019, doi: 10.1007/s00170-018-2870-4.

[82] M. Boujelbene, “Investigation and modeling of the tangential cutting force of the Titanium alloy Ti-6Al-4V in the orthogonal turning process,” *Procedia Manuf.*, vol. 20, pp. 571–577, 2018, doi: 10.1016/j.promfg.2018.02.085.

[83] E. M. Rubio, A. Bericua, B. De Agustina, and M. M. Marín, “Analysis of the surface roughness of titanium pieces obtained by turning using different cooling systems,” *Procedia CIRP*, vol. 79, pp. 79–84, 2019, doi: 10.1016/j.procir.2019.02.015.

[84] B. J. Kadam and K. A. Mahajan, “Materials Today : Proceedings Optimization of cutting temperature in machining of titanium alloy using Response Surface Method , Genetic Algorithm and Taguchi method,” *Mater. Today Proc.*, no. xxxx, 2021, doi: 10.1016/j.matpr.2021.05.252.

[85] A. Kumar and K. Maity, “Modeling of machining parameters affecting flank wear and surface roughness in hot turning of Monel-400 using response surface methodology (RSM),” *Measurement*, vol. 137, pp. 375–381, 2019, doi: 10.1016/j.measurement.2019.01.070.

[86] “Machining with Advanced CO2 Machining Spray Technology : MoldMaking Technology,” 2019. [Online]. Available: https://web.archive.org/web/20200709020717/https://www.moldmakingtechnology.com/articles/machining-with-advanced-co2machining-spray-technology.

[87] P. K Nag, *Engineering Thermodynamics*, 5 th Editi. Tata McGraw-Hill Education.

[88] V. K. Pasam and P. Neelam, “Effect of vegetable oil-based hybrid nano-cutting fluids on surface integrity of titanium alloy in machining process,” *Smart Sustain. Manuf. Syst.*, vol. 4, no. 1, pp. 1–18, 2020, doi: 10.1520/SSMS20190050.

[89] S. Subudhi and M. Sen, “Review of Ranque-Hilsch vortex tube experiments using air,” *Renew. Sustain. Energy Rev.*, vol. 52, pp. 172–178, 2015, doi: 10.1016/j.rser.2015.07.103.

[90] T. S. Ogedengbe, S. Abdulkareem, and J. O. Aweda, “Effect of Coolant Temperature on Surface Finish during Turning of Titanium Alloy Ti6Al4V,” *Int. J. Eng. Mater. Manuf.*, vol. 3, no. 4, pp. 237–244, 2018, doi: 10.26776/ijemm.03.04.2018.08.

[91] A. K. Sharma, G. Venkatesh, S. Rajesha, and P. Kumar, “Experimental investigations into ultrasonic-assisted abrasive flow machining (UAAFM) process,” *Int. J. Adv. Manuf. Technol.*, vol. 80, no. 1–4, pp. 477–493, 2015, doi: 10.1007/s00170-015-7009-2.

[92] M. Nur, H. Mat, N. Z. Asmuin, and F. Basir, “Effect of impact force for dual-hose dry blasting nozzle geometry for various pressure and distance : an experimental work,” 2020, doi: http://dx.doi.org/10.1140/epjp/s13360-020-00251-9.

[93] S. K. Khare, S. Agarwal, and S. Srivastava, “Analysis of Surface Roughness during Turning Operation by Taguchi Method,” *Mater. Today Proc.*, vol. 5, no. 14, pp. 28089–28097, 2018, doi: 10.1016/j.matpr.2018.10.050.

[94] S. Joshi, P. Pawar, S. Joshi, and A. Tewari, “Deformation mechanism in orthogonal machining of titanium alloys with varying alpha-beta phase fraction,” *AIMTDR Conf.*, vol. 1, no. 311, pp. 311–315, 2012.

[95] C. Agrawal, J. Wadhwa, A. Pitroda, C. I. Pruncu, M. Sarikaya, and N. Khanna, “Comprehensive analysis of tool wear, tool life, surface roughness, costing and carbon emissions in turning Ti–6Al–4V titanium alloy: Cryogenic versus wet machining,” *Tribol. Int.*, vol. 153, no. June 2020, 2021, doi: 10.1016/j.triboint.2020.106597.

[96] N. K. Sahu and A. B. Andhare, “Prediction of residual stress using RSM during turning of Ti–6Al–4V with the 3D FEM assist and experiments,” *SN Appl. Sci.*, vol. 1, no. 8, pp. 1–14, 2019, doi: 10.1007/s42452-019-0809-5.